We would like to thank the two reviewers for their thorough and constructive reviews of our manuscript. We have completely revised the manuscript based on the reviews. In summary, the most important changes are the following.

- We moved a large part of global inversion results and discussion to the supplementary materials and changed the manuscript title to "Inverse modeling of pan-Arctic methane emissions at high spatial resolution: What can we learn from assimilating satellite retrievals and using different process-based wetland and lake biogeochemical models?";
- We did an ensemble of pan-Arctic inversions for each prior emission scenario to calculate the posterior estimate uncertainty using a Monte Carlo stochastic approximation method. And the new results are now shown in Fig. 5 and the old results in Table 3 are removed;
- We redid the bias correction of SCIAMACHY retrievals overpassing the pan-Arctic using a new method and showed the results in Fig. 3) shows the new bias correction;
- We reanalyzed the comparison between the inversion considering lake emissions and the inversion w/o considering lake emissions. The corresponding new figure (Fig. 6) shows that their difference is pronounced;
- We redrew the inversion evaluation figures (now Fig. 7 and Fig. S6). In Fig. 7, due to a direct comparison between global inversions and nested-grid inversions, We showed that the gain of using high-resolution nested grid inversion could be very promising;
- We rewrote the further discussion section to focus on the gain of assimilating satellite retrievals, using high-resolution nested-grid inversions and incorporating methane emissions from lakes. We also illustrated the impact of prior wetland emissions and the uncertainty of this study and future directions.

This response file includes (1) the point-to-point response letter to the first reviewer; (2) the point-to-point response letter to the second reviewer; (3) the manuscript revision with all changes highlighted; (4) the supplementary material revision with all changes highlighted.

General Comments

Though the authors already carried out an extensive work and analysis, the following points need clarification and revision publication in ACP.

Response: We appreciate the valuable comments from the reviewer. These comments help us improve the manuscript in both readability and scientific values.

1.1 Satellite observations and bias correction

Using satellite observations in an inversion system is a difficult task. Using SCHIAMACHY at high latitudes in support to surface in situ observations is even more difficult. The authors acknowledge this difficulty and apply filters on satellite data. They also worked on bias correction to minimize any misuse of satellite data in the inversion. However, in its current form, some questions remain unanswered and should be discussed.

1. Satellite bias is corrected along natural parameters (latitude, air mass factor, etc.) before inversion. Using the same data for debiasing and then for the inversion can be very hazardous. One should make sure that the bias patterns are totally decorrelated from the patterns used in the inversion (concentration gradients in this case). As methane emissions are dominant in tropical regions, concentration patterns could be somehow correlated with satellite bias. In this case, you risk misleading the inversion or at best reduce the number of usable information in the satellite observations. Has it be tried to include the bias correction in the inversion procedure?

Response: We have not tried to include the bias correction in the inversion procedure. In previous studies, some included and some did not. There is no claim that including the bias correction in the inversion procedure is better than the ones not including or vice versa. Given the risk that the further optimization of bias correction functions in the inversion cycle could cause bias correction to incorrectly account for the uncertainties brought by unaccounted model errors or even the uncertain sources and sinks (Houweling et al., 2014) and the inclusion also makes the inverse modeling system more complex, thus the inclusion was not chosen in this study. But as the pan-Arctic inversions are our focus, we did make an effort to detect the bias using independent observations. Specifically, we used the observed CH_4 vertical profiles from the NOAA/ESRL aircraft mission over Alaska, the NIES aircraft mission over Siberia and the NASA/ARCTAS aircraft mission over northern Canada to build a relationship between the satellite bias and specific humidity averaged over the lower 3 km. It should make the debiasing process more reliable. See Fig. 3 for details.

2. Though efforts are done to deploy new observation sites around the Arctic ocean, satellite datasets could fill some gap in the observations. In my opinion, this paper has all the elements to partly address this question and should address it. What is the impact of using satellite data on the inversions? This could be estimated by computing

the sensitivity matrix (Cardinali et al., 2004). It could also be inquired into by comparing inversions with and without assimilating satellite observations.

Response: Thanks very much for this suggestion! Accordingly, we have used a Monte Carlo stochastic approximation method to calculate the inversion uncertainty with and without assimilating satellite retrievals. It shows that assimilating satellite retrievals does reduce the inversion uncertainty.

1.2 Inversion system and uncertainties

1. The description of the system is somehow hard to follow. Section 3.3 should be clarified, in particular, concerning the nesting procedure and the spin-up periods. It looks like observations are used several times in the different inversions, spin up and nesting procedure. This could artificially increase the weight of the observations multiply used, compared with those used only once. Please discuss this point. It may be necessary to stop the spin-up period when the inversion period starts to avoid multiple use of information, biasing the inversion.

Response: The surface sites in the pan-Arctic were used in both global and nested-grid inversions. It could increase the weight of the NOAA/ESRL observations. But if it was not used in global inversions, we believe the boundary conditions of the nested-grid inversions would have much more errors. Since the NOAA/ESRL sites in the pan-Arctic provide much less observations (sometimes less than 1/50), this double counting should introduce much less errors than the method the reviewer suggested. Also, using surface measurements in both global and nested-grid inversions can be found in other previous studies such as Wecht et al. (2014). In addition, we have rewritten the description of the optimization and spin-up processes.

Wecht, K. J., Jacob, D. J., Frankenberg, C., Jiang, Z. and Blake, D. R.: Mapping of North American methane emissions with high spatial resolution by inversion of SCIAMACHY satellite data, J. Geophys. Res. Atmos., 119, 7741–7756, doi:10.1002/2014JD021551, 2014.

2. The global inversions are used as boundary conditions for the regional inversions. It would be interesting to see the impact of the higher resolution on the inversion results. Could the posterior fluxes from the global and the regional inversions be compared for equivalent regions? Anyway, I have some concerns about the way the nesting is carried out. If I understand well, the nested regional model is run on a grid, which does not extend north of 80°. This means that the transport across the Arctic ocean is totally excluded from the regional inversion. Thus, for instance, ZEP only sees the influence of the global boundary conditions as it is really close from the side of your regional domain. ALT is excluded from the regional domain while it is expected to provide some regional information, etc. In the best case, this is a pity of missing some potential information with air masses crossing the Arctic ocean and reaching remote sites. In the

worst case, it totally biases the regional inversion and, at the end, the regional is not better (or maybe worse) than the global inversion. This problem must be addressed, especially as you use a relatively scarce network with Arctic sites relatively close to the border of the regional domain.

That being said, I finally do not see what exactly brings the regional inversion to this study.

Response: We acknowledge that the exclusion of the North Pole in the nested grid could introduce some uncertainty to our estimates but do not agree with the reviewer's claim that this exclusion can totally bias the regional inversion and make the regional not better than the global inversion. We argue that, due to the following reasons, our regional inversion can do a much better job in helping understand CH_4 emissions from the pan-Arctic. First, as we replied to one specific comment below, studies showed that in the summer time which we are interested in, vertical and zonal transport are much stronger than meridional transport. It is true that ALT is excluded from the regional domain. But we do not think that the exclusion of this site would make important regional information missed. The ALT site is located in a region far from possible CH_4 emission hotspots. And because satellite retrievals in northern Canada are much more abundant than the ALT measurements, even if they are of less quality, the regional information they can provide is much better. Thus the scenario to damage our inversions as pointed out would hardly occur. Compared to coarse grid inversions, high-resolution inversions have many advantages: 1) because the footprint of satellite retrievals becomes more consistent with the finer grid cells, the chance they can be represented well in the GEOS-Chem model is much larger; 2) the impact of earth topography on the usability of satellite retrievals (tessellation error) is largely reduced. In summary, it is very unlikely that there is a large bias in our regional inversions due to the exclusion of the North Pole.

3. Concerning the prior uncertainties in the inversion, the current system uses a regularization term γ to control the weight of prior information compared with observations. How this term is computed? Is it based on a χ^2 criterion? Couldn't the same procedure be used to also adjust the in situ vs satellite observations? It has been proven that prior uncertainties play a key role in inversion, and wrong uncertainty matrices can lead to totally biased or inconsistent results. Furthermore, a critical point in inversions is a correct specification of posterior uncertainties. Posterior fluxes without posterior uncertainties are mostly worthless numbers produced by very elaborated black boxes (to caricature...). The authors acknowledge this issue and try to address it by comparing inversion results for 6 different wetland prior fluxes. I am confident that these different scenarios can be sufficient to qualitatively discuss the performance of the inversion. In addition, it seems that the 6 scenarios are sufficient (by chance?) to reproduce a realistic range of uncertainty when comparing to Berchet et al. (2014) numbers for Siberian Lowlands. However, as the author try to draw some

conclusions about the emissions from lakes, dominated by other sources, uncertainties might be too high. This is especially critical as the regional inversions seem kind of unsound. Additional inversions with different observation and prior uncertainty matrices would be necessary to really address this issue.

Response: The term γ is determined by analyzing its influence on the minimum of the cost function. It is a usual way to balance the prediction error and assimilation error in adjoint methods. More details can be found in Hakami et al. (2005), Yumimoto and Uno (2006) and Kopacz et al. (2009). For the emissions from lakes, we showed in Fig. 6 of the revision that the agreement between the GEOS-Chem model and SCIMACHY over a yedoma permafrost region (circled by a black polygon in Fig. 1) gets much better when the emissions from lakes were considered. There is a non-negligible possibility that the missed emissions by the DLEM scenario are from lakes because as illustrated, 56% of the water-inundated landscapes in this region are lakes. And it is possible that emissions counted for wetlands in other wetland models actually are from lakes. But we are cautious to draw a conclusion that CH_4 emissions from lakes must be included in inversions or are significant across the pan-Arctic because there is still very large uncertainty. But the point is that the inversions in this study can shed light on this source at large spatial scales that are unachievable from field observations and the inversions are more reliable than biogeochemical models.

Hakami, A., D. K. Henze, J. H. Seinfeld, T. Chai, Y. Tang, G. R. Carmichael, and A. Sandu (2005), Adjoint inverse modeling of black carbon during the Asian Pacific Regional Aerosol Characterization Experiment, J. Geophys. Res., 110(D14), D14301, doi:10.1029/2004JD005671.

Kopacz, M., D. J. Jacob, D. K. Henze, C. L. Heald, D. G. Streets, and Q. Zhang (2009), Comparison of adjoint and analytical Bayesian inversion methods for constraining Asian sources of carbon monoxide using satellite (MOPITT) measurements of CO columns, J. Geophys. Res., 114, D04305, doi:10.1029/2007JD009264.

Yumimoto, K., and I. Uno (2006), Adjoint inverse modeling of CO emissions over eastern Asia using four-dimensional variational data assimilation, Atmos. Environ., 40(35), 6836–6845, doi:10.1016/j.atmosenv.2006.05.042.

1.3 Structure, content and title of the manuscript

The manuscript in its current form lacks some consistency between the title, structure and content.

The title makes the reader expects an atmospheric inversion accounting for lake and wetland emissions. Section 4.1 deviates in my opinion from the main topic of the paper. What is the objective of this section? In the current state, it looks like an enumeration of aggregated emissions on global regions and compared with previous work. Though by itself

not uninteresting, I don't think it is relevant for Arctic inversions. Maybe the entire section could be moved to supplementary materials (or to a different paper dedicated to global inversions).

On the other hand, Section 3.4 seems to me a key part of the manuscript. But the authors chose to put it only at the end of the method section with only limited details. I consider the satellite measurements play a key role in this work, especially as the Arctic in situ sites are very scarce during the inversion window. As noted by the authors, bias correction is essential for using both satellite and surface measurements. An amended version of the manuscript should include an extended discussion on the bias correction, on the performance of the different models, on the relative weight of satellite data in the inversion compared to surface measurements. This discussion is already partly done in Section 3.4 but should be extended and moved to Section 4. Some elements of Section 4.1 may also be used for this discussion.

The title should render the use of satellite observations as it is not common in Northern latitude.

Response: We have changed the title to "Inverse modeling of pan-Arctic methane emissions at high spatial resolution: What can we learn from assimilating satellite retrievals and using different process-based wetland and lake biogeochemical models?" In the revision, we mainly focused on the following questions: 1) how large the impacts do the wetland biogeochemical models have on pan-Arctic CH_4 inversions and in which direction can the wetland biogeochemical model can be improved for the use of inverse modeling? 2) Can the inclusion of CH_4 emissions from lakes improve the results of inverse modeling? 3) Can the assimilation of satellite retrievals reduce the uncertainty of the posterior estimates? and 4) to compare the possible debiasing method for global or pan-Arctic scale inversions? And we have moved the most part of description about the optimization steps and results of global inversions to the supplementary materials.

Technical Comments

The following points are mostly technical points that need reformulation or some clarification.

p. 32471 l. 20: the last sentence might over-sell the paper or is too vague

Response: This sentence has been deleted.

p. 32472 l. 24: I think putting together ")(" should be avoided as much as possible. There are other occurrences of this typo point in the manuscript

Response: We have revised all these occurrences of ")(" in the manuscript.

p. 32474 l. 9: inversions are even more sensitive to uncertainty matrices; that should be at least partly addressed

Response: Thanks very much! In this revision, we have calculated the uncertainty of posterior estimates of methane emissions from the pan-Arctic. It shows that by using satellite retrievals the uncertainty is reduced.

p. 32476 l. 10: are the outliers numerous? What is the impact of this filtering on the inversion?

Response: We only find one outlier that can pass other quality tests in our study period. Thus we expect this filtering only has a trivial impact on the inversion.

p. 32476 l. 19: the selection is relevant, but some details on how it is done are needed for the reader. Couldn't the excluded sites be used for evaluation? A map of all the sites excluded from the inversion, assimilated in the inversion and used for validation should be provided (at least in the supplementary material), with the borders of the nested model.

Response: For the global scale, we excluded the same sites as in Alexe et al. (2015). We have added this citation for reference. For the nested model, we now added a new figure (Fig. 1) to show the sites assimilated in the inversion and used for validation. There are no surface sites excluded from both assimilation and validation in the nested inversions.

Alexe, M., Bergamaschi, P., Segers, A., Detmers, R., Butz, A., Hasekamp, O., Guerlet, S., Parker, R., Boesch, H., Frankenberg, C., Scheepmaker, R. A., Dlugokencky, E., Sweeney, C., Wofsy, S. C. and Kort, E. A.: Inverse modeling of CH_4 emissions for 2010–2011 using different satellite retrieval products from GOSAT and SCIAMACHY, Atmos. Chem. Phys., 15, 113–133, doi:10.5194/acp-15-113-2015, 2015.

p. 32476: Maybe I missed it but I couldn't find anywhere whether surface observations are continuous or flask measurements.

Response: The surface observations are weekly flask measurements. We have added this information in this section.

p. 32478 l. 17: Can you give an exact definition of "lake"? This seems obvious, but the difference between wetlands and lake could be very tiny in some conditions? Does the map of lakes evolve with time?

Response: The lakes north of 60° N were retrieved from Global Lakes and Wetlands Database (GLWD). This map does not evolve with time. Tan and Zhuang (2015) have detailed description of the lake map processing. According to GLWD, lakes are defined as permanent still-water bodies (lentic water bodies) without direct connection to the sea. And wetlands are by nature

transitional between terrestrial and aquatic ecosystems and have the presence of standing water for some period during the growing season, either at the surface or within the root zone. At least in GLWD, there is no double counting of lakes or wetlands. And we have acknowledged the possible uncertainty introduced by the double counting in the revision.

We have added the definition of "lake" into this section.

Tan, Z. and Zhuang, Q.: Arctic lakes are continuous methane sources to the atmosphere under warming conditions, Environ. Res. Lett., 10, 054016, doi:10.1088/1748-9326/10/5/054016, 2015.

p. 32479 l. 10: Is there any citation comparing GEOS-4 and GEOS-5? As you use different meteorological forcings for the different inversion windows, it could have an impact on the results. The two datasets are probably very consistent and the impact is probably very limited, but this should at least be mentioned.

Response: In our revision, the GEOS-4 meteorological forcing was only used for constructing initial conditions on January 1, 2004. Thereafter, all inversions used the GEOS-5 meteorological forcing, including global scale and nested grid inversions. Additionally, in the revision, we moved the start time of nested grid inversions from July 1, 2004 to July 1, 2005. With such a change, we expect that any signals that could be caused by the inconsistency between GEOS-4 and GEOS-5, if any, should have disappeared after the transport and assimilation processes of one and a half years.

p. 32479 l. 14: if I understand well, for instance, if an air mass from Canada crosses the pole and reaches a site in Siberia, you wouldn't be able to recover any information on the emission with your way of dealing with the pole? It would be then mixed with "boundary" polar conditions? You might lose a lot of information on Arctic emissions considering the fast transport of air masses over the Arctic Ocean. Wasn't it possible to implement the procedure of the global system in the nested system?

Response: We did not include the polar area for the following reasons. First, in GEOS-Chem, with the concern of numerical stability, there is a special treatment of advection in the polar region (Lin and Rood, 1996), but this treatment has not been applied and tested for the nested grid. Second, according to Miyazaki et al. (2008), the Northern Hemisphere (NH) extratropics during summer has slow mean-meridional circulation and inactive wave activity but strong vertical transport. Thus there should be very few air masses from Canada crossing the pole and reaching a site in Siberia or vice versa. Third, it is true that the boundary conditions of the nested model could miss the signals out of boundaries. But this is the drawback of all the similar applications, regardless whether it is in North America or in the pan-Arctic. The possible solution is to construct the boundaries by real data but it is out of focus of this paper. Instead, we have acknowledged this problem in our discussion and called for the improvement of the GEOS-Chem model.

Lin, S.-J. and Rood, R. B.: Multidimensional Flux-Form Semi-Lagrangian Transport Schemes, Mon. Weather Rev., 124, 2046–2070, 1996.

Miyazaki, K., Patra, P. K., Takigawa, M., Iwasaki, T. and Nakazawa, T.: Global-scale transport of carbon dioxide in the troposphere, J. Geophys. Res., 113, D15301, doi:10.1029/2007JD009557, 2008.

p. 32480 l. 10: people unfortunately do not always define Arctic the same way... Please give your definition, so that the reader knows on which region your emissions are defined.

Response: We have removed the word "Arctic" here and the nested domain has defined in the previous paragraph (180°W–180°E and 80°N–56°N).

p. 32482 l. 22: does the system guarantee that it is not stuck in a local minimum? I guess it does, but mentioning only the 0.5% criterion might be insufficient

Response: Yes, the system guarantees that the iteration is not stuck in a local minimum. We have mentioned in the sentence "optimization changes its course automatically if local minimum reaches".

p. 32483 l. 14: BIC seems a reasonable score but it is not commonly used, so please give a little bit of details on it.

Response: We added some descriptions of the method: "The BIC criterion is widely used for regression model selection and aims to award a model that fit measurements with the least model parameters."

p. 32483 l. 25: Does filtering outliers influence the bias correction? What is the portion of data filtered out along this criterion?

Response: The grid squares with RSD in excess of 20 ppb are not outliers but just as indicated by Turner et al. (2015) they are more likely dominated by bias in prior emissions or strong local emissions. If these values are included, the bias correction will either remove local emission signals or account for biases not belonging to SCIAMACHY retrievals.

p. 32484 l. 15: is there a known reason for the opposite dependence of model-data differences in East Asia? This only comes from wrong emission inventories or is there a relation with regional meteorology or other?

Response: According to Peng et al. (2016), the EDGAR dataset could overestimate anthropogenic CH_4 emissions from China.

Peng, S. S., Piao, S. L., Bousquet, P., Ciais, P., Li, B. G., Lin, X., Tao, S., Wang, Z. P., Zhang, Y., and Zhou, F.: Inventory of anthropogenic methane emissions in Mainland China from 1980 to 2010, Atmos. Chem. Phys. Discuss., doi:10.5194/acp-2016-139, in review, 2016.

p. 32484 l. 22: I do not understand why you need these polynomial trends? Is it that you use monthly or 2-weekly flask measurements and extrapolate them to hourly residuals? If so, I think this might be a problem for the inversion. Extrapolating data before inversion can only bring additional uncertainties.

Response: In the revision, we directly compared the weekly flask measurements (the data records include the measurement date and UTC information) to the model.

p. 32486 l. 3: Please remind the inversion windows here. It is not always clear when the satellite data are used.

Response: The global scale inversion window is from January 2004 to December 2004 and January 2005 to December 2005. The inversions of the second time window are for analysis.

p. 32488 l. 20: it would be easier for the reader to draw a picture if the same area were compared.

Response: Our results cannot directly compare with Monteil et al. (2013) because they only reported the CH_4 emissions from the areas north of 50°N.

p. 32489 l. 13: without uncertainties on the posterior, it is hard to see the impact and the confidence of the inversion. The subsequent discussion is thus very speculative in my opinion. The DLEM scenario with no lakes only shows the limitation of inversion methods, I think... I do not really get the choice of DLEM. The way you put it, it only confirms that the inversion has not enough information to redistribute fluxes. But the missing fluxes could also be wetland fluxes.

Response: We have calculated posterior uncertainty in the revision.

p. 32490 l. 18: both numbers looks pretty high, especially for the total column. What the difference between observed and prior total columns? Is the improvement significant? I think this is the most important here. If with the inversion, you only shift the total columns of 1 ppb without the lakes and of 2 ppb with the lakes, you got a signal; but conversely, if the inversion shifts the total columns by e.g., 30 ppb without the lakes and 31 ppb with the lake, you got nothing...

Response: We have drawn another figure to show the difference. As shown in Fig. 6, there are visible differences.

p. 32490 l. 22: I think this citation is not relevant. They could have achieved 15 ppb of improvement if taking wrong prior fluxes...

Response: We have removed this citation.

p. 32491 l. 26: Berchet et al. (2014) did find methane emissions of 1–13 TgCH4/y from Siberian wetlands, which is amazingly consistent with your figure.

Response: Our newly estimated methane emissions from Siberian wetlands are 1.6–7.6 Tg yr^{-1}.

Tab. 1: Maybe you could add correlation coefficients as you show one R in Figure 1.

Response: We have added it.

Figure 1c: it would be interesting to compare on the same figure before and after optimization and to have the same figure for all debiasing method (probably in supplementary material to avoid having dozens of figures...)

Response: As shown in Table 1, the fitting between model and SCIAMACHY does not differ too much among several methods, e.g. between "Latitude only" and "Latitude + Humidity". Thus such plots probably will not bring much information.

Figure 4: Could you please add the prior and posterior uncertainties? Why does the seasonal cycle vanishes after 1998 in the Tropics? As for Section 4.1, I am not sure this figure is really relevant regarding the topic of the paper

Response: We think you are right – this figure seems irrelevant to our topic. It only shows the process of initial condition construction. We have removed it in the revision. For the vanishing of the seasonal cycle after 1998 in the tropics, it is related to the discontinuation of the biomass burning emission dataset. In GEOS-Chem, the GFED3 dataset covers only from 1997 to 2010 and all simulations before 1997 have to use the data of year 1997. Compared to the other years, biomass burning emissions have more apparent seasonal cycle in 1997.

Figure 8-9: Please add the prior RMS for each different scenario, so that one can see the improvement after inversion.

Response: For both figures, we have added the prior RMS for each different scenario.

Several studies have pointed to the importance of methane emissions from lakes, but so far no attempt has been made to include those estimates into global atmospheric transport model and assess their influence on inverse modeling results. This study makes a useful contribution by filling this gap. Estimates are provided of Arctic lake and wetland emissions before and after optimization using inverse modeling. This is all fine, but in the end it is still not so clear whether or not the model has improved by the inclusion of lake emission and what it means for the overall Arctic methane budget. In my opinion, some more in depth analysis in this direction would increase the usefulness of this study. Right now, the conclusion section has some general statements that don't seem to be supported by the results, or at least not in the way the results are presented. Improvements in this direction will be needed, as explained in further detail below, to make this manuscript suitable for publication.

Response: We appreciate the valuable comments from the reviewer. To address the concerns raised by the reviewer, we have used a Monte Carlo stochastic approximation method to calculate the uncertainty of posterior estimates. Fig. 5 shows that assimilating satellite retrievals reduced the uncertainty. In Fig. 6, we did a more detailed comparison between the inversion considering lake emissions and the inversion not considering lake emissions. It shows that there should be strong CH_4 emissions in the specified yedoma permafrost region that is missed by the DLEM model. Since 56% of the water-inundated landscapes are lakes in the region, there is a non-negligible possibility that the missed emissions by the DLEM scenario could be from lakes. And it is possible that emissions counted for wetlands in other wetland models actually are from lakes. We are cautious to draw a conclusion that CH_4 emissions from lakes must be included in inversions or are significant across the pan-Arctic because there is still very large uncertainty. But the point is that the inversions in this study can shed light on this source at large spatial scales that are unachievable from field observations and the inversions are more reliable than biogeochemical models. Also, we have changed the structure of the manuscript to focus on the following questions: 1) how large the impacts do the wetland biogeochemical models have on pan-Arctic CH_4 inversions and in which direction can the wetland biogeochemical model can be improved for the use of inverse modeling?; 2) can the inclusion of CH_4 emissions from lakes improve the results of inverse modeling?; 3) can the assimilation of satellite retrievals reduce the uncertainty of the posterior estimates?; and 4) to compare the possible debiasing method for global or pan-Arctic scale inversions?

General Comments

The statement in the conclusion section that "biogeochemical models tend to overestimate natural sources in the Arctic" calls for a comparison of numbers, together with their uncertainties and a discussion of possible factors influencing the comparison. The numbers are given in Table 3. Looking at the ranges they seem to support the conclusion. However, does the range of posterior estimates reflect the posterior uncertainty? If not, the difference between prior and posterior fluxes may not be significant. Since only a single lake estimate

is used this part of the uncertainty is in any case not accounted for judging only emission ranges. What factors could influence the comparison? Without the lake emission estimates the biogeochemical models would be fine. Could it be that by simply adding up lake emission estimates to the process model results, emissions end up being double counting? For example, if lakes appear in places that already count as wetlands in those models. Particularly when the model prescribes inundated area using satellite data there is no clear boundary between the two. Some further discussion is needed of how these contributions fit together and what the implications are for the uncertainty of the estimates.

Response: In the revision, the posterior uncertainty was calculated. According to Fig. 5, we can still claim that biogeochemical models could overestimate CH_4 emissions in the pan-Arctic. But now this is not a conclusion we are urgent to draw. Rather, we want to say that according to this figure, in addition to Table 2, the estimated uncertainty caused by unrealistic spatial and temporal patterns of biogeochemical models could be larger than the uncertainty caused by observation and prior emission magnitude uncertainties. This emphasizes the importance of improving biogeochemical models to achieve consistent spatial and temporal variabilities. The value of the estimates for lake emissions here is to shed light on the upper and lower bounds of this source. Because the lake model is combined with different wetland models in which some could have stricter definitions of wetland area and some could have wider definitions, in addition to data assimilation, the results can give us more insights on the magnitude of the source than the lake model alone. It can also be true for CH_4 emissions from wetlands.

It is difficult to judge the added value of the regional inversion from the way in which results are presented. Table 3 is the only place where a direct comparison between prior and posterior is made. Looking at the ranges, the results actually suggest that the inversion increases uncertainty. Otherwise the plots for the regional inversions show either prior or posterior fluxes, but no differences between the two. This makes it hard to judge where inversion results converge or diverge in the inversion process. The impact of accounting for lakes is discussed in the text – where suggestions are made that it is important to do so. This is the kind of discussion that is expected from a paper, which investigates the role of lakes. However, only one figure in the supplementary information shows any results supporting this discussion. Since it only shows posterior results, it is difficult to compare with any of the other figures. The point about the importance of including lake emissions has to be demonstrated more convincingly.

Response: To address these issues, we calculated the posterior uncertainty of emission estimates and showed it in Fig. 5. Fig. 6 shows that the inclusion of lake emissions improves the agreement between the GEOS-Chem model and satellite retrievals. We also compared the RMS of the posterior global and pan-Arctic inversions over the pan-Arctic surface and aircraft observations.

Figure 8 and 9 demonstrate how the inversion-optimized fluxes improve the fit to various measurements. What I find missing in these figures is the range of a priori RMS values (I

mean from each inversion). I wonder also whether posterior RMS's correlate with the priors. In other words, does the pattern of posterior mismatches reflect that of the prior or not? A more important omission, however, is a quantification of the role of lakes in these figures. Is there any gain in terms of RMS by including a pattern of lake emissions in the inversion?

Response: We have improved these two figures according to the comments (see Fig. 7 and Fig. S6). Now the RMS from the prior of each scenario shows together with the RMS from the posterior. For lake emissions, Fig. 6 can show some gain in terms of RMS if lake emissions are included. We think it is difficult to explain the gain in terms of RMS using other observations because both surface sites and aircraft missions are far from the regions where lakes are obvious dominant in the GLWD map.

The final conclusion that the nested modeling approach improves the simulation of methane mixing ratios is not supported by results. The same is true for the sentence that follows about the understanding that is gained about Arctic emissions by simulating methane with more spatial detail. Either provide the supporting evidence or otherwise remove the conclusions.

Response: We have revised the discussion and conclusion according to our results. According to the results, the following conclusions can be drawn: 1) the realistic spatial and temporal variability of prior CH_4 emissions from wetlands are important for inverse modeling; 2) satellite retrievals can be used to reduce the uncertainty of the estimates of CH_4 emissions in the pan-Arctic; 3) high-resolution nested grid inversions improve the performance of inverse modeling; and 4) there could be large spatial scale CH_4 emissions from pan-Arctic lakes in some specific regions.

Specific Comments

Abstract, line 13: "Canadian and Siberian lakes contribute most of the estimated lake emissions" What do you mean here, to Global or Arctic lake emissions?

Response: We mean that "Canadian and Siberian lakes contributed most of the estimated CH_4 emissions from pan-Arctic lakes."

Page 32475, equation 2: where does "XCO2" come from?

Response: The XCO_2 comes from the CarbonTracker CO_2 measurement and modeling system. We have added this information in the revision.

Page 32479, line 16: The Southern bound of the Arctic nested grid is 56N. Does this mean that all reported total fluxes from the nested grid inversion represent fluxes northward of

56N? In several places there is mentioning of 60N, and somewhere even 50N. Confusion should be avoided on what is called "Arctic".

Response: Although the inversions were conducted northward of 56°N, only emissions northward of 60°N were analyzed. In the revision, we changed "Arctic" to "pan-Arctic" and defined "pan-Arctic" as a region northward of 60°N. For the place 50°N, it is because the cited study does not calculate methane emissions from 60°N separately. In that case, we have not tried to imply the emissions from 60°N and 50°N should agree.

Page 32483, line 25: Why is this condition restricted to measurements between 50S and 50N? It hints at something that requires further specification. In the studies by Bergamaschi et al and Houweling et al, SCIAMACHY retrievals are filtered out outside this latitude interval. Figure S1, indicates that higher latitude measurements are used in this study, although this line 25 suggests that data are treated differently. This should be clarified.

Response: Following Bergamaschi et al. (2009) and Houweling et al. (2014), we also filtered out measurements outside 50°S and 50°N because in these regions SCIAMACHY only delivered good-quality retrievals in local summer times and we run whole-year inversion at the global scale. Before, we applied the regression relationship of Fig. 1c to the pan-Arctic inversions. We realized that it could be problematic. In this revision, following the method of Wecht et al. (2014), we used aircraft campaign measurements from Alaska, Canada and Siberia to calculate a linear regression between bias and specific humidity. This relationship was then applied to all nested grid inversions. We showed this new regression and aircraft campaign sites in Fig. 2 and 3.

Wecht, K. J., Jacob, D. J., Frankenberg, C., Jiang, Z. and Blake, D. R.: Mapping of North American methane emissions with high spatial resolution by inversion of SCIAMACHY satellite data, J. Geophys. Res. Atmos., 119, 7741–7756, doi:10.1002/2014JD021551, 2014.

Page 32486, line 8: "this suggests that the global emissions . . ." It should be noted here that the convergence of global totals relies on the assumed atmospheric lifetime being correct. There is no mentioning that atmospheric sinks are optimized. If they were, then the measurement constraint on the global total emission would have been substantially less.

Response: We have added this assumption into the sentence: "This convergence probably suggests that surface measurements from the NOAA/ESRL network are of sufficient density and accuracy to represent the global CH_4 burden if the CH_4 lifetime is correct".

Page 32487, line 24: "They probably underestimated . . ." This difference could be caused by a different assumption on the methane lifetime, the uncertainty of which may well exceed 10 TgCH4/yr.

Response: You are right. We have changed the tongue of this sentence.

Page 32488, line 4: "This adjustment could be primarily driven . . ." Then a list follows of every element in the inversion that influences the a priori fluxes. Therefore, effectively this sentence doesn't say anything. However, it would actually be interesting to know the relative importance, for example, of the satellite and surface data. This has been studied in the past by others for the global domain, but not specifically for the Arctic sub domain.

Response: As our focus is on the inverse modeling of CH_4 emissions from the pan-Arctic, we did not do more work to investigate the possible reasons. But it is possibly very complex. We have deleted the sentence to reduce confusion.

Page 32490, line 11: "We conducted a nested grid inversion . . ." Somewhere in the part that follows a reference is missing to figure S3.

Response: We have added the reference to Fig. S3

Page 32493, line 27: "But our study also suggests that . . ." Here a reference is missing to Berchet et al, ACPD, 2015 (doi:10.5194/acpd-15-25477-2015).

Response: We have added this reference.

Page 32512, fig 3: It is not clear if the totals refer to Global or Arctic emission totals. Furthermore, please put the totals under the figures to improve readability.

Response: The totals refer to pan-Arctic emission totals. We have put the numbers under the wetland scenario or source names to make the figure more readable.

Page 32512: figure 3: Is the resolution of CLM4Me indeed so much lower than the other models?

Response: Yes, the CLM4Me model has a spatial resolution of 1.9° × 2.5° but many others have a spatial resolution of half degree (SDGVM has a resolution of one degree).

Page 32473, line 24: "Previous" i.o. "And previous".

Response: We have revised it.

Page 32483, line 23: "SIAMACHY"

Response: We have revised it.

Page 32489, line 3: "by that the"

Response: This sentence has been removed in the revision.

Page 32491, line 26: "the CH4 budget of"

Response: We have revised it.

Page 32492, line 24: “help”?

Response: “help transport” was replaced by “quickly transport”.

Page 32510, figure c: axis titles are missing (they should be along the axis instead of in the caption).

Response: The problem is that there is no enough space to put them; otherwise this subplot will become too small. As this figure has been move to the supplement, we chose to keep the current format.

Inverse modeling~~Mapping~~ of pan-Arctic methane emissions at high spatial resolution: ~~using~~ W~~w~~hat can we learn from assimilating satellite retrievals ~~an adjoint atmospheric transport and inversion method~~ and using different process-based wetland and lake biogeochemical models?

Zeli Tan[1,2], Qianlai Zhuang[1,2,3], Daven K. Henze[4], Christian Frankenberg[5], Ed Dlugokencky[6], Colm Sweeney[6], Alexander J. Turner[7], Motoki Sasakawa[8], Toshinobu Machida[8]

[1]Department of Earth, Atmospheric, and Planetary Sciences, Purdue University, West Lafayette, Indiana, USA

[2]Purdue Climate Change Research Center, Purdue University, West Lafayette, Indiana, USA

[3]Department of Agronomy, Purdue University, West Lafayette, Indiana, USA

[4]Department of Mechanical Engineering, University of Colorado, Boulder, Colorado, USA

[5]Jet Propulsion Laboratory/California Institute of Technology, Pasadena, California, USA

[6]Global Monitoring Division, NOAA Earth System Research Laboratory, Boulder, Colorado, USA

[7]School of Engineering and Applied Sciences, Harvard University, Cambridge, Massachusetts, USA

[8]National Institute for Environmental Studies, Tsukuba, Japan

Correspondence to: Qianlai Zhuang (qzhuang@purdue.edu)

Abstract: Understanding methane emissions from the Arctic, a fast warming carbon reservoir, is important for projecting future changes in the global methane cycle ~~under future climate scenarios~~. Here we optimized ~~Arctic~~ methane emissions north of 60°N (pan-Arctic) using~~with~~ a nested-grid high-resolution inverse model ~~by assimilating~~ that assimilates both high-precision surface measurements and column-average SCIAMACHY satellite retrievals of methane mole fraction. For the first time, methane emissions from lakes were~~are~~ integrated into an atmospheric transport and inversion estimate, together with prior wetland emissions estimated by six different biogeochemical models. In our estimates~~We find that~~, ~~the~~ in 2005, global methane emissions ~~during July 2004–June 2005 ranged from~~ were in the range of 496.4 ~~to~~ 511.5 Tg yr^{-1}~~, with wetland methane emissions ranging from 130.0 to 203.3 Tg yr^{-1}. The~~ and pan-Arctic methane emissions ~~during July 2004–June 2005~~ were in the range of 11.9–28.5 ~~14.6–30.4~~ Tg yr^{-1}~~,~~. Methane emissions from~~with~~ pan-Arctic wetlands and lakes were~~emissions ranging from 8.8 to 20.4~~5.5–14.2 Tg yr^{-1} and ~~from 5.4 to 7.9~~2.4–14.2 Tg yr^{-1}~~,~~, respectively. ~~Canadian and Siberian lakes contributed most of the estimated lake emissions.~~ Methane emissions from Siberian wetlands and lakes could be the largest and also have the largest uncertainty. Our results indicate that the uncertainty introduced by different wetland models could be much larger than the uncertainty of each inversion. We also show that assimilating satellite retrievals can reduce the uncertainty of the nested-grid inversions. The significance of lake emissions cannot be identified across the pan-Arctic by high-resolution inversions but it is possible to identify high lake emissions in some specific regions. In contrast to global inversions, high-resolution nested-grid inversions ~~can~~ perform better in estimating ~~representing~~ near surface CH_4 concentrations.~~Due to insufficient measurements in the region, Arctic methane emissions are less constrained in~~

~~northern Russia than in Alaska, northern Canada and Scandinavia. Comparison of different inversions indicates that the distribution of global and Arctic methane emissions is sensitive to prior wetland emissions. Evaluation with independent datasets shows that the global and Arctic inversions improve estimates of methane mixing ratios in boundary layer and free troposphere. The high-resolution inversions provide more details about the spatial distribution of methane emissions in the Arctic.~~

1. Introduction

Methane (CH_4) is ~~an important long-lived atmospheric trace gas. It is~~ the second most powerful carbon-based greenhouse gas in the atmosphere behind carbon dioxide (CO_2) and also plays a significant role in the cycles of ozone ~~(O_3)~~, hydroxyl radicals (OH) and stratospheric water vapor ~~(H_2O)~~ (Myhre et al., 2013; Shindell et al., 2009). The atmospheric burden of CH_4 is now more than factor of 2.5 greater than the pre-industrial value of about 700 ppb (Etheridge et al., 1998), mainly due to anthropogenic emissions. Major sources and sinks of CH_4 have been identified (Denman et al., 2007); however their quantification is still of large uncertainties~~their individual strengths~~ and the annual~~causes of the observed concentration trends~~ and inter-annual ~~variabilities~~variability~~fluctuations~~ of atmospheric CH_4 are not well explained~~known~~. For instance, scientists have not yet agreed on what caused the leveling off of atmospheric CH_4 since the

1980s (Dlugokencky et al., 2003; Bousquet et al., 2006; Aydin et al., 2011; Kai et al., 2011; Levin et al., 2012; Simpson et al., 2012; Kirschke et al., 2013) and the recent rebounding of its growth since 2007 (Rigby et al., 2008; Dlugokencky et al., 2009; Nisbet et al., 2014).

~~Given the uncertainty regarding drivers of trends in CH_4 concentrations, I~~ To reduce the quantification uncertainty of CH_4 sources and sinks ~~the research of atmospheric CH_4~~, much effort has been made ~~focused on refining~~ using Bayesian inference ~~estimates of CH_4 sources using one of two types of general approaches for estimating the contribution of individual CH_4 sources or sinks to the overall CH_4 budget~~(Bergamaschi et al., 2007, 2009, 2013; Meirink et al., 2008; Cressot et al., 2014; Houweling et al., 2014; Alexe et al., 2015)~~: "bottom-up" and "top-down" methods~~. In these studies, in-situ and/or satellite observations of CH_4 that are representative of large spatial scales were assimilated into a chemical transport model (CTM) to constrain the initial estimates of CH_4 sources and sinks that are inventoried ~~we inferred~~ from field studies, industrial investigations and biogeochemical models (Fung et al., 1991; Zhuang et al., 2004; Walter et al., 2006; Zhu et al., 2013; Tan and Zhuang, 2015a and 2015b). ~~Bottom-up estimates are scaled up from small scale studies of emissions factors (e.g., CH_4 flux) and activity data (e.g., global area that applies to the particular wetland studied) or from biogeochemical models (e.g. wetlands) with environmental conditions (Fung et al., 1991; Zhuang et al., 2004; Walter et al., 2006; Tan and Zhuang, 2015a and 2015b). In contrast, top-down estimates use in situ and satellite observations of CH_4 that are representative of large spatial scales with a chemical transport model (CTM) to infer strengths of CH_4 sources and sinks (e.g., Enting, 2002; Bergamaschi et al., 2009). In Bayesian theory, a top-down estimate can reduce uncertainty in bottom-up inventories through the use of model and ambient observations. This method, called Bayesian inference, has been successfully employed in numerous studies for estimating the~~

~~global CH_4 budget at coarse spatial resolutions (over 300 km) (Bergamaschi et al., 2007, 2009, 2013; Meirink et al., 2008; Cressot et al., 2014; Houweling et al., 2014; Alexe et al., 2015).~~ ~~Many of these studies have assimilated s~~Space-borne observations of atmospheric CH_4 ~~concentrations~~ are especially useful in inverse modeling ~~to constrain CH_4 emissions~~ because they can deliver dense and continuous coverage unachievable by surface networks or aircraft campaigns (Bergamaschi et al., 2007). There are two types of nadir satellite CH_4 retrievals: one from solar backscatter in the shortwave infrared (SWIR) and the other from thermal infrared radiation (TIR). Between them, SWIR retrievals were more widely used in atmospheric inversion of CH_4 emissions (Bergamaschi et al., 2007, 2009, 2013; Fraser et al., 2013; Cressot et al., 2014; Houweling et al., 2014; Monteil et al., 2014; Wecht et al., 2014; Alexe et al., 2015; Turner et al., 2015) because they can provide column concentrations with near-uniform vertical sensitivity down to the surface. To date, most of the inversions were operated at coarse spatial resolutions over 300 km. However, partly owing to their coarse resolutions, ~~such coarse-resolution global inversions~~it is impossible for these inversions ~~have not been able~~ to constrain ~~the strength of~~ different CH_4 sources that are spatially co-located~~and the locations of CH_4 flux hotspots~~ (Fung et al., 1991; Wecht et al., 2014). To address this issue, regional inverse models at fine spatial resolutions were developed (Miller et al., 2013; Wecht et al., 2014; Thompson et al., 2015). For example, Wecht et al. (2014) and Turner et al. (2015) have used the 1/2° × 2/3° horizontal resolution GEOS-Chem adjoint model to constrain CH_4 emissions over North America.

Estimating CH_4 emissions from the Arctic is important for understanding the global carbon cycle because the fast warming of Arctic permafrost, one of the largest organic carbon reservoirs (Tarnocai et al., 2009), could lead to a rapid rise of CH_4 emissions (Zhuang et al., 2006; Walter et al., 2007; Koven et al., 2011). Natural sources dominate the Arctic CH_4

inventory (Fisher et al., 2011), e.g. wetlands (McGuire et al., 2012), lakes (Walter et al., 2006; Bastviken et al., 2011), sea shelves (Shakhova et al., 2013) and oceans (Kort et al., 2012). As the factors governing natural CH_4 production (methanogenesis) and oxidation (methanotrophy) are notoriously heterogeneous, estimates of Arctic CH_4 emissions are still poorly constrained, even with decades of site-level and modeling studies (Zhuang et al., 2004; Bastviken et al., 2011; Schuur et al., 2015; Tan and Zhuang, 2015a; Tan and Zhuang, 2015b). Previous~~And previous~~ CH_4 inversions over the Arctic only assimilated surface measurements that were too sparse to constrain~~provide constraints for~~ fine-scale CH_4 fluxes. Also, possibly important CH_4 sources that were newly identified, e.g. CH_4 emissions from Arctic lakes (Walter et al., 2006 and 2007; Bastviken et al., 2011; Tan and Zhuang, 2015a) and the East Siberian Shelf (Shakhova et al., 2013; Berchet et al., 2016) have not been included in these studies. ~~Further, an important consideration is specification of realistic prior fluxes, g~~Given the ill-posed nature of trace-gas inversions, realistic prior fluxes could be important for successful inverse modeling of CH_4 emissions from the Arctic (Kaminski and Heimann, 2001). ~~While CH_4 emissions from lakes could be of comparable magnitude to CH_4 emissions from wetlands in the Arctic (Walter et al., 2006 and 2007; Bastviken et al., 2011; Tan and Zhuang, 2015a), this source has not been included in past global or regional inverse modeling studies.~~

To address these issues, we used~~this study uses~~ the adjoint of a 3-D CTM~~chemical transport model~~ at high spatial resolution (less than 60 km) to improve the quantification of pan-Arctic CH_4 emissions in 2005. We explored the feasibility of using satellite CH_4 retrievals overpassing the pan-Arctic to further constrain regional CH_4 emissions. ~~with the integration of both process-based wetland and lake biogeochemical models and atmospheric CH_4 mixing fractions to improve the quantification of Arctic CH_4 emissions for July 2004–June 2005.~~ For the

first time, ~~we include~~ CH_4 emissions from pan-Arctic lakes were included in ~~a~~ high-resolution ~~Bayesian~~ inverse modeling~~inversion~~ of CH_4 emissions~~fluxes in the Arctic~~. As wetland emissions are likely the largest pan-Arctic CH_4 source, we also investigated~~this study also considers~~ the sensitivity of our estimates~~inversion~~ to ~~prior wetland fluxes~~the use of different wetland emission scenarios. Section 2 describes the observation data of atmospheric ~~satellite retrievals and surface~~ CH_4 ~~observations~~ that were~~are~~ used to infer CH_4 emissions~~fluxes~~ and evaluate posterior estimates. Section 3 ~~describes the details of~~ details the wetland and lake biogeochemical models that were used in this study~~for wetland and lake emissions~~ (Section 3.1), the pan-Arctic nested-grid CTM~~chemical transport model and the prior budgets of other CH_4 sources and sinks~~ (Section 3.2), and the adjoint-based inversion method (Section 3.3). Section 4 presents the posterior CH_4 emissions, ~~and~~ their evaluation and further discussion.

2. Observations

2.1. Satellite Retrievals

SWIR CH_4 retrievals are available from SCanning Imaging Absorption spectroMeter for Atmospheric CHartogrphY (SCAMACHY) for 2003–2012 (Frankenberg et al., 2006, 2008, 2011) and Greenhouse Gases Observing SATellite (GOSAT) for 2009 to present (Parker et al., 2011). SCIAMACHY, aboard the European Space Agency's environmental research satellite ENVISAT retrieves column-averaged CH_4 mixing ratios (XCH_4) from the SWIR nadir spectra (channel 6: 1.66–1.67 μm) using the IMAP-DOAS algorithm (Frankenberg et al., 2006, 2008, 2011). The satellite operates in a near polar, sun-synchronous orbit at an altitude of 800 km. At channel 6, the ground pixel size of the retrievals is about 30 km (along-track) × 60 km (across-track). We use version 6.0 proxy CH_4 retrievals from Frankenberg et al. (2011) that provide a weighted

column average dry-mole fraction of CH_4 with 10-layer averaging kernels and prior CH_4 profiles. The averaging kernels show near-uniform vertical sensitivity in the troposphere and declining sensitivity above the tropopause (Butz et al., 2010). Some auxiliary data, e.g. the air mass factor A_F ($A_F = 1/\cos\theta + 1/\cos\xi$, where θ is the solar zenith angle and ξ is the viewing angle of the satellite), water column density and dry air column density, are also published with the IMAP-DOAS v6.0 XCH_4 product.

The estimated single-retrieval precision is scene-dependent and averages roughly 1.5% or 25 ppb (Frankenberg et al., 2011). With this order of instrument precision, SCIAMACHY cannot resolve day-to-day variability of emissions but can strongly constrain a multi-year average (Turner et al., 2015). The retrieving algorithm firstly calculates CH_4 total column density Ω_{CH4} (molecules cm^{-2}):

$$\Omega_{CH_4} = \Omega_{\mathbf{A}} + \mathbf{a}^{\mathrm{T}}\left(\omega - \omega_{\mathbf{A}}\right) \qquad (1)$$

where ω is the true 10-layer sub-column densities of CH_4 (molecules cm^{-2}), $\omega_{\mathbf{A}}$ is the 10-layer prior CH_4 sub-column density (molecules cm^{-2}), $\Omega_{\mathbf{A}}$ is the corresponding a priori CH_4 total column density, and **a** is an averaging kernel vector that defines the sensitivity of the retrieved total column to each sub-column in ω. To account for the impact of aerosol scattering and instrument effects on the observed light path, Frankenberg et al. (2006) used the CO_2 column density Ω_{CO2} as a proxy to normalize and convert Ω_{CH4} to a column mixing ratio XCH_4 (ppb):

$$XCH_4 = \left(\Omega_{CH_4}/\Omega_{CO_2}\right) XCO_2 \qquad (2)$$

where XCO_2 is the column-weighted mixing ratio of CO_2 from NOAA's CarbonTracker CO_2 measurement and modeling system. CO_2 is used as a proxy because it is retrieved in a spectrally

neighboring fitting window and, relative to CH_4, its mixing ratio is known with much higher precision.

~~As general retrieval quality deteriorates after November 2005 due to the dysfunction of two important detector pixels (Frankenberg et al., 2011), only observations during the period of January 2003 to October 2005 are used.~~ The quality of SCIAMACHY observations is controlled by a filtering scheme that selects only daytime, over land and with cloud free or partially cloud scenes and good fitting accuracy (http://www.temis.nl/climate/docs/TEMIS_SCIA_CH4_IMAPv60_PSD_v2_6.pdf). Further, a surface elevation filter is applied to filter out observations that are different from the model grids at surface altitude by more than 250 m (Bergamaschi et al., 2009; Alexe et al., 2015). This filtering process ensures that the atmospheric columns seen by SCIAMACHY are well represented by the model columns. To avoid spurious outliers that may have a large impact on the inversion, XCH_4 retrievals of less than 1500 ppb or larger than 2500 ppb are discarded (Alexe et al., 2015). For the pan-Arctic, most of qualified XCH_4 retrievals were recorded in the summer time when local solar zenith angles are higher, surface reflectance is lower and impact of Arctic vortex is smaller. Fig. 1~~S1~~ shows the SCIAMACHY retrievals (n = 3774~~3989~~) of the weighted column-average CH_4 dry mixing ratio for July 2005~~4~~–September 2005~~4~~ in the pan-Arctic that have passed all quality control tests.

2.2. Surface Observations

The NOAA/ESRL Carbon Cycle Cooperative Global Air Sampling Network provides high-precision weekly flask measurements of surface atmospheric CH_4 dry-air mole fraction (Dlugokencky et al., 2014)~~. CH_4 measurements~~ that were calibrated against the WMO X2004 CH_4 standard scale maintained at NOAA (Dlugokencky et al., 2005). Due to the coarse

resolution of the GEOS-Chem model, we include only marine and continental background sites and exclude sites that are strongly influenced by sub-grid local sources (Alexe et al., 2015), as listed in Table S1. The flask-air samples in the NOAA/ESRL network that were taken from regular ship cruises in Pacific Ocean serve to evaluate simulated surface mixing ratios of global inversions over the remote ocean and downwind the continental sources (Alexe et al., 2015). Fig. 1 shows~~One~~ the Arctic sites that were used for data assimilation and nested-grid inversion evaluation. ~~(Pallas-Sammaltunturi, Finland (PAL)) that was excluded from the assimilation is used to evaluate the nested-grid inversions~~.

2.3. Aircraft Campaign Observations

To derive the bias of SCIAMACHY CH_4 retrievals overpassing the pan-Arctic and evaluate the~~The~~ modeled CH_4 vertical profiles in the troposphere, we used CH_4 measurements that were collected by three aircraft campaigns: ~~are evaluated by~~ the NOAA/ESRL Carbon Cycle Cooperative Global Air Sampling Network's aircraft program (http://www.esrl.noaa.gov/gmd/ccgg/aircraft/data.html; Sweeney et al., 2015), the National Institute for Environmental Studies (NIES) aircraft program (Machida et al., 2001; Sasakawa et al., 2013), and the NASA's Arctic Research of the Composition of the Troposphere from Aircraft and Satellite (ARCTAS) mission. For the NOAA/ESRL aircraft mission~~observations~~, CH_4 was routinely collected using 0.7 L silicate glass flasks on planned flights with maximum altitude limits of 300–350 hPa. The sampling vertical resolution is up to 400 m in the boundary layer and all samples were analyzed by NOAA/ESRL in Boulder, Colorado. For the NIES aircraft mission, air samples were collected in 550 mL glass flasks over Surgut, West Siberia (61.5°N, 73.0°E) at altitude ranging from 0.5 to 7 km with 0.5–1.5 km intervals. The precision of gas chromatograph analysis for CH_4 measurement was estimated to be 1.7 ppb and the NIES-94

scale used in analysis was higher than the NOAA/GMD scale by 3.5–4.6 ppb in a range of 1750–1840 ppb. In ARCTAS, CH_4 was measured over northern Canada by the DACOM tunable diode laser instrument with an estimated accuracy/precision of 1%/0.1%. Central locations of their flights in the pan-Arctic are shown in Fig. 1. Table S2 lists the locations and profiles of the NOAA/ESRL aircraft mission flights used in evaluation.

3. Modeling

Here we describe the prior emissions, the forward model, and the inversion method used to optimize CH_4 emissions in the pan-Arctic on the basis of SCIAMACHY and NOAA/ESRL observations.

3.1. Wetland and Lake CH_4 Emissions

CH_4 emissions estimated by the inverse modeling method can be sensitive to the choice of prior wetland CH_4 fluxes (Bergamaschi, 2007). To assess this sensitivity, we used wetland CH_4 emissions simulated by six well-known wetland biogeochemical models (CLM4Me, DLEM, LPJ-Bern, LPJ-WSL, ORCHIDEE and SDGVM) to setup six different inverse modeling experiments~~our inverse model~~. All wetland CH_4 simulations follow the same protocol of WETland and Wetland CH_4 Inter-comparison of Models Project (WETCHIMP) as described in ~~(~~Melton et al.~~,~~ (2013)~~);~~ and Wania et al.~~,~~ (2013). Melton et al. (2013) demonstrated that the difference of these estimates primarily arises from the model distinction in CH_4 biogeochemistry and wetland hydrology. These models estimated that the annual global CH_4 emissions from wetlands during 2004–2005 were in the range of 121.7–278.1 Tg yr^{-1} (Fig. S1~~2 and Table 2~~) and wetland CH_4 emissions are the highest in tropical regions (e.g., Amazon, Southeast Asia and Tropical Africa) where extensive floodplains and warm environment coexist. In the pan-Arctic,

the modeled annual wetland CH_4 emissions in 2005~~during 2004–2005~~ were in the range of 9.1~~11.4~~–20.9~~25.6~~ Tg yr^{-1} (Fig. 2~~3 and Table 3~~), and their spatial distribution was mainly controlled by the modeled or mapped wetland coverage (Melton et al., 2013). As shown in Fig. 2~~3~~, because of some consistency in simulating wetland hydrology, nearly all models suggest that there are~~were~~ high CH_4 fluxes in West Siberia Lowlands, Finland and Canadian Shield. ~~As our focus is on 2004–2005, we only use one wetland emission scenario from LPJ-WSL in our inverse model during 1993–2003 to construct initial conditions. As presented in Fig. S2, before optimization, this prior wetland scenario gives the best fit between GEOS-Chem modeled CH_4 and GLOBALVIEW-CH4 (GLOBALVIEW-CH4, 2009).~~

Lakes, permanent still-water bodies without direct connection to the sea, are abundant in the pan-Arctic (Lehner and Döll, 2004). Recent studies indicated that pan-Arctic lakes could contribute a significant amount of CH_4 to the atmosphere (Walter et al., 2006; Tan and Zhuang, 2015a) and the emissions could be driven by factors different from wetland emissions, e.g. the supply of labile yedoma permafrost carbon (Walter et al., 2006) and water deep mixing (Schubert et al., 2012). Because the WETCHIMP models cannot account for this source, ~~The biogeochemical models involved in the WETCHIMP project have not included CH_4 emissions from lakes. As CH_4 emissions from pan-Arctic lakes could be significant (Walter et al., 2006; Tan and Zhuang, 2015a) and have different drivers relative to wetland emissions, e.g. the supply of labile yedoma permafrost carbon (Walter et al., 2006) and water deep mixing (Schubert et al., 2012), it is necessary to include this source into the Arctic CH_4 inventory.~~ we ~~instead Prior~~prior ~~CH_4 emissions from pan-Arctic lakes are simulated~~ used~~with~~ a one-dimension process-based lake biogeochemical model, bLake4Me, to simulate CH_4 emissions from pan-Arctic lakes (Tan et al., 2015; Tan and Zhuang, 2015a). The bLake4Me model explicitly parameterizes the control

of temperature and carbon substrate availability on methanogenesis, the control of temperature and oxygen level on methanotrophy and the transport of gaseous CH_4 by diffusion and ebullition. ~~The model also includes two thermal modules, governing the heat transport and water phase change in both water and sediments column of lakes.~~ A detailed model description and evaluation can be found~~is given~~ in Tan et al. (2015). Model quantification~~estimates~~ of CH_4 emissions from all lakes north of 60°N was~~are~~ described by Tan and Zhuang (2015a and 2015b). On average, the estimated CH_4 emissions from pan-Arctic lakes during the studied period are approximately 11 Tg CH_4 yr^{-1}, see Fig. 2~~3~~.

3.2. GEOS-Chem Model

Atmospheric CH_4 mole fractions are simulated by GEOS-Chem v9-01-03 (http://acmg.seas.harvard.edu/geos/index.html), a global 3-D CTM model (Bey et al., 2001). For the period of 2004–2005, GEOS-Chem ~~could be~~ is driven by ~~either GEOS-4 or~~ GEOS-5 meteorological (met) data from NASA's Global Modeling Assimilation Office (GMAO). ~~As GEOS-5 is available only from December 2003, in this study we use GEOS-4 met data from 1993 to 2005 for inverse simulations when only surface measurements are assimilated and GEOS-5 met data from 2004 to 2005 for inverse simulations when both satellite retrievals and surface measurements are assimilated. Both the GEOS-4 and~~ The GEOS-5 met data have horizontal resolution of 1/2° latitude × 2/3° longitude~~, and 6-hour~~ temporal resolution of 6 hours and ~~. There are 55 and~~ 72 hybrid sigma-pressure levels extending from Earth's surface to 0.01 hPa ~~for GEOS-4 and GEOS-5 met data respectively~~. In contrast to the global GEOS-Chem model, the nested-grid version does not include~~contain~~ algorithms for handling advection near the North and South Poles (Lin and Rood, 1996). To avoid polar grid boxes, we crop the native 1/2° × 2/3° resolution GEOS-5 met data to a window region (180°W–180°E and 80°N–56°N) for

the pan-Arctic ~~the Arctic~~ nested grid. To make it consistent with the bLake4Me model, only CH_4 emissions north of 60°N are ~~would be~~ analyzed. We expect that the avoidance of the North Pole only has a minor impact on our inversions because according to Miyazaki et al. (2008) the Northern Hemisphere (NH) extratropics during summer has slow mean-meridional circulation and inactive wave activity but strong vertical transport. Boundary conditions for nested grid simulations are produced using ~~for the same period with~~ ~~by~~ the same period GEOS-Chem 4° × 5° resolution global scale forward runs at 3-hour intervals.

The GEOS-Chem CH_4 simulation was originally introduced by Wang et al. (2004) and updated by Pickett-Heaps et al. (2011). As described by Wecht et al. (2014), the prior anthropogenic sources, including oil/gas production, coal mining, livestock, waste treatment, rice paddies, biofuel burning and other processes, were~~are~~ extracted from Emission Database for Global Atmospheric Research v4.2 (EDGAR4.2) with 0.1° × 0.1° resolution and no seasonality (European Commission, Joint Research Centre/Netherlands Environmental Assessment Agency, 2009). CH_4 emissions from termites and biomass burning were~~are~~ obtained from the study of Fung et al. (1991) and daily Global Fire Emissions Database Version 3 (GFED3) ~~(~~of van der Werf et al.~~,~~ (2010), respectively. CH_4 emissions from wetlands and lakes ~~are from the model simulations~~ were simulated by biogeochemical models described in Section 3.1. Atmospheric CH_4 is mainly removed by tropospheric oxidation initiated by reaction with tropospheric OH, which was computed using a 3-D OH climatology of monthly average concentrations from a previous simulation of tropospheric chemistry (Park et al., 2004). The global mean pressure-weighted tropospheric OH concentration is 10.8×10^5 molecules cm^{-3}. For minor sinks, CH_4 uptake by upland soils was~~is~~ derived from Fung et al. (1991) and CH_4 oxidation in the stratosphere was~~is~~ calculated from the archived CH_4 loss frequency described by Murray et al.

(2012). The resulting atmospheric lifetime of CH_4 is about 8.9 years, consistent with the observational constraint of 9.1±0.9 years (Prather et al., 2012). We regridded and cropped the anthropogenic and natural CH_4 emissions in EDGAR4.2, GFED3 and Fung et al. (1991) for ourthe nested pan-Arctic domain using the Harvard-NASA Emissions Component (HEMCO) software (Keller et al., 2014), marked as "other" in Fig. 23. Compared to CH_4 emissions from natural sourcesArctic wetlands and lakes, these emissionssources are relatively small in 2005 (~2.13.2 Tg yr^{-1}).

3.3. Inversion Method

Atmospheric inversion is a procedure for using observations of atmospheric gases as constraints to estimate surface gas fluxes. The inverse problem can be characterized by solution of

$$\mathbf{y} = \mathbf{F}(\mathbf{x}) + \varepsilon \qquad (3)$$

By applying Bayesian theorem and assuming Gaussian errors, the inverse problem can be solved by minimizing the cost function, $J(\mathbf{x})$, that measures the model deviations from both prior assumptions and observations (Enting et al., 2002; Kopacz et al., 2009):

$$J(\mathbf{x}) = (\mathbf{F}(\mathbf{x}) - \mathbf{y})^{\mathrm{T}} \mathbf{C}_{\mathrm{d}}^{-1} (\mathbf{F}(\mathbf{x}) - \mathbf{y}) + \gamma (\mathbf{x} - \mathbf{x}_0)^{\mathrm{T}} \mathbf{C}_{\mathbf{x}_0}^{-1} (\mathbf{x} - \mathbf{x}_0) \qquad (4)$$

where $\mathbf{y}$ is a vector of observations from SCIAMACHY and NOAA/ESRL, $\mathbf{F}$ is a model operator that maps emissions to observations, $\mathbf{x}$ represents CH_4 emissions to be constrained, $\mathbf{x}_0$ is the a priori estimate of $\mathbf{x}$, $\mathbf{C}_{\mathrm{d}}$ is the observational error covariance matrix that includes contributions from model error, representation error (sampling mismatch between observations and the model) and measurement error, and $\mathbf{C}_{\mathbf{x}_0}$ is the parameter error covariance matrix (containing the uncertainties of the parameters and their correlations). The regularization parameter γ controls

the relative constraints applied by the observational and a priori parts of $J(\mathbf{x})$ (Kopacz et al., 2009). In the adjoint method, γ is not fixed at unity but determined by analyzing its influence on the minimum of $J(\mathbf{x})$ (Henze et al., 2007; Kopacz et al., 2009).

Minimization of $J(\mathbf{x})$ yields the following expression for the maximum a posteriori solution for the state vector ~~(~~ $\hat{\mathbf{x}}$ ~~)~~ and its associated error covariance ~~(~~ $\hat{\mathbf{C}}_{\mathbf{x}}$ ~~)~~ (Rodgers, 2000):

$$\hat{\mathbf{x}} = \mathbf{x}_0 + \left(\left(\nabla_{\mathbf{x}} \mathbf{F} \right)^{\mathrm{T}} \mathbf{C}_{\mathrm{d}}^{-1} \nabla_{\mathbf{x}} \mathbf{F} + \gamma \mathbf{C}_{\mathbf{x}_0}^{-1} \right)^{-1} \left(\nabla_{\mathbf{x}} \mathbf{F} \right)^{\mathrm{T}} \mathbf{C}_{\mathrm{d}}^{-1} \left(\mathbf{y} - \mathbf{F}\left(\mathbf{x}_0 \right) \right) \quad (5)$$

$$\hat{\mathbf{C}}_{\mathbf{x}}^{-1} = \left(\nabla_{\mathbf{x}} \mathbf{F} \right)^{\mathrm{T}} \mathbf{C}_{\mathrm{d}}^{-1} \nabla_{\mathbf{x}} \mathbf{F} + \gamma \mathbf{C}_{\mathbf{x}_0}^{-1} \quad (6)$$

where $\nabla_{\mathbf{x}} \mathbf{F}$ is the Jacobian matrix of the forward model. $J(\mathbf{x})$ is minimized iteratively through successive forward and backward simulations with the GEOS-Chem model and its adjoint, developed by Henze et al. (2007) and previously applied to CO, CO_2 and CH_4 source inversions (Jiang et al., 2011; Deng et al., 2014; Wecht et al., 2014). The GEOS-Chem adjoint model is a 4DVAR inverse modeling system that allows optimization of a very large number of parameters using at the same time very large sets of observational data, such as satellite data. Rather than optimizing CH_4 emissions directly, it optimizes an exponential scale factor $\mathbf{e_x}$ ($\mathbf{e_x} = \ln\left(\mathbf{x}/\mathbf{x}_0 \right)$) at each grid cell to avoid negative emissions. The posterior error covariance $\hat{\mathbf{C}}_{\mathbf{x}}$ could be approximated by the Davidon-Fletcher-Powell (DFP) or the Limited-memory Broyden–Fletcher–Goldfarb–Shanno (L-BFGS) optimization algorithm (Singh et al., 2011; Deng et al., 2014). But the performances of these deterministic methods are usually not promising, subjecting to the choice of initial Hessian, so-called preconditioning (Bousserez et al., 2015). In contrast, approximating $\hat{\mathbf{C}}_{\mathbf{x}}$ by stochastic methods, i.e. Monte-Carlo sampling and Gradient-based randomization, could help avoid the impact of setting initial Hessian (Bousserez et al., 2015). For example, Bousserez et al. (2015) demonstrated that for high-dimensional inverse problems using

a Monte Carlo stochastic approach that samples ensemble members by perturbing x_0 and y in line with $\mathbf{C}_{x_0}$ and $\mathbf{C}_d$ respectively, could guarantee a low relative error (10%) in the variance with as few as 50 members. In this study, the posterior uncertainty of nested-grid inversions was estimated using this method.

For prior emissions, their uncertainties were~~are~~ set as 100% in each grid box and ~~the~~ spatial correlation was~~is~~ set as an e-folding function with spatial correlation lengths of 500 km at the global ~~coarse~~ 4° × 5° resolution ~~(4° × 5°)~~ and of 300 km at the nested grid 1/2° × 2/3° resolution ~~(1/2° × 2/3°)~~ (Bergamaschi et al., 2009). Six global coarse-resolution inversions using different wetland emission scenarios and assimilating both surface CH_4 measurements and satellite CH_4 retrievals were performed during the period of 2005/01–2005/12. These inversions provided boundary conditions for the following nested-grid inversions. For 1/2° × 2/3° nested-grid inversions, we ran the adjoint model for 50 times over the period of 2005/07–2005/09 for each of twelve scenarios: six wetland scenarios by two data assimilation scenarios. The two data assimilation scenarios include one scenario assimilating only NOAA/ESRL measurements and another scenario assimilating both NOAA/ESRL measurements and SCIAMACHY retrievals. As described above, the 50-member ensemble run is for the calculation of posterior estimate uncertainty. The steps to construct optimal initial conditions for global and nested inversions are described in the supplementary materials. ~~Optimization is performed in three steps. First, a global coarse-resolution inversion using the LPJ-WSL wetland scenario is run from 1993 to 2005 using surface measurements only. This inversion provides the optimized CH_4 fields for the calculation of bias correction functions and initial conditions for the next set of inversions. Next, we run six global coarse-resolution inversions using the wetland CH_4 scenarios described in Section 3.1 at two time windows: 2004/01–2004/12 and 2004/07–2005/06. In these global~~

~~inversions, both surface measurements and satellite retrievals are assimilated. The inverse modeling at the 1st time block servers as a spin-up period and the analysis time period is from July 2004 to June 2005 (Deng et al., 2014; Alexe et al., 2015). Besides optimizing global CH_4 fluxes, the global inversions also provide boundary conditions for our nested grid inversions. Following Turner et al. (2015), we construct time-dependent boundary conditions for the nested simulations of the adjoint model from the forward model at 4° × 5° horizontal resolution using the posterior emissions from a global inversion performed first. This is different from the method of Wecht et al. (2014) where both emissions and boundary conditions were optimized by minimizing two separate cost functions iteratively. The last step is thus to run nested grid inversions in the Arctic at 1/2° × 2/3° resolution to optimize Arctic CH_4 emissions. The modeling period is from June 24, 2004 to Oct 1, 2004 and the real analysis time is from July 1, 2004 to Oct 1, 2004.~~ As in Wecht et al. (2014), observations in the first week were not~~are not~~ assimilated and each optimization was run iteratively at least 40 times until the reduction of its cost function became less than 0.5% with each successive iteration. ~~This time period is selected based on two factors. First, due to snow cover and large solar zenith angle, the quality of SCIAMACHY retrievals in winter is usually low. Second, CH_4 fluxes from pan-Arctic wetlands and lakes are the most pronounced in summer.~~ In the GEOS-Chem adjoint model~~all steps~~, optimization changes its course automatically if local minimum reaches~~is run iteratively at least 40 times until the reduction of the cost function becomes less than 0.5% with each successive iteration (Wecht et al., 2014)~~.

3.4. Satellite Retrieval Bias Correction

The importance of bias correction for ~~to~~ the assimilation of satellite retrievals ~~in inversion of CH_4 fluxes~~ has been discussed~~emphasized~~ in many earlier studies (Bergamaschi et al., 2007,

2009, 2013; Fraser et al., 2013; Cressot et al., 2014; Houweling et al., 2014; Wecht et al., 2014; Alexe et al., 2015; Turner et al., 2015). Usually, these studies represented satellite retrieval bias as a regression function of one proxy parameter, ~~These methods relied on regression between a proxy parameter (~~i.e.~~,~~ latitude, air mass factor or specific humidity~~) and retrieval bias~~. Air mass factor was used as a proxy parameter by some studies due to its correlation to spectroscopic errors and residual aerosol errors ~~Air mass factor was chosen because of the co-variation of spectroscopic errors with the sampled air mass and residual aerosol errors~~ (Cressot et al., 2014; Houweling et al., 2014) and specific humidity was used~~chosen~~ because water vapor is the main cause of SCIAMACHY seasonal bias that lags the variations of solar zenith angle (Houweling et al., 2014). Relative to air mass factor and humidity, ~~Many studies used seasonal and latitudinally varying functions for bias correction~~ because latitude~~they~~ can represent the changes in both solar zenith angle and climate variables (Bergamaschi et al., 2007, 2009, 2013), it was used by more studies. Considering that different proxies can account for different errors, the system bias of satellites may be better represented by multiple proxy parameters~~It is likely that retrieval bias can be better represented if the effects of air mass change and climate system change can be accounted for together~~.

To test this hypothesis, we compared the performance~~s~~ of three traditional one-proxy methods (latitude φ, air mass factor A_F, specific humidity H_S) and two new two-proxy methods (latitude + humidity, air mass factor + humidity), listed in Table 1. These methods were evaluated using two reference values: the difference between the satellite-retrieved and the GEOS-Chem modeled CH_4 column mixing ratios and the Bayesian Information Criterion (BIC) score. The BIC criterion is widely used for regression model selection and aims to award a model that fit measurements with the least model parameters. ~~After constraining the GEOS-~~

~~Chem model with surface measurements, t~~In the study, we would select the bias correction method that gives the smallest difference ~~between the measured and modeled CH_4 column mixing ratios~~ and the lowest ~~Bayesian Information Criterion (BIC)~~ BIC score ~~will be used~~. ~~Specific humidity is taken from the European Centre for Medium-Range Weather Forecasts (ECMWF)'s ERA-20C reanalysis product (http://apps.ecmwf.int/datasets/data/era20c-daily), averaged by the column between the surface and 3 km altitude (Houweling et al., 2014). The air mass factor and central latitude of CH_4 retrievals are directly available in the SCIAMACHY IMAP v6.0. For bias correction, we first optimize the GEOS-Chem 4-D CH_4 mixing ratios by an inversion using surface measurements and then sample the modeled XCH_4 at the coordinates and time of SCIAMACHY retrievals and with local averaging kernels applied. The difference between SIAMACHY and GEOS-Chem values (Fig. 1a) is regressed with proxy factors to obtain the optimal bias correction. As suggested by Turner et al. (2015), it is more likely that grid squares between 50°S and 50°N with residual standard deviation (RSD) in excess of 20 ppb are dominated by model bias in prior emissions. Thus, we exclude such grid squares in regressions. Further, satellite retrievals with low precisions (the ratio of retrieval precision error to retrieval is larger than 3%) are removed from analysis.~~ In our experiments, all bias correction functions were~~are~~ updated monthly. ~~Unlike Bergamaschi et al. (2009), we do not further optimize bias correction functions in the inversion cycle because such an optimization could make bias correction account for the uncertainties that should not be dealt with by correction, e.g. unaccounted model errors or even the sources and sinks (Houweling et al., 2014).~~ As listed in Table 1, the "latitude only" correction performs the best among~~within~~ the three single~~-~~-proxy correction methods and is only slightly worse than the ~~best correction method~~ "latitude + humidity" correction method~~in our test~~. The "air mass factor only" method does not work as well

in our experiment. Turner et al. (2015) suggested that it could be attributed to a potential bias in the GEOS-Chem simulation of CH_4 in the polar stratosphere. ~~This implies that the latitude polynomial correction used in most previous CH_4 inversions is appropriate.~~ As the "latitude + humidity" method~~-~~ has the smallest model-data differencet~~et~~ and the lowest BIC score~~performs the best~~, we applied it ~~is applied~~ for satellite bias correction in all global inversions~~this study~~.

For SCIAMACHY retrievals overpassing the pan-Arctic, because the modeled atmospheric CH_4 could be less reliable, we used another bias correction method. According to a comparison between SCIAMACHY and the high-precision Total Carbon Column Observing Network (TCCON) measurements, the system bias of SCIAMACHY retrievals could be closely correlated with specific humidity averaged over the lowest 3 km of the atmosphere (Houweling et al., 2014). And Wecht et al. (2014) has demonstrated that this humidity-proxy method shows promising performance in debiasing SCIAMACHY retrievals overpassing North America. In this study, we sought a similar linear regression relationship between SCIAMACHY bias and specific humidity. First, we detected the SCIAMACHY bias by comparing SCIAMACHY retrievals with CH_4 vertical profiles measured by the NOAA/ESRL aircraft mission over Alaska, USA, the NIES aircraft mission over Siberia, Russia and the NASA/ARCTAS aircraft mission over Alberta, Canada. Before comparison, these CH_4 vertical profiles had been mapped to the SCIAMACHY retrieval pressure grid using Eq. (1) and (2). Fig. 3 (left) shows that the retrieved system bias (ΔXCH_4) has a negative relationship with air humidity. Because the pan-Arctic is normally dry, SCIAMACHY retrievals could be lower than atmospheric CH_4 column average mixing ratios in most of days.

After bias correction, ~~we estimated~~ the error variances of SCIAMACHY ~~observations~~ retrievals were estimated ~~(Fig. 1b)~~ using the~~a~~ relative residual error (RRE) method described by

Heald et al. (2004). Fig. S2 shows the error variances of SCIAMACHY retrievals in the global scale and Fig. 3 (right) shows the error variances in the nested grid. In both global and nested grid inversions, the total error of individual SCIAMACHY retrievals is assumed to be at least 1.5% (Bergamaschi et al., 2007; Frankenberg et al., 2011). ~~Fig. 1d indicates that the correction greatly reduces model-satellite differences in tropical areas of America, Africa and South Asia and also reduces the difference in Australia and some areas of the United States. As shown in Fig. 1c, the agreement between GEOS-Chem and SCIAMACHY XCH_4 is also improved at the global scale. However, because the model-data difference in East Asia has an opposite latitude dependence to that in other areas of the same latitudes (Fig. 1a), the correction deteriorates the model-satellite agreement there (Fig. 1d).~~ The observational error of the NOAA/ESRL CH_4 mixing ratios is estimated as the sum of measurement error (~0.2%) and representation error. Similar to satellite retrievals, the representation error of surface measurements is defined as the standard deviation of ~~the difference of~~surface CH_4 concentration~~residuals~~ differences between NOAA/ESRL measurements and GEOS-Chem. ~~And the CH_4 residuals are calculated by subtracting the simulated or observed CH_4 mixing ratios by a fitted polynomial trend (Masarie and Tans, 1995).~~

4. Results and Discussion

4.1. Optimized Global CH_4 Emissions

~~As shown in Fig. 4, the posterior global and regional CH_4 emissions exhibit a strong seasonal variability during 1993–2005, which is mainly driven by the sensitivity of methanogenesis in natural sources to temperature (e.g., wetlands). During this period, there are prominently positive CH_4 emission anomalies in 1994 (+27.4 Tg CH_4) and 1998 (+34.6 Tg CH_4), and prominently negative anomalies in 1997 (−18.4 Tg CH_4), 2001 (−20.5 Tg CH_4) and 2005 (−~~

~~22.3 Tg CH_4). The 1998 CH_4 emission peak has been documented in many studies (e.g., Dlugokencky et al., 2001; Rigby et al., 2008). Dlugokencky et al. (2001) attributed this anomaly to an increase in the imbalance between CH_4 sources and sinks equal to ~24 Tg CH_4, suggested to be caused by an increase of wetland emissions in both tropical regions (13 Tg CH_4) and the Northern Hemisphere (11.6 Tg CH_4) and a severe fire year in boreal regions (5.7 Tg CH_4). However, according to Fig. 4, wetlands only contributed a small amount of emission increase during 1998 (9.1 Tg CH_4) and most of the increase was from other sources (e.g., biomass burning) in both tropical and high-latitude regions. Our findings are consistent with the claim of Langenfelds et al. (2002) that two CH_4 emission pulses in 1994 and 1998 could be linked with large biomass burning events in tropical and boreal regions. During 1993–1996, the annual mean of global CH_4 emissions was 534 Tg CH_4 yr^{-1}, slightly lower than the estimate (549±7 Tg CH_4 yr^{-1}) of Dlugokencky et al. (1998). During 1993–2005, there are no visible trends for wetland emissions in tropical, northern mid-latitude and northern high-latitude regions. Also, the annual mean of global CH_4 emissions did not change between 1993 and 2004, coinciding with the leveling off of CH_4 growth rate since the 1990s (Dlugokencky et al., 1998 & 2003). Kai et al. (2011) claimed that the evolution of CH_4 mixing ratios in the recent decades was a result of long-term reduction in agricultural emissions (i.e. rice paddies) or landfills emissions within the Northern Hemisphere. In Fig. 4b, the long-term decline of CH_4 emissions from tropical non-wetland sources seems to provide some support to this argument. But as the finding of inter-hemispheric $\delta^{13}CH_4$ is questionable (Levin et al., 2012), it is uncertain whether this declined tropical source is in the Northern Hemisphere.~~

As listed in Table 2, when both NOAA/ESRL measurements and SCIAMACHY retrievals were assimilated, the posterior estimates of total emissions in 2005 show good

convergence at a narrow range of 496.4–511.5 Tg CH_4 yr^{-1}, albeit our six prior scenarios span in a wide range (471.5–627.8 Tg CH_4 yr^{-1}). ~~The posterior global CH_4 emissions using both NOAA/ESRL and SCIAMACHY observations and different prior wetland scenarios are shown in Fig. 5 and also listed in Table 2. Since total emissions are constrained by the atmospheric burden of CH_4 and the CH_4 lifetime, while the prior CH_4 fluxes in six scenarios are different in a wide range of estimates (471.5–627.8 Tg CH_4 yr^{-1}), the posterior global CH_4 emissions converge into a very narrow zone (496.4–511.5 Tg CH_4 yr^{-1}).~~ Because the total of global emissions is constrained by the atmospheric CH_4 burden and lifetime, this~~This~~ convergence probably suggests that ~~the~~ surface measurements from the NOAA/ESRL network~~observations~~ are of sufficient density and accuracy to represent the global CH_4 burden~~constrain the global emissions~~ if ~~assuming~~ the CH_4 lifetime is ~~being~~ correct. ~~However,~~ In contrast, the posterior CH_4 emissions differ largely between different wetland emission scenarios in the TransCom3 land regions. For example, in the DLEM inversion, the estimated CH_4 emissions from the Eurasian temperate region are as large as 146.1 Tg CH_4 yr^{-1}. But in the CLM inversion, the total of these emissions is only 84.9 Tg CH_4 yr^{-1}. Also, for CH_4 emissions from the South American tropical region, the estimate is 31.4 Tg CH_4 yr^{-1} in the DLEM inversion but nearly two times larger (62.3 Tg CH_4 yr^{-1}) in the SDGVM inversion. There are several possible explanations for the large differences between the scenarios: high-precision surface measurements could be not of sufficient density in regional scales, satellite retrievals could be not of sufficient accuracy, and the GEOS-Chem model and its priors could be not of high temporal and spatial resolutions to resolve satellite retrievals.~~there are still not enough high-precision measurements at regional scales, resulting in large differences between the posterior emissions in the TransCom3 land regions (Table 2).~~ A

detailed comparison between our estimates and previous inversion studies at the global scale is presented in the supplementary materials.

~~There have been many studies that assimilated surface and/or satellite observations into a CTM inverse model to constrain global CH_4 fluxes, see Kirschke et al. (2013) for review. For instance, using the same observations suite, Bergamaschi et al. (2009) estimated that in 2004, CH_4 emissions in global, tropical (30°S–30°N), northern extratropical (30°N–90°N) and southern extratropical (90°S–30°S) zonal areas were 506.7 Tg CH_4 yr^{-1}, 323.5 Tg CH_4 yr^{-1}, 172.8 Tg CH_4 yr^{-1} and 10.4 Tg CH_4 yr^{-1}, respectively. These large-scale estimates are consistent with our calculations: 284.5–319.6 Tg CH_4 yr^{-1} (tropical), 165.3–206.6 Tg CH_4 yr^{-1} (northern extratropical) and 10.0–13.9 Tg CH_4 yr^{-1} (southern extratropical). This agreement reflects that GEOS-Chem adjoint and TM5-4DVAR are consistent in the atmospheric transport, chemistry and inverse modeling methods. In contrast to Bergamaschi et al. (2009), our inversions tend to allocate more emissions to extratropical regions. As a result, the tropical total (SATr + NAF + SAF + TrA) of the six inversions is in the range of 114.1–169.7 Tg CH_4 yr^{-1}, which is much lower than their estimate of 203.2 Tg CH_4 yr^{-1}. The most likely reason for this discrepancy from Bergamaschi et al. (2009) is that we use a much larger correction to the SCIAMACHY data in tropical regions. The posterior CH_4 emissions from wetlands in our four scenarios (Bern, CLM4Me, SDGVM and WSL) are close to the estimate (~161 Tg CH_4 yr^{-1}) of Bloom et al. (2010) for 2003–2007 based on CH_4 and gravity spaceborne data to constrain large-scale methanogenesis. Our estimates are also close to the inferred CH_4 emissions (175±33 Tg CH_4 yr^{-1}) from natural wetlands by Kirschke et al. (2013). By using artificial neural networks, Zhu et al. (2013) estimated that from 1990 to 2009, annual wetland CH_4 emissions from northern high latitudes (>45°N) are in the~~

range of 44.0–53.7 Tg CH_4 yr^{-1}, agreeing with the estimates of the Bern, CLM4Me and SDGVM scenarios.

The renewed growth of atmospheric CH_4 since 2007 has been observed by several studies (Rigby et al., 2008; Dlugokencky et al., 2009; Nisbet et al., 2014). According to Nisbet et al. (2014), the global growth rate was about 6 ppb yr^{-1} from 2007 to 2012. Assuming 1 ppb equivalent to 2.75 Tg CH_4 in the entire atmosphere (Khalil et al., 2007) and the lifetime of atmospheric CH_4 constant, the estimated global CH_4 emissions during 2010–2011 should be at most 49.5 Tg larger than the estimated during 2004–2005. The higher CH_4 emissions after 2007 were also demonstrated by other top-down studies: 539 Tg CH_4 yr^{-1} during 2009–2011 (Turner et al., 2015) and 538±15 Tg CH_4 yr^{-1} during August 2009–July 2010 (Cressot et al., 2014). When comparing the estimate of Alexe et al. (2015) for 2010–2011 with our estimates (Table 2), the difference is in the range of 29–44.1 Tg CH_4 (Table 2), consistent with these independent studies. Our estimates also agree well with the inference of Houweling et al. (2014) that global CH_4 emissions in 2004 were close to 500 Tg CH_4 yr^{-1} and the emissions rose by 27–35 Tg CH_4 yr^{-1} after July 2006. In contrast, the ensemble Kalman filter assessment in Fraser et al. (2013) involving GOSAT observations and GEOS-Chem is 510.6±18.4 Tg CH_4 yr^{-1} for the period June 2009–December 2010 (Table 2). If we assume GEOS-Chem simulated correct CH_4 sink, Theyit means Fraser et al. (2013) may probably underestimated the emissions during this period because the calculated increase from 2004 to 2009 is too low (~10 Tg CH_4 yr^{-1}).

As shown in Fig. 5a, the highest CH_4 fluxes are located in the Amazon, China, Southeast Asia, North America and Europe where extensive wetlands or large population exist. Our inversions indicate that the Eurasian temperate regions, including China, North America and Europe, emitted much more CH_4 than other regions (Table 2), showing the dominance of

~~anthropogenic sources in the global CH_4 inventory. As presented in Fig. 5c, our inverse model reduces the CH_4 emissions from China, the Amazon basin and Eurasian boreal region (scale factor < 1) but enhances the emissions in Europe and Southeast Asia (scale factor > 1) relative to the prior. This adjustment could be primarily driven by the constraints of the surface measurements and satellite retrievals and secondarily by the satellite bias correction.~~

4.2. Optimized pan-Arctic CH_4 Emissions

When using both surface measurements and satellite retrievals, our estimated CH_4 emissions over the pan-Arctic are in the range of 11.9–28.5 Tg CH_4 yr^{-1}. The simulation is the largest in the ORCHIDEE scenario and the smallest in the SDGVM scenario: 24.9±3.6 Tg CH_4 yr^{-1} and 16.1±4.2 Tg CH_4 yr^{-1}, respectively. Regionally, posterior CH_4 emissions from Alaska, northern Canada, northern Europe and Siberia are 0.3–3.4 Tg CH_4 yr^{-1}, 1.3–7.9 Tg CH_4 yr^{-1}, 0.8–8.1 Tg CH_4 yr^{-1} and 4.4–14.9 Tg CH_4 yr^{-1}, respectively. Same as the global inversions, the difference of the nested-grid inversions between different scenarios is much larger than the total uncertainty of priors and observations of each scenario: 16.6 Tg CH_4 yr^{-1} vs. 5.5 Tg CH_4 yr^{-1}. In these regions, CH_4 emissions from Siberia are more uncertain (Fig. 5), a possible indication of the lack of high-quality measurements in Siberia for assimilation. Our results also indicate that the assimilation of SCIAMACHY retrievals overpassing the pan-Arctic can reduce the estimate uncertainty. For example, for the BERN scenario, the posterior uncertainty is about 18%, much smaller than the inversion that only assimilates NOAA/ESRL measurements (27%). And for the CLM scenario, the posterior uncertainty increases from 16% to 23% when only surface measurements were assimilated. ~~In contrast to the global CH_4 inversions, total posterior CH_4 emissions from the Arctic nested-grid inversions span a wide range: 14.6–30.4 Tg CH_4 yr^{-1} (Table 3). It reflects a strong influence from both the priors (Fig. 3) and the nested-grid~~

~~boundaries (Berchet et al., 2015) on the posteriors (Fig. 6). Across six Arctic inversions, the range of the posterior is not smaller than the range of the prior (25.7–39.9 Tg CH_4 yr^{-1}) and the mean departure of the posterior from the prior is 10.1 Tg CH_4 yr^{-1}. This divergence implies that due to uncertain boundary conditions (Berchet et al., 2015), the surface and satellite observations in the Arctic cannot provide sufficient constrains to reduce the estimate uncertainty. Further, as presented in Table 3 and Fig. 6, this lack of constraint from the observations mainly occurs in Siberia and causes large uncertainties in the estimates of Siberian wetland CH_4 emissions (2.0–12.7 Tg CH_4 yr^{-1}).~~ Our estimates are consistent with other inverse modeling estimates. For example, Kirschke et al. (2013) reviewed a series of top-down estimation of CH_4 emissions and suggested that CH_4 emissions north of 60°N could be in the range of 12–28 Tg CH_4 yr^{-1}, very close to our estimate. This consistency could reflect the robustness of our nested-grid GEOS-Chem adjoint model and the good constraint of the NOAA/ESRL sites over the pan-Arctic on the atmospheric CH_4 field. Our estimates also imply that CH_4 emission from the pan-Arctic could constitute a large fraction of CH_4 emissions in the northern high latitudes (> 50°N). ~~In comparison with the inverse modeling of~~ Based on the estimate (50 Tg CH_4 yr^{-1}) of Monteil et al. (2013), we calculated that ~~we estimate that the annual total CH_4 emission from the pan-Arctic (> 60°N) is~~ 29.2-60.8% of ~~their estimate (50 Tg CH_4 yr^{-1}) for~~ CH_4 emissions in the northern high latitudes could be emitted from the pan-Arctic (> 60°N). For all scenarios, the inverse modeling adjusts total CH_4 emissions downward compared to prior emissions. It is possible that CH_4 emissions are overestimated by the biogeochemical models or double counted between the wetland and lake models or both. This adjustment could also be explained by the underestimate of CH_4 absorption by soils in biogeochemical models due to the missing of high-affinity methanotrophy (Oh et al., 2016). ~~Because all inversions estimate lower CH_4 emissions than the~~

priors, it is possible that CH_4 emissions from Arctic wetlands, lakes and other sources are overestimated by the biogeochemistry models and EDGAR dataset. In contrast to other sources, the estimated CH_4 emissions from Arctic lakes are less divergent in the nested-grid inversions except for the ORCHIDEE scenario, as presented in Fig. 7 and Table 3. There are two reasons for this convergence: 1) CH_4 fluxes from lakes are low in those poorly constrained regions, e.g. Northeastern Europe and Central Siberia, and 2) we only use one lake prior scenario in the inversions. The exception of the ORCHIDEE inversion could be explained by that the ORCHIDEE model simulates very high wetland CH_4 fluxes in Canadian Shield, West Siberia Lowlands and East Siberia Coastal Lowlands where high CH_4 fluxes from lakes are also possible (Fig. 3). For CH_4 emissions from Arctic lakes, our estimates, 5.4–7.9 Tg CH_4 yr^{-1}, are close to the lower bound of the estimate (7.1–17.3 Tg CH_4 yr^{-1}) in Bastviken et al. (2011) with upscaling site-level observations. Even if the lake source is reduced, on average, by 40% by the inversions, the remaining amounts are still much higher than the previous estimate of ~4 Tg CH_4 yr^{-1} in Gao et al. (2013). This emphasizes the importance of including pan-Arctic lakes in the carbon cycle. When the ORCHIDEE scenario is excluded, annual CH_4 emissions from lakes in Alaska, northern Canada, northern Europe and northern Siberia are, on average, 1.0 Tg CH_4 yr^{-1}, 3.1 Tg CH_4 yr^{-1}, 0.6 Tg CH_4 yr^{-1} and 2.8 Tg CH_4 yr^{-1}, respectively. These estimates correspond to 1.2 Tg CH_4 yr^{-1}, 5.0 Tg CH_4 yr^{-1}, 0.6 Tg CH_4 yr^{-1} and 5.0 Tg CH_4 yr^{-1} in Tan and Zhuang (2015a) without optimization. The posterior CH_4 emissions from lakes in northern Canada are closer to the estimate of 2.6±0.4 Tg CH_4 yr^{-1} in Tan and Zhuang (2015b) because thermokarst lakes in northern Canada can be better identified by a high-resolution landscape evolution model in Tan and Zhuang (2015b) than by coarse-resolution geographic datasets in Tan and Zhuang (2015a). The posterior lake emissions from northern Siberia are much smaller than the modeled (Tan and

~~Zhuang, 2015a; Tan and Zhuang, 2015b). There are two possible reasons for the larger estimates of the lake model: 1) the model overestimates thermokarst active zone of yedoma lakes; and 2) four high-flux yedoma lakes that are used for calibration are not good representative of all yedoma lakes. For European lakes, Saarnio et al. (2009) estimated that they are a CH_4 source of 1.48 Tg CH_4 yr^{-1}. This means that CH_4 emissions from lakes in northern Europe (>60°N) could constitute 40% of CH_4 emissions from all European lakes. By upscaling site observations to northern Canada, Laurion et al. (2010) found that annual diffusive CH_4 emission from Canadian thaw ponds was 1.0 Tg CH_4. Since ebullition could be much stronger than diffusion in transporting CH_4 (Bastviken et al., 2011), our estimate of 3.1 Tg CH_4 yr^{-1} from Canadian lakes should not be considered a large overestimate, as indicated in Tan and Zhuang (2015b).~~

In contrast to CH_4 emissions from pan-Arctic wetlands, CH_4 emissions from pan-Arctic lakes at large spatial scales are still largely unknown. Consensus has not been reached yet on how to apply the knowledge learnt from individual lakes to the pan-Arctic scale, because even lakes in a small area could have much different transport pathways (ebullition vs. diffusion), morphology (deep vs. shallow and large vs. small), eutrophication (eutrophic vs. oligotrophic) and carbon source (thermokarst vs. non-thermokarst and yedoma vs. non-yedoma). ~~scientists have not reached a consensus on the importance of Arctic lakes to the global CH_4 cycle because only a limited number of Arctic lakes have been observed and their characteristics (e.g., morphology, eutrophication and carbon input) are more heterogeneous.~~ Because wetlands and lakes, both inundation landscapes, are usually neighbored, it is difficult to use inverse modeling at coarse spatial scales to detect strong CH_4 emissions that are emitted solely by lakes. To test whether high-resolution inversions can better represent CH_4 emissions from lakes, we conducted a comparison test ("DLEM only") over the East Siberia Coastal Lowlands (Fig. 1) using the

DLEM model and excluding CH_4 emissions from lakes. We chose the East Siberia Lowlands to test our hypothesis as lakes there occupy 56% of the water-inundated landscapes, i.e. lakes, wetlands and rivers (Lehner and Döll, 2004) and a large fraction of lakes in the region are high-flux yedoma lakes (Walter et al., 2006). We chose the DLEM model considering that the simulated wetland CH_4 emissions in this model are weak for the East Siberia Lowlands. This design is also aimed to alleviate the impact of one major shortcoming: because there are not sufficient high-quality observations, ~~In this study, as the constraints of observations are limited,~~ we ~~only~~ optimized ~~total~~ CH_4 emission in each grid cell separately for wetlands and lakes~~and fix the weight of each source during our inversions. Since wetlands and lakes are usually spatially neighbored, this operation could attribute~~ and in this manner a fraction of lake emissions could be attributed incorrectly to wetlands or vice versa. ~~To verify the possibility of large CH_4 emissions from pan-Arctic lakes, we conducted a nested-grid inversion in the Arctic based on the DLEM scenario that did not include CH_4 emissions from lakes as a comparison. The DLEM scenario was chosen because as presented in Fig. 3 its simulated wetland emissions are less spatially overlapped with the simulated lake emissions.~~ The inversion of the "DLEM only" scenario is shown in Fig. S5. In comparison to Fig. 4c, CH_4 emissions from the East Siberia Coastal Lowlands are low in Fig. S5. A further comparison of model-satellite agreement between the DLEM scenario and this no-lake scenario reveals that the agreement improves impressively when lake emissions are considered (see Fig. 6). It implies that CH_4 emissions from regional lakes could be significant. As illustrated above, however, the spatial neighborhood of wetlands and lakes makes it difficult to conduct ~~operate~~ similar experiments in other areas. Thus we are cautious to claim that CH_4 emissions from lakes are ubiquitously strong across the pan-Arctic. Rather, since we used six wetland models that can simulate very different wetland emission

distributions at~~i~~ ~~n~~ spatial and temporal scales, our estimates of 2.4–14.2 Tg CH_4 yr^{-1} for lake emissions could be more useful in explaining the range of this source. ~~This no-lake inversion shows that there are low CH_4 fluxes in the East Siberia Coastal Lowlands, a region with extensive high-flux yedoma lakes (Walter et al., 2006). In comparison with the original test, this no-lake inversion produces a larger mean difference between the observed and simulated posterior SCIAMACHY XCH_4, 27.4 ppb vs. 26.5 ppb. The 0.9 ppb difference is impressive considering the influence of nested-grid model boundaries. For instance, Berchet et al. (2015), even using high-precision surface measurements collected from eight West Siberian Plain sites, only reduced the difference of the observed and simulated posterior GOSAT XCH_4 by 1.5 ppb in a Eurasian-scale inversion. Another sign that SCIAMACHY XCH_4 can be much better represented by including lake emissions is that the no-lake inversion only reduces the simulated prior SCIAMACHY XCH_4 deviation by 0.1 ppb. Thus, the no-lake scenario probably misses some significant CH_4 emissions in the coastal lowlands. Because 56% of the water-inundated landscapes (i.e., lakes, wetlands and rivers) in this region are lakes (Lehner and Döll, 2004), lakes, especially yedoma lakes, could have contributed a large fraction of the missed CH_4 emissions.~~ The lower bound of our estimate is much smaller than the estimate of 7.1–17.3 Tg CH_4 yr^{-1} by Bastviken et al. (2011) in the use of extensive site-level observations. In contrast, the upper bound of our estimate is within the range. Given the wide span of this estimate, it is difficult to say whether CH_4 emissions from pan-Arctic lakes can be significant across the region.

Arctic tundra is regarded as an important source of CH_4 in the northern high latitudes. By using process-based models and atmospheric CH_4 observations, McGuire et al. (2012) estimated that Arctic tundra was a source of 25 Tg CH_4 yr^{-1} to the atmosphere during 1990–2006. By using the TM5-4DVAR inverse model and assimilating~~with~~ SCIAMACHY and NOAA/ESRL

observations, Alexe et al. (2015) estimated that CH_4 emissions from Arctic wetlands were 18.2 Tg CH_4 yr^{-1} for 2010–2011. A similar estimate of 16±5 Tg CH_4 yr^{-1} was also made by Bruhwiler et al. (2014) ~~with~~ using the CarbonTracker-CH_4 assimilation system. Our estimate~~s~~ of 5.5~~8.8~~–14.2~~20.4~~ Tg CH_4 yr^{-1} overlaps with the estimate of Bruhwiler et al. (2014) but is much lower than the estimates of Alexe et al. (2015) and McGuire et al. (2012). However, McGuire et al. (2012) did not use complex inverse models and Alexe et al. (2015) used the coarse-resolution TM5-4DVAR inverse model. As our global inversions (Table 2) are consistent with the estimate of Alexe et al. (2015), this difference is likely introduced by the use of the nested-grid inverse model. In other words, the nested-grid inverse model reveals some information that could be missed in global coarse-resolution inversions. ~~encompass the estimates of Alexe et al. (2015) and Bruhwiler et al. (2014) but are lower than that of McGuire et al. (2012).~~ For Siberian wetlands, they could emit much more CH_4 (1.6–7.6 Tg yr^{-1}) than any other areas. But the uncertainty of this source is also the largest. Using several flux towers near to Siberian wetlands, Berchet et al. (2015) estimated that CH_4 emissions from Siberian wetlands were in the range of 1–13 Tg CH_4 yr^{-1}, wider ~~larger~~ than our estimated range. In addition, our estimate is also much smaller than the estimate of 21.63 ± 5.25 Tg CH_4 yr^{-1} by Kim et al. (2012) for annual mean CH_4 emissions from Siberian wetlands during 2005–2010. ~~As discussed, the uncertainty mainly arises from CH_4 emissions from Siberian wetlands. Regionally, when the ORCHIDEE scenario is excluded,~~ ~~annual~~ According to our inversions, CH_4 emissions from wetlands in Alaska, northern Canada, northern Europe ~~and northern Siberia~~ are~~, on average,~~ 0–1.2~~0~~ Tg CH_4 yr^{-1}, 0.4–4.8~~3.3~~ Tg CH_4 yr^{-1}~~,~~ and 0.7–3.6~~4.2~~ Tg CH_4 yr^{-1} ~~and 5.8 Tg CH_4 yr^{-1}~~, respectively. For Alaskan wetlands, t~~T~~he ~~estimated~~ total of posterior CH_4 emission~~s from Alaskan wetlands~~ is much lower than the inferred value of 4.1 Tg CH_4 yr^{-1} for the Alaskan Yukon River basin during 1986–2005 using the

modeling of process-based CH_4 biogeochemistry and large-scale hydrology (Lu and Zhuang, 2012) and also much lower than the inferred value of 3 Tg CH_4 yr^{-1} for the whole ~~of~~ Alaska (Zhuang et al., 2007). ~~As wetlands in Europe are predominantly located north of 60°N, o~~Our estimate of wetland emissions from northern Europe compasses~~is very close to~~ a European-scale estimate of 3.6 Tg CH_4 yr^{-1} by Saarnio et al. (2009), agreeing with the investigation that wetlands in Europe are predominantly located north of 60°N. ~~The posterior CH_4 emissions from Siberian wetlands show a wide range (2.0–12.7 Tg CH_4 yr^{-1}), which are much smaller than the estimate of 21.63 ± 5.25 Tg CH_4 yr^{-1} by Kim et al. (2012) for the annual mean CH_4 emissions from Siberian wetlands during 2005–2010. Assimilating in situ CH_4 measurements collected at 13 Eurasian sites in Siberia, Finland, Mongolia, China and South Korea, Berchet et al. (2015) estimated that CH_4 budget on the West Siberian Plain was 5–28 Tg CH_4 for 2010. It is also larger than our estimate but shows a similar large uncertainty.~~

~~4.3. Method Evaluation~~

~~Fig. 8 shows the difference between the modeled and observed CH_4 mixing ratios at NOAA ship board sampling stations and aircraft vertical profile sites under different wetland scenarios before and after the global scale inversions. For most scenarios, inversion improves the representation of CH_4 mixing ratios in GEOS-Chem at both marine and inland boundary layers and free troposphere. Specifically, the CLM4Me scenario performs best in the evaluation by reducing the difference by more than 10 ppb. Because this scenario also produces global and wetland CH_4 fluxes consistent with earlier studies (as described in Section 4.1), it is likely that the spatial pattern of CH_4 fluxes simulated by the CLM4Me model is more realistic than the other scenarios at the global scale.~~

As shown in Fig. 7, in most of scenarios, the nested grid inversions perform much better than both the forward simulations and the global inversions at NOAA/ESRL pan-Arctic flask sites (Fig. 1). For example, for the ORCHIDEE scenario, the nested grid inversion reduces the model bias by 44 ppb relative to the forward run and by 20 ppb relative to the global inversion, respectively. Also, for the SDGVM scenario, it reduces the model bias by 22 ppb relative to the forward run and by 13 ppb relative to the global inversion, respectively. But for aircraft CH_4 measurements, it is more complex. The nested grid inversions can reduce the model bias in some scenarios greatly, i.e. the CLM4Me scenario and the SDGVM scenario. But in many cases, they do not perform visibly better than the forward runs and the global inversions. One possible reason is that the aircraft CH_4 RMS has already been low and thus the remaining errors, including the representation error of model diurnal variability, cannot be resolved by our current inversion system. For example, CH_4 emissions from Alaska can be well constrained by three NOAA/ESRL surface sites in Alaska (BRW, CBA and SHM) and the CH_4 mixing ratios at the aircraft PFA site are representative of the interior of Alaska as pointed out in Sweeney et al. (2015). It is also possible that the increase of grid cells in the nested grid inversions introduced more transport and computation errors.~~Fig. 9 compares the modeled and observed CH_4 mixing ratios at the PAL surface station, in Finland and the PFA aircraft vertical profile site, in Alaska before and after the nested grid inversions. These two stations are near the main CH_4 sources in northern Europe and Alaska, respectively. For PFA, the nested-grid inversions perform better than the nested-grid forward run but do not have clear advantage over the global inversions. The reason for this could be that CH_4 emissions from Alaska can be well constrained by three NOAA/ESRL surface sites in Alaska (BRW, CBA and SHM) and the CH_4 mixing ratios at PFA are representative of the interior of Alaska as was pointed out in Sweeney et al. (2015).~~

4.34. Further Discussion

Both the global and nested-grid inversions indicate that the inverse modeling is more sensitive to different wetland models than prior emission error and data error. Thus, to gain better understandings of the global and pan-Arctic CH_4 cycles, it is important to develop more realistic biogeochemical models. Especially, from the perspective of inverse modeling, focus should be ~~put~~ on improving the spatial and temporal representation of the models rather than emission magnitude.

For the high-resolution inverse modeling, transport and computation errors of the nested-grid CTMs need to be reduced for better performance. These CTMs can also benefit the efforts to assimilate aircraft CH_4 measurements. For the purpose of satellite data bias correction, more coordination between satellite missions and aircraft missions is demanded. The treatment of the SCIAMACHY bias could be an important uncertainty source for our estimates, as suggested by Houweling et al. (2014). Future top-down studies could benefit from a more reasonable bias correction method, even for low bias satellite products, e.g. GOSAT (Alexe et al., 2015).

~~As described in Section 4, there are still several issues limiting the accuracy of our estimates. First, although the stronger zonal and weaker vertical transport characteristics of northern high latitudes is thought to help transport flux information to the pan-Arctic sites (e.g., Shemya, Barrow and Cold Bay), CH_4 sources in some regions of the Arctic, e.g. Siberia, are still poorly constrained by the assimilated measurements. In theory, because surface and aircraft measurements have much lower uncertainties than satellite retrievals, it is possible to refine our estimates by incorporating site measurements near Siberia, such as the Surgut site of National Institute for Environmental Studies (NIES) (Machida et al., 2001). The uncertainty of~~

~~SCIAMACHY retrievals likely also needs to be revisited. The assumed 1.5% minimum uncertainty for SCIAMACHY retrievals in this study could be somewhat overestimated (Bergamaschi et al., 2007), which limits their potentials to provide constraints on CH_4 fluxes. The treatment of the SCIAMACHY bias could be an important uncertainty source for our estimates, as suggested by Houweling et al. (2014). Future top-down studies could benefit from a more reasonable bias correction method, even for low bias satellite products, e.g. GOSAT (Alexe et al., 2015).~~

T~~Second, t~~he attribution of CH_4 fluxes to spatially overlapped sources, e.g. wetlands and lakes, could be problematic~~a problem~~ for even high-resolution inversions. Carbon isotope measurements ($\delta^{13}CH_4$) are widely used to separate biogenic and geologic CH_4 sources (Langenfelds et al., 2002) but are not useful for two biogenic sources with similar carbon isotope ratios (Walter et al., 2008; Fisher et al., 2011). In our study, lake and wetland emissions were simulated separately by different models. This raised the possibility of double counting emissions of the two sources. A possible solution is to simulate them in a single earth system model using a consistent wetland and lake pixel identification method.~~One possible solution is to constrain the flux ratio of wetlands to lakes using very fine resolution geographical information. For instance, the flux ratio should be well constrained by the area ratio of these two landscapes. Another possible solution is to jointly constrain CO_2 and CH_4 fluxes in a nested-grid inversion. As known, although both wetlands and lakes are CH_4 sources, wetlands are a CO_2 sink and lakes are a CO_2 source (Zhu et al., 2013; Walter Anthony et al., 2014). This opposite correlations of CH_4 and CO_2 emissions could possibly be used to constrain the optimization of the flux ratio in inverse models.~~

Our nested grid adjoint model currently does not cover the regions near ~~to~~ the North Pole. While it could be rare in the summer time, if air mass transports across the Arctic Ocean, it may not be represented in the model. In the following studies, we will ~~try to~~ adapt the advection algorithm for the polar region from the global adjoint model to the nested-grid model and validate the adaptation. These refinements shall ~~may~~ reduce the uncertainty of our estimates. It is also valuable to discuss the integration of other natural CH_4 sources found in the pan-Arctic, such as CH_4 emission ~~s~~from subsea permafrost of East Siberian shelf (Shakhova et al., 2013).

~~Our Arctic inversions did not include natural CH_4 sources (e.g., CH_4 emissions from subsea permafrost of East Siberian shelf) other than wetlands and lakes in the Arctic. It could lead to more uncertainties in our estimates. But our study also suggests that it is unlikely that CH_4 emissions from sea shelf are as large as 17 Tg CH_4 yr^{-1} as suggested by Shakhova et al. (2013) because the posterior CH_4 emissions from Arctic wetlands are no more than 20.4 Tg CH_4 yr^{-1}.~~

5. Conclusion

In this study, we used a ~~nested-grid~~ high-resolution nested-grid ~~chemical transport inverse~~ adjoint model in the pan-Arctic domain to constrain CH_4 emissions from pan-Arctic wetlands, lakes and anthropogenic sources. The sensitivity of the method to different prior wetland CH_4 fluxes was~~is also~~ tested. When assimilating both NOAA/ESRL measurements and SCIAMACHY retrievals ~~observations~~, we estimated that ~~during July 2004–June 2005,~~ in 2005, the total of global ~~total~~ CH_4 emissions was~~is~~ in the range of 496.4–511.5 Tg CH_4 yr^{-1}, with wetlands contributing 130.0–203.3 Tg CH_4 yr^{-1}. Both of these estimates are consistent with some widely accepted expert assessments. The estimated CH_4 emissions in the pan-Arctic were in the

range of 11.9–28.5 Tg yr^{-1}, with wetland and lake emissions ranging from 5.5 to 14.2 Tg yr^{-1} and from 2.4 to 14.2 Tg yr^{-1}, respectively. The largest CH_4 emissions in the pan-Arctic are from Siberian wetlands and lakes. The study demonstrates that the assimilation of satellite retrievals can reduce the uncertainty of the nested grid inversions. ~~The nested-grid inversions demonstrate that biogeochemical models tend to overestimate CH_4 emissions from natural sources of the Arctic (e.g., wetlands and lakes). The posterior CH_4 emissions from Arctic lakes from July 2004 to June 2005 are 5.4–7.9 Tg CH_4 yr^{-1}, a significant contribution to the Arctic CH_4 cycle. CH_4 emissions from lakes in Alaska, northern Canada, northern Europe and northern Siberia, on average, are estimated to be 1.0 Tg CH_4 yr^{-1}, 3.1 Tg CH_4 yr^{-1}, 0.6 Tg CH_4 yr^{-1} and 2.8 Tg CH_4 yr^{-1}, respectively. Except for the emissions from northern Siberia, other estimates are consistent with the lake biogeochemical model simulations. The posterior CH_4 emissions from Arctic wetlands from July 2004 to June 2005 are 8.8–20.4 Tg CH_4 yr^{-1}. CH_4 emissions from wetlands in Alaska, northern Canada, northern Europe and northern Siberia are, on average, 1.0 Tg CH_4 yr^{-1}, 3.3 Tg CH_4 yr^{-1}, 4.2 Tg CH_4 yr^{-1} and 5.8 Tg CH_4 yr^{-1}, respectively. The nested-grid inversions indicate that CH_4 emissions from northern Canada, Alaska, Scandinavia and East Siberia Coastal lowlands are better constrained by the inversions than from other Arctic regions, e.g. most of Siberian wetlands.~~ Evaluation with independent datasets shows that ~~the global inversions and the Arctic inversions with a nested approach~~ the nested inversions can better improve ~~estimates~~ the representation of CH_4~~methane~~ mixing ratios in lower boundary layer rather than top boundary layer and free troposphere. ~~The high-resolution inversions provide more details about the spatial distribution of methane emissions in the Arctic, which helps understand the CH_4 cycle in this climate sensitive region.~~

Acknowledgements: We would like to thank the WETCHIMP investigators for making their simulations of wetland methane emissions available. We appreciate the help from Guang-Dih Lei and Bhagirath M. Trivedi at NASA and Robert Yantosca at Harvard for processing nested grid GOES-5 met data and the help from Christoph A. Keller at Harvard for processing nested grid emission data by HEMCO. This study is supported through projects funded to Q. Z. by the NASA Land Use and Land Cover Change program (NASA-NNX09AI26G), Department of Energy (DE-FG02-08ER64599), the NSF Division of Information and Intelligent Systems (NSF-1028291), and the NSF Carbon and Water in the Earth Program (NSF-0630319). This research is also in part supported by the Director, Office of Science, Office of Biological and Environmental Research of the US Department of Energy under Contract No. DE-AC02-05CH11231 as part of their Earth System Modeling Program. D. K. H. acknowledges NOAA grant no. NA14OAR 4310136. A. J. T. was supported by a Department of Energy (DOE) Computational Science Graduate Fellowship (CSGF). The supercomputing resource is provided by Rosen Center for Advanced Computing at Purdue University.

References

Alexe, M., Bergamaschi, P., Segers, A., Detmers, R., Butz, A., Hasekamp, O., Guerlet, S., Parker, R., Boesch, H., Frankenberg, C., Scheepmaker, R. A., Dlugokencky, E., Sweeney, C., Wofsy, S. C. and Kort, E. A.: Inverse modeling of CH_4 emissions for 2010–2011 using different satellite retrieval products from GOSAT and SCIAMACHY, Atmos. Chem. Phys., 15, 113–133, doi:10.5194/acp-15-113-2015, 2015.

Aydin, M., Verhulst, K. R., Saltzman, E. S., Battle, M. O., Montzka, S. A, Blake, D. R., Tang, Q. and Prather, M. J.: Recent decreases in fossil-fuel emissions of ethane and methane derived from firn air, Nature, 476(7359), 198–201, 2011.

Bastviken, D., Tranvik, L., Downing, J., Crill, P. M. and Enrich-Prast, A.: Freshwater methane emissions offset the continental carbon sink, Science, 331, 50–50, 2011.

Berchet, A., Pison, I., Chevallier, F., Paris, J.-D., Bousquet, P., Bonne, J.-L., Arshinov, M. Y., Belan, B. D., Cressot, C., Davydov, D. K., Dlugokencky, E. J., Fofonov, A. V., Galanin, A., Lavrič, J., Machida, T., Parker, R., Sasakawa, M., Spahni, R., Stocker, B. D. and Winderlich, J.: Natural and anthropogenic methane fluxes in Eurasia: a meso-scale quantification by generalized atmospheric inversion, Biogeosciences, 12, 5393–5414, doi:10.5194/bg-12-5393-2015, 2015.

Berchet, A., Bousquet, P., Pison, I., Locatelli, R., Chevallier, F., Paris, J.-D., Dlugokencky, E. J., Laurila, T., Hatakka, J., Viisanen, Y., Worthy, D. E. J., Nisbet, E. G., Fisher, R. E., France, J. L., Lowry, D. and Ivakhov, V.: Atmospheric constraints on the methane emissions from the East Siberian Shelf, Atmos. Chem. Phys., 16, 4147–4157, doi:10.5194/acp-16-4147-2016, 2016.

Bergamaschi, P., Krol, M., Dentener, F., Vermeulen, A., Meinhardt, F., Graul, R., Ramonet, M. , Peters, W. and Dlugokencky, E. J.: Inverse modelling of national and European CH_4 emissions using the atmospheric zoom model TM5, Atmos. Chem. Phys., 5, 2431–2460, 2005.

Bergamaschi, P., Frankenberg, C., Meirink, J. F., Krol, M., Dentener, F., Wagner, T., Platt, U., Kaplan, J. O., Körner, S., Heimann, M., Dlugokencky, E. J. and Goede, A.: Satellite chartography of atmospheric methane from SCIAMACHY on board ENVISAT: 2. Evaluation based on inverse model simulations, J. Geophys. Res., 112, D02304, doi:10.1029/2006JD007268, 2007.

1492 Bergamaschi, P., Frankenberg, C., Meirink, J. F., Krol, M., Villani, M. G., Houweling, S.,
1493 Dentener, F., Dlugokencky, E. J., Miller, J. B., Gatti, L. V., Engel, A. and Levin, I.: Inverse
1494 modeling of global and regional CH4 emissions using SCIAMACHY satellite retrievals, J.
1495 Geophys. Res., 114, D22301, doi:10.1029/2009JD012287, 2009.

1496 Bergamaschi, P., Houweling, S., Segers, A., Krol, M., Frankenberg, C., Scheepmaker, R. A.,
1497 Dlugokencky, E., Wofsy, S. C., Kort, E. a., Sweeney, C., Schuck, T., Brenninkmeijer, C., Chen,
1498 H., Beck, V. and Gerbig, C.: Atmospheric CH4 in the first decade of the 21st century: Inverse
1499 modeling analysis using SCIAMACHY satellite retrievals and NOAA surface measurements, J.
1500 Geophys. Res. Atmos., 118, 1-20, doi:10.1002/jgrd.50480, 2013.

1501 Bey, I., Jacob, D. J., Yantosca, R. M., Logan, J. A., Field, B. D., Fiore, A. M., Li, Q., Liu, H. Y.,
1502 Mickley, L. J., and Schultz, M. G.: Global modeling of tropospheric chemistry with assimilated
1503 meteorology: model description and evaluation, J. Geophys. Res., 106, 23073-23095, 2001.

1504 Bloom, A. A., Palmer, P. I., Fraser, A., Reay, D. S. and Frankenberg, C.: Large-Scale Controls of
1505 Methanogenesis Inferred from Methane and Gravity Spaceborne Data, Science, 327, 322–325,
1506 doi:10.1038/nchem.467, 2010.

1507 Bousquet, P., Ciais, P., Miller, J. B., Dlugokencky, E. J., Hauglustaine, D. A, Prigent, C., Van
1508 der Werf, G. R., Peylin, P., Brunke, E.-G., Carouge, C., Langenfelds, R. L., Lathière, J., Papa, F.,
1509 Ramonet, M., Schmidt, M., Steele, L. P., Tyler, S. C. and White, J.: Contribution of
1510 anthropogenic and natural sources to atmospheric methane variability, Nature, 443(7110), 439–
1511 443, doi:10.1038/nature05132, 2006.

1512 Bousserez, N., Henze, D. K., Perkins, A., Bowman, K. W., Lee, M., Liu, J., Deng, F. and Jones,
1513 D. B. A.: Improved analysis-error covariance matrix for high-dimensional variational inversions:

application to source estimation using a 3D atmospheric transport model, Q. J. R. Meteorol. Soc., doi:10.1002/qj.2495, 2015.

Bruhwiler, L. M., Dlugokencky, E., Masarie, K., Ishizawa, M., Andrews, A., Miller, J., Sweeney, C., Tans, P. and Worthy, D.: CarbonTracker-CH_4: an assimilation system for estimating emissions of atmospheric methane, Atmos. Chem. Phys., 14, 8269–8293, doi:10.5194/acp-14-8269-2014, 2014.

Butz, A., Hasekamp, O. P., Frankenberg, C., Vidot, J., and Aben, I.: CH_4 retrievals from space-based solar backscatter measurements: Performance evaluation against simulated aerosol and cirrus loaded scenes, J. Geophys. Res. Atmos., 115, D24302, doi:10.1029/2010JD014514, 2010.

Cressot, C., Chevallier, F., Bousquet, P., Crevoisier, C., Dlugokencky, E. J., Fortems-Cheiney, A., Frankenberg, C., Parker, R., Pison, I., Scheepmaker, R. A., Montzka, S. A., Krummel, P. B., Steele, L. P. and Langenfelds, R. L.: On the consistency between global and regional methane emissions inferred from SCIAMACHY, TANSO-FTS, IASI and surface measurements, Atmos. Chem. Phys., 14, 577–592, doi:10.5194/acp-14-577-2014, 2014.

Deng, F., Jones, D. B. A., Henze, D. K., Bousserez, N., Bowman, K. W., Fisher, J. B., Nassar, R., O'Dell, C., Wunch, D., Wennberg, P. O., Kort, E. A., Wofsy, S. C., Blumenstock, T., Deutscher, N. M., Griffith, D. W. T., Hase, F., Heikkinen, P., Sherlock, V., Strong, K., Sussmann, R. and Warneke, T.: Inferring regional sources and sinks of atmospheric CO_2 from GOSAT XCO_2 data, Atmos. Chem. Phys., 14, 3703–3727, doi:10.5194/acp-14-3703-2014, 2014.

Denman, K. L., Brasseur, G., Chidthaisong, A., Ciais, P., Cox, P. M., Dickinson, R. E., Hauglustaine, D., Heinze, C., Holland, E., Jacob, D., Lohmann, U., Ramachandran, S., da Silva Dias, P. L., Wofsy, S. C., and Zhang, X.: Couplings Between Changes in the Climate System and

Biogeochemistry. In: Climate Change 2007: The Physical Science Basis. Contribution of Working Group I to the Fourth Assessment Report of the Intergovernmental Panel on Climate Change, edited by Solomon, S., Qin, D., Manning, M., Chen, Z., Marquis, M., Averyt, K. B., Tignor, M., and Miller, H. L., Cambridge University Press, Cambridge, United Kingdom and New York, N. Y., USA, 2007.

Dlugokencky, E., Masarie, K. and Lang, P.: Continuing decline in the growth rate of atmospheric methane burden, Nature, 393, 447–450, 1998.

Dlugokencky, E. J., Houweling, S., Bruhwiler, L., Masarie, K. A., Lang, P. M., Miller, J. B, and Tans, P. P.: Atmospheric methane levels off: Temporary pause or a new steady-state?, Geophys. Res. Lett., 30, No. 19, doi: 10.1029/2003GL018126, 2003.

Dlugokencky, E. J., Myers, R. C., Lang, P. M., Masarie, K. A., Crotwell, A. M., Thoning, K. W., Hall, B. D., Elkins, J. W., and Steele, L. P.: Conversion of NOAA atmospheric dry-air CH_4 mole fractions to a gravimetrically prepared standard scale, J. Geophys. Res. Atmos., 110, D18306, doi:10.1029/2005JD006035, 2005.

Dlugokencky, E. J., Bruhwiler, L., White, J. W. C., Emmons, L. K., Novelli, P. C., Montzka, S. A., Masarie, K. A., Lang, P. M., Crotwell, A. M., Miller, J. B. and Gatti, L. V.: Observational constraints on recent increases in the atmospheric CH_4 burden, Geophys. Res. Lett., 36, L18803, doi:10.1029/2009GL039780, 2009.Dlugokencky, E. J., Lang, P. M., Crotwell, A.M., Masarie, K.A. and Crotwell M.J.: Atmospheric Methane Dry Air Mole Fractions from the NOAA ESRL Carbon Cycle Cooperative Global Air Sampling Network, 1983-2013, Version: 2014-06-24, ftp://aftp.cmdl.noaa.gov/data/trace_gases/ch4/flask/surface/ (last access: 9 June 2015), 2014.

1557 Enting, I. G.: Inverse problems in atmospheric constituent transport, Cambridge University Press,
1558 2002.

1559 Etheridge, D. M., Steele, L. P., Francey, R. J., and Langenfelds, R. L.: Atmospheric methane
1560 between 1000 A.D. and present: Evidence of anthropogenic emissions and climatic variability, J.
1561 Geophys. Res., 103(D13), 15,979-15,993, 1998.

1562 European Commission, Joint Research Centre/Netherlands Environmental Assessment Agency:
1563 Emission Database for Global Atmospheric Research (EDGAR), release version 4.0.,
1564 http://edgar.jrc.ec.europa.eu (last access: 11 June 2015), 2009.

1565 Fiore, A. M., Horowitz, L. W., Dlugokencky, E. J. and West, J. J.: Impact of meteorology and
1566 emissions on methane trends, 1990–2004, Geophys. Res. Lett., 33, L12809,
1567 doi:10.1029/2006GL026199, 2006.

1568 Fisher, R. E., Sriskantharajah, S., Lowry, D., Lanoisellé, M., Fowler, C. M. R., James, R. H.,
1569 Hermansen, O., Lund Myhre, C., Stohl, A., Greinert, J., Nisbet-Jones, P. B. R., Mienert, J. and
1570 Nisbet, E. G.: Arctic methane sources: Isotopic evidence for atmospheric inputs, Geophys. Res.
1571 Lett., 38, L21803, doi:10.1029/2011GL049319, 2011.

1572 Frankenberg, C., Meirink, J. F., Bergamaschi, P., Goede, A. P. H., Heimann, M., Kröner, S.,
1573 Platt, U., van Weele, M., and Wagner, T.: Satellite chartography of atmospheric methane from
1574 SCIAMACHY on board ENVISAT: Analysis of the years 2003 and 2004, J. Geophys. Res., 111,
1575 D07303, doi:10.1029/2005JD006235, 2006.

1576 Frankenberg, C., Bergamaschi, P., Butz, A., Houweling, S., Meirink, J. F., Notholt, J., Petersen,
1577 A. K., Schrijver, H., Warneke, T., and I. Aben: Tropical methane emissions: A revised view

from SCIAMACHY onboard ENVISAT, Geophys. Res. Lett., 35, L15811, doi:10.1029/2008GL034300, 2008.

Frankenberg, C., Aben, I., Bergamaschi, P., Dlugokencky, E. J., van Hees, R., Houweling, S., van der Meer, P., Snel, R., and Tol, P.: Global column-averaged methane mixing ratios from 2003 to 2009 as derived from SCIAMACHY: Trends and variability, J. Geophys. Res., 116, D02304, doi:10.1029/2010JD014849, 2011.

Fraser, A., Palmer, P. I., Feng, L., Boesch, H., Cogan, A., Parker, R., Dlugokencky, E. J., Fraser, P. J., Krummel, P. B., Langenfelds, R. L., O'Doherty, S., Prinn, R. G., Steele, L. P., van der Schoot, M. and Weiss, R. F.: Estimating regional methane surface fluxes: the relative importance of surface and GOSAT mole fraction measurements, Atmos. Chem. Phys., 13, 5697–5713, doi:10.5194/acp-13-5697-2013, 2013.

Fung, I., John, J., Lerner, J., Matthews, E., Prather, M., Steele, L. P., and Fraser, P. J.: Three-dimensional model synthesis of the global methane cycle, J. Geophys. Res., 96, 13,033–13,065, doi:10.1029/91JD01247, 1991.

~~Gao, X., Schlosser, C. A., Sokolov, A., Walter Anthony, K., Zhuang, Q., and Kicklighter, D.: Permafrost degradation and methane: low risk of biogeochemical climate-warming feedback, Environ. Res. Lett., 8, 035014, doi:10.1088/1748-9326/8/3/035014, 2013.~~

GLOBALVIEW-CH4: Cooperative Atmospheric Data Integration Project - Methane. CD-ROM, NOAA ESRL, Boulder, Colorado, available at: ftp://ftp.cmdl.noaa.gov (last access: 19 August 2015), Path: products/globalview/ch4, 2009.

1598 Gurney, K. R., Law, R. M., Denning, A. S., Rayner, P. J., Baker, D., Bousquet, P., Bruhwiler, L.,
1599 Chen, Y.-H., Ciais, P., Fan, S., Fung, I. Y., Gloor, M., Heimann, M., Higuchi, K., John, J., Maki,
1600 T., Maksyutov, S., Masarie, K., Peylin, P., Prather, M., Pak, B. C., Randerson, J., Sarmiento, J.,
1601 Taguchi, S., Takahashi, T., and Yuen, C.-W.: Towards robust regional estimates of CO_2 sources
1602 and sinks using atmospheric transport models, Nature, 415, 626–630, doi:10.1038/415626a, 2002.

1603 Heald, C. L., Jacob, D. J., Jones, D. B. A., Palmer, P. I., Logan, J. A., Streets, D. G., Sachse, G.
1604 W., Gille, J. C., Hoffman, R. N. and Nehrkorn, T.: Comparative inverse analysis of satellite
1605 (MOPITT) and aircraft (TRACE-P) observations to estimate Asian sources of carbon monoxide,
1606 J. Geophys. Res., 109, D23306, doi:10.1029/2004JD005185, 2004.

1607 Henze, D. K., Hakami, A., and Seinfeld, J. H.: Development of the adjoint of GEOS-Chem,
1608 Atmos. Chem. Phys., 7, 2413–2433, 2007.

1609 Houweling, S., Krol, M., Bergamaschi, P., Frankenberg, C., Dlugokencky, E. J., Morino, I.,
1610 Notholt, J., Sherlock, V., Wunch, D., Beck, V., Gerbig, C., Chen, H., Kort, E. a., Röckmann, T.
1611 and Aben, I.: A multi-year methane inversion using SCIAMACHY, accounting for systematic
1612 errors using TCCON measurements, Atmos. Chem. Phys., 14, 3991–4012, doi:10.5194/acp-14-
1613 3991-2014, 2014.

1614 Jiang, Z., Jones, D. B. A., Kopacz, M., Liu, J., Henze, D. K., and Heald, C.: Quantifying the
1615 impact of model errors on top-down estimates of carbon monoxide emissions using satellite
1616 observations, J. Geophys. Res., 116, D15306, doi:10.1029/2010JD015282, 2011.

1617 Kai, F. M., Tyler, S. C., Randerson, J. T. and Blake, D. R.: Reduced methane growth rate
1618 explained by decreased Northern Hemisphere microbial sources, Nature, 476(7359), 194–197,
1619 doi:10.1038/nature10259, 2011.

Kaminski, T. and Heimann, M.: Inverse modeling of atmospheric carbon dioxide fluxes, Science, 294, 259–259, 2001.

Keller, C. A., Long, M. S., Yantosca, R. M., Da Silva, A. M., Pawson, S., and Jacob, D. J.: HEMCO v1.0: a versatile, ESMF-compliant component for calculating emissions in atmospheric models, Geosci. Model Dev., 7, 1409-1417, doi:10.5194/gmd-7-1409-2014, 2014.

Khalil, M. A. K., Butenhoff, C. L. and Rasmussen, R. A.: Atmospheric methane: trends and cycles of sources and sinks, Environ. Sci. Technol., 41, 2131–2137, 2007.

Kim, H., Machida, T., Sasakawa, M., Belikov, D., Saeki, T., Ito, A. and Maksyutov, S.: Recent variation of Siberian CH_4 fluxes estimated from atmospheric observations of CH_4, AGU Fall Meeting Abstracts, 1, GC24A-08, 2012.

Kirschke, S., Bousquet, P., Ciais, P., Saunois, M., Canadell, J. G., Dlugokencky, E. J., Bergamaschi, P., Bergmann, D., Blake, D. R., Bruhwiler, L., Cameron-Smith, P., Castaldi, S., Chevallier, F., Feng, L., Fraser, A., Heimann, M., Hodson, E. L., Houweling, S., Josse, B., Fraser, P. J., Krummel, P. B., Lamarque, J.-F., Langenfelds, R. L., Le Quéré, C., Naik, V., O'Doherty, S., Palmer, P. I., Pison, I., Plummer, D., Poulter, B., Prinn, R. G., Rigby, M., Ringeval, B., Santini, M., Schmidt, M., Shindell, D. T., Simpson, I. J., Spahni, R., Steele, L. P., Strode, S. A., Sudo, K., Szopa, S., van der Werf, G. R., Voulgarakis, A., van Weele, M., Weiss, R. F., Williams, J. E., and Zeng, G.: Three decades of global methane sources and sinks, Nat. Geosci., 6, 813–823, doi:10.1038/ngeo1955, 2013.

Kopacz, M., Jacob, D. J., Henze, D. K., Heald, C. L., Streets, D. G. and Zhang, Q.: Comparison of adjoint and analytical Bayesian inversion methods for constraining Asian sources of carbon

monoxide using satellite (MOPITT) measurements of CO columns, J. Geophys. Res., 114, D04305, doi:10.1029/2007JD009264, 2009.

Kort, E. A., Wofsy, S. C., Daube, B. C., Diao, M., Elkins, J. W., Gao, R. S., Hintsa, E. J., Hurst, D. F., Jimenez, R., Moore, F. L., Spackman, J. R. and Zondlo, M. A.: Atmospheric observations of Arctic Ocean methane emissions up to 82° north, Nat. Geosci., 5, 1–4, doi:10.1038/ngeo1452, 2012.

Koven, C. D., Ringeval, B., Friedlingstein, P., Ciais, P., Cadule, P., Khvorostyanov, D., Krinner, G. and Tarnocai, C.: Permafrost carbon-climate feedbacks accelerate global warming, Proc. Natl. Acad. Sci., 108, 14769–14774, doi:10.1073/pnas.1103910108, 2011.

Langenfelds, R. L., Francey, R. J., Pak, B. C., Steele, L. P., Lloyd, J., Trudinger, C. M. and Allison, C. E.: Interannual growth rate variations of atmospheric CO_2 and its $\delta^{13}C$, H_2, CH_4, and CO between 1992 and 1999 linked to biomass burning, Global Biogeochem. Cycles, 16(3), 1048, doi:10.1029/2001GB001466, 2002.

~~Laurion, I., Vincent, W., MacIntyre, S., Retamal, L., Dupont, C., Francus, P. and Pienitz, R.: Variability in greenhouse gas emissions from permafrost thaw ponds, Limnol. Oceanogr., 55, 115–133, doi:10.4319/lo.2010.55.1.0115, 2010.~~

Lehner, B. and Döll, P.: Development and validation of a global database of lakes, reservoirs and wetlands, J. Hydrol., 296, 1–22, 2004.

Levin, I., Veidt, C., Vaughn, B. H., Brailsford, G., Bromley, T., Heinz, R., Lowe, D., Miller, J. B., Poβ, C. and White, J. W. C.: No inter-hemispheric $\delta^{13}CH_4$ trend observed, Nature, 486, E3–E4, doi:10.1038/nature11175, 2012.

Lin, S.-J. and Rood, R. B.: Multidimensional Flux-Form Semi-Lagrangian Transport Schemes, Mon. Weather Rev., 124, 2046–2070, 1996.

Lu, X. and Zhuang, Q.: Modeling methane emissions from the Alaskan Yukon River basin, 1986–2005, by coupling a large-scale hydrological model and a process-based methane model, J. Geophys. Res., 117, G02010, doi:10.1029/2011JG001843, 2012.

Machida, T., Nakazawa, T., Muksyutov, S., Tohjima, Y., Takahashi, Y.,Watai, T., Vinnichenko, N., Panchenko, M., Arshinov, M., Fedoseev, N., and Inoue, G.: Temporal and spatial variations of atmospheric CO_2 mixing ratio over Siberia, paper presented at the Sixth International CO_2 Conference, Sendai, Japan, 1–5, 2001.

~~Masarie, K. A. and Tans, P. P.: Extension and integration of atmospheric carbon dioxide data into a globally consistent measurement record, J. Geophys. Res., 100, 11593–11610, doi:10.1029/95JD00859, 1995.~~

McGuire, A. D., Christensen, T. R., Hayes, D., Heroult, A., Euskirchen, E., Kimball, J. S., Koven, C., Lafleur, P., Miller, P. A., Oechel, W., Peylin, P., Williams, M., and Yi, Y.: An assessment of the carbon balance of Arctic tundra: comparisons among observations, process models, and atmospheric inversions, Biogeosciences, 9, 3185-3204, doi:10.5194/bg-9-3185-2012, 2012.

Meirink, J. F., Bergamaschi, P. and Krol, M. C.: Four-dimensional variational data assimilation for inverse modelling of atmospheric methane emissions: method and comparison with synthesis inversion, Atmos. Chem. Phys., 8, 6341–6353, doi:10.5194/acp-8-6341-2008, 2008.

Melton, J. R., et al.: Present state of global wetland extent and wetland methane modelling: conclusions from a model inter-comparison project (WETCHIMP), Biogeosciences, 10, 753-788, 2013.

Meng, L., Paudel, R., Hess, P. G. M. and Mahowald, N. M.: Seasonal and interannual variability in wetland methane emissions simulated by CLM4Me' and CAM-chem and comparisons to observations of concentrations, Biogeosciences, 12, 4029–4049, doi:10.5194/bg-12-4029-2015, 2015.

Miller, S. M., Wofsy, S. C., Michalak, A. M., Kort, E. A., Andrews, A. E., Biraud, S. C., Dlugokencky, E. J., Eluszkiewicz, J., Fischer, M. L., Janssens-Maenhout, G., Miller, B. R., Miller, J. B., Montzka, S. A., Nehrkorn, T. and Sweeney, C.: Anthropogenic emissions of methane in the United States, Proc. Natl. Acad. Sci., 110(50), 20018–20022, doi:10.1073/pnas.1314392110, 2013.

Miller, S. M., Worthy, D. E. J., Michalak, A. M., Wofsy, S. C., Kort, E. A., Havice, T. C., Andrews, A. E., Dlugokencky, E. J., Kaplan, J. O., Levi, P. J., Tian, H. and Zhang, B.: Observational constraints on the distribution, seasonality, and environmental predictors of North American boreal methane emissions, Global Biogeochem. Cycles, 28, 146–160, doi:10.1002/2013GB004580, 2014.

Miyazaki, K., Patra, P. K., Takigawa, M., Iwasaki, T. and Nakazawa, T.: Global-scale transport of carbon dioxide in the troposphere, J. Geophys. Res., 113, D15301, doi:10.1029/2007JD009557, 2008.

Monteil, G., Houweling, S., Butz, A., Guerlet, S., Schepers, D., Hasekamp, O., Frankenberg, C., Scheepmaker, R., Aben, I. and Röckmann, T.: Comparison of CH_4 inversions based on 15

months of GOSAT and SCIAMACHY observations, J. Geophys. Res. Atmos., 118, 1–17, doi:10.1002/2013JD019760, 2013.

Murray, L. T., Jacob, D. J., Logan, J. A., Hudman, R. C., and Koshak, W. J.: Optimized regional and interannual variability of lightning in a global chemical transport model constrained by LIS/OTD satellite data, J. Geophys. Res., 117, D20307, doi:10.1029/2012JD017934, 2012.

Myhre, G., Shindell, D., Bréon, F.-M., Collins, W., Fuglestvedt, J., Huang, J., Koch, D., Lamarque, J.-F., Lee, D., Mendoza, B., Nakajima, T., Robock, A., Stephens, G., Takemura, T., and Zhang, H.: Anthropogenic and natural radiative forcing, in: Climate Change 2013: the Physical Science Basis, contribution of Working Group I to the Fifth Assessment Report of the Intergovernmental Panel on Climate Change, edited by: Stocker, T. F., Qin, D., Plattner, G.-K., Tignor, M., Allen, S. K., Boschung, J., Nauels, A., Xia, Y., Bex, V., and Midgley, P. M., Cambridge University Press, Cambridge, UK and New York, NY, USA, 2013.

Nisbet, E. G., Dlugokencky, E. J. and Bousquet, P.: Methane on the Rise--Again, Science, 343, 493–495, doi:10.1126/science.1247828, 2014.

Oh, Y., Stackhouse, B., Lau, M. C. Y., Xu, X., Trugman, A. T., Moch, J., Onstott, T. C., Jørgensen, C. J., Ludovica, D., Elberling, B., Emmerton, C. A., St. Louis, V. L. and Medvigy, D.: A scalable model explaining methane consumption in arctic mineral soils, Geophys. Res. Lett., 43, 5143–5150, doi:10.1002/2016GL069049, 2016.

Park, R. J., Jacob, D. J., Field, B. D., Yantosca, R. M., and Chin, M.: Natural and transboundary pollution influences on sulfate-nitrate-ammonium aerosols in the United States: Implications for policy, J. Geophys. Res., 109, D15204, doi:10.1029/2003JD004473, 2004.

Parker, R., Boesch, H., Cogan, A., Fraser, A., Feng, L., Palmer, P. I., Messerschmidt, J., Deutscher, N., Griffith, D. W. T., Notholt, J., Wennberg, P. O., and Wunch, D.: Methane observations from the Greenhouse Gases Observing SATellite: Comparison to ground-based TCCON data and model calculations, Geophys. Res. Lett., 38, L15807, doi:10.1029/2011GL047871, 2011.

Peng, S. S., Piao, S. L., Bousquet, P., Ciais, P., Li, B. G., Lin, X., Tao, S., Wang, Z. P., Zhang, Y., and Zhou, F.: Inventory of anthropogenic methane emissions in Mainland China from 1980 to 2010, Atmos. Chem. Phys. Discuss., doi:10.5194/acp-2016-139, in review, 2016.

Pickett-Heaps, C. A., Jacob, D. J., Wecht, K. J., Kort, E. A., Wofsy, S. C., Diskin, G. S., Worthy, D. E. J., Kaplan, J. O., Bey, I., and Drevet, J.: Magnitude of seasonality of wetland methane emissions from the Hudson Bay Lowlands (Canada), Atmos. Chem. Phys., 11, 3773–3779, doi:10.5194/acp-11-3773-2011, 2011.

Prather, M. J., Holmes, C. D., and Hsu, J.: Reactive greenhouse gas scenarios: systematic exploration of uncertainties and the role of atmospheric chemistry, Geophys. Res. Lett., 39, L09803, doi:10.1029/2012gl051440, 2012.

Rigby, M., Prinn, R. G., Fraser, P. J., Simmonds, P. G., Langenfelds, R. L., Huang, J., Cunnold, D. M., Steele, L. P., Krummel, P. B., Weiss, R. F., O'Doherty, S., Salameh, P. K., Wang, H. J., Harth, C. M., Mühle, J. and Porter, L. W.: Renewed growth of atmospheric methane, Geophys. Res. Lett., 35, L22805, doi:10.1029/2008GL036037, 2008.

Rodgers, C. D.: Inverse Methods for Atmospheric Sounding: Theory and Practice, Vol. 2, edited by: Rodgers, C. D., World Scientific Publishing Co. Pte. Ltd., Singapore, 2000.

Saarnio, S., Winiwarter, W. and Leitão, J.: Methane release from wetlands and watercourses in Europe, Atmos. Environ., 43, 1421–1429, doi:10.1016/j.atmosenv.2008.04.007, 2009.

Sasakawa, M., Machida, T., Tsuda, N., Arshinov, M., Davydov, D., Fofonov, A. and Krasnov, O.: Aircraft and tower measurements of CO_2 concentration in the planetary boundary layer and the lower free troposphere over southern taiga in West Siberia: Long-term records from 2002 to 2011, J. Geophys. Res., 118, 9489–9498, doi:10.1002/jgrd.50755, 2013.

Schubert, C. J., Diem, T. and Eugster, W.: Methane Emissions from a Small Wind Shielded Lake Determined by Eddy Covariance, Flux Chambers, Anchored Funnels, and Boundary Model Calculations: A Comparison, Environ. Sci. Technol., 46, 4515–4522, 2012.

Schuur, E. A. G., McGuire, A. D., Schädel, C., Grosse, G., Harden, J. W., Hayes, D. J., Hugelius, G., Koven, C. D., Kuhry, P., Lawrence, D. M., M.Natali, S., Olefeldt, D., Romanovsky, V. E., Schaefer, K., Turetsky, M. R., Treat, C. C. and Vonk, E. J.: Climate change and the permafrost carbon feedback, Nature, 520, 171–179, doi:10.1038/nature14338, 2015.

Shakhova, N., Semiletov, I., Leifer, I., Sergienko, V., Salyuk, A., Kosmach, D., Chernykh, D., Stubbs, C., Nicolsky, D., Tumskoy, V. and Gustafsson, Ö.: Ebullition and storm-induced methane release from the East Siberian Arctic Shelf, Nat. Geosci., 7, doi:10.1038/ngeo2007, 2013.

Shindell, D. T., Faluvegi, G., Koch, D. M., Schmidt, G. A., Unger, N., and Bauer, S. E.: Improved attribution of climate forcing to emissions, Science, 326, 716-718, 2009.

Simpson, I. J., Sulbaek Andersen, M. P., Meinardi, S., Bruhwiler, L., Blake, N. J., Helmig, D., Rowland, F. S. and Blake, D. R.: Long-term decline of global atmospheric ethane concentrations and implications for methane, Nature, 488, 490–494, doi:10.1038/nature11342, 2012.

1768 Singh, K., Jardak, M., Sandu, A., Bowman, K., Lee, M., and Jones, D.: Construction of non-
1769 diagonal background error covariance matrices for global chemical data assimilation, Geosci.
1770 Model Dev., 4, 299-316, 2011.

1771 Sweeney, C., Karion, A., Wolter, S., Newberger, T., Guenther, D., Higgs, J. A., Andrews, A. E.,
1772 Lang, P. M., Neff, D., Dlugokencky, E., Miller, J. B., Montzka, S. A., Miller, B. R., Masarie, K.
1773 A., Biraud, S. A., Novelli, P. C., Crotwell, M., Crotwell, A. M., Thoning, K. and Tans, P. P.:
1774 Seasonal climatology of CO_2 across North America from aircraft measurements in the
1775 NOAA/ESRL Global Greenhouse Gas Reference Network, J. Geophys. Res. Atmos., 120, 5155–
1776 5190, doi:10.1002/2014JD022591, 2015.

1777 Tan, Z., Zhuang, Q. and Walter Anthony, K.: Modeling methane emissions from arctic lakes:
1778 Model development and site-level study, J. Adv. Model. Earth Syst., 7, 459-483,
1779 doi:10.1002/2014MS000314, 2015.

1780 Tan, Z. and Zhuang, Q.: Arctic lakes are continuous methane sources to the atmosphere under
1781 warming conditions, Environ. Res. Lett., 10, 054016, doi:10.1088/1748-9326/10/5/054016,
1782 2015a.

1783 Tan, Z. and Zhuang, Q.: Methane emissions from pan-Arctic lakes during the 21st century: An
1784 analysis with process-based models of lake evolution and biogeochemistry, J. Geophys. Res.
1785 Biogeosciences, 120, 2641–2653, doi:10.1002/2015JG003184, 2015b.

1786 Tarnocai, C., Canadell, J. G., Schuur, E. A. G., Kuhry, P., Mazhitova, G. and Zimov, S.: Soil
1787 organic carbon pools in the northern circumpolar permafrost region, Global Biogeochem. Cycles,
1788 23, GB2023, doi: 10.1029/2008GB003327, 2009.

1789 Thompson, R. L., Stohl, A., Zhou, L. X., Dlugokencky, E., Fukuyama, Y., Tohjima, Y., Kim, S.-
1790 Y., Lee, H., Nisbet, E. G., Fisher, R. E., Lowry, D., Weiss, R. F., Prinn, R. G., O'Doherty, S.,
1791 Young, D. and White, J. W. C.: Methane emissions in East Asia for 2000 – 2011 estimated using
1792 atmospheric Bayesian inversion, J. Geophys. Res. Atmos., 120, 4352–4369,
1793 doi:10.1002/2014JD022394, 2015.

1794 Turner, A. J., Jacob, D. J., Wecht, K. J., Maasakkers, J. D., Biraud, S. C., Boesch, H., Bowman,
1795 K. W., Deutscher, N. M., Dubey, M. K., Griffith, D. W. T., Hase, F., Kuze, A., Notholt, J.,
1796 Ohyama, H., Parker, R., Payne, V. H., Sussmann, R., Velazco, V. A., Warneke, T., Wennberg, P.
1797 O. and Wunch, D.: Estimating global and North American methane emissions with high spatial
1798 resolution using GOSAT satellite data, Atmos. Chem. Phys., 15, 7049–7069, doi:10.5194/acp-
1799 15-7049-2015, 2015.

1800 van der Werf, G. R., Randerson, J. T., Giglio, L., Collatz, G. J., Mu, M., Kasibhatla, P. S.,
1801 Morton, D. C., DeFries, R. S., Jin, Y., and van Leeuwen, T. T.: Global fire emissions and the
1802 contribution of deforestation, savanna, forest, agricultural, and peat fires (1997–2009), Atmos.
1803 Chem. Phys., 10, 11,707–11,735, doi:10.5194/acp-10-11707-2010, 2010.

1804 Walter, K. M., Zimov, S. A., Chanton, J. P., Verbyla, D. and Chapin III, F. S.: Methane bubbling
1805 from Siberian thaw lakes as a positive feedback to climate warming, Nature, 443, 71–75,
1806 doi:10.1038/nature05040, 2006.

1807 Walter, K. M., Smith, L. C. and Chapin III, F. S.: Methane bubbling from northern lakes: present
1808 and future contributions to the global methane budget, Philos. T. Roy. Soc. A, 365(1856), 1657–
1809 76, doi:10.1098/rsta.2007.2036, 2007.

Wania, R., Melton, J. R., Hodson, E. L., Poulter, B., Ringeval, B., Spahni, R., Bohn, T., Avis, C. A., Chen, G., Eliseev, A. V., Hopcroft, P. O., Riley, W. J., Subin, Z. M., Tian, H., van Bodegom, P. M., Kleinen, T., Yu, Z. C., Singarayer, J. S., Zürcher, S., Lettenmaier, D. P., Beerling, D. J., Denisov, S. N., Prigent, C., Papa, F. and Kaplan, J. O.: Present state of global wetland extent and wetland methane modelling: methodology of a model inter-comparison project (WETCHIMP), Geosci. Model Dev., 6, 617–641, doi:10.5194/gmd-6-617-2013, 2013.

Wang, J. S., Logan, J. L., McElroy, M. B., Duncan, B. N., Megretskaia, I. A., and Yantosca, R. M.: 3-D model analysis of the slowdown and interannual variability in the methane growth rate from 1988 to 1997, Global Biogeochem. Cycles, 18, GB3011, doi:10.1029/2003GB002180, 2004.

Wecht, K. J., Jacob, D. J., Frankenberg, C., Jiang, Z. and Blake, D. R.: Mapping of North American methane emissions with high spatial resolution by inversion of SCIAMACHY satellite data, J. Geophys. Res. Atmos., 119, 7741–7756, doi:10.1002/2014JD021551, 2014.

Zhu, X., Zhuang, Q., Qin, Z., Glagolev, M. and Song, L.: Estimating wetland methane emissions from the northern high latitudes from 1990 to 2009 using artificial neural networks, Global Biogeochem. Cycles, 27, 1–13, doi:10.1002/gbc.20052, 2013.

Zhuang, Q., Melillo, J. M., Kicklighter, D. W., Prinn, R. G., McGuire, A. D., Steudler, P. A., Felzer, B. S., and Hu, S.: Methane fluxes between terrestrial ecosystems and the atmosphere at northern high latitudes during the past century: A retrospective analysis with a process-based biogeochemistry model, Global Biogeochem. Cycles, 18, GB3010, doi:10.1029/2004GB002239, 2004.

Zhuang, Q., Melillo, J. M., Sarofim, M. C., Kicklighter, D. W., McGuire, a. D., Felzer, B. S., Sokolov, A., Prinn, R. G., Steudler, P. a. and Hu, S.: CO_2 and CH_4 exchanges between land ecosystems and the atmosphere in northern high latitudes over the 21st century, Geophys. Res. Lett., 33, L17403, doi:10.1029/2006GL026972, 2006.

Zhuang, Q., Melillo, J. M., McGuire, A. D., Kicklighter, D. W., Prinn, R. G., Steudler, P. A., Felzer, B. S. and Hu, S.: Net emissions of CH_4 and CO_2 in Alaska: Implications for the region's greenhouse gas budget, Ecol. Appl., 17, 203–212, 2007.

Figure Captions

Figure 1. SCIAMACHY retrievals (n = 37743) of the weighted column-average CH_4 dry mole fractions for July 2005–September 2005 in the pan-Arctic that have passed all quality control tests described in Section 2.1 and the locations of surface flask stations and aircraft missions used for data assimilation or inversion evaluation.

~~Figure 1. Comparison of column averaged CH_4 mole fractions from SCIAMACHY with those from GEOS-Chem model calculated with prior emissions. (a and b) show the mean bias and residual standard deviation of the satellite-model difference, (c) shows the comparison of the model (x-axis) and satellite (y-axis) XCH_4 after applying the "latitude + humidity" correction from the linear regression (weighted R^2 is shown inset and the red 1:1 line is also shown), and (d) shows the satellite-model difference after bias removal.~~

~~Figure 2. Prior average wetland CH_4 emissions during 2004–2005 from different wetland biogeochemical models used for the GEOS-Chem global inversion at 4° × 5° resolution. Annual total emission (orange) is presented in units of Tg CH_4 yr^{-1}.~~

Figure 2~~3~~. Prior average CH_4 fluxes from wetlands, lakes and other sources (i.e. anthropogenic and biomass burning) in 2005~~during 2004–2005~~ used for~~in~~ the ~~GEOS-Chem~~ pan-Arctic nested grid inversions at 1/2° × 2/3° resolution. Annual total emission ~~(orange)~~ for each pan-Arctic source is presented in units of Tg CH_4 yr^{-1}.

Figure 3. Bias correction function (left) and standard deviation (right) for SCIAMACHY retrievals overpassing the pan-Arctic. ΔXCH_4 is the difference between SCIAMACHY and column-average mixing ratios mapped from aircraft vertical profiles. The red line in the left shows a linear regression weighted by the number of SCIAMACHY retrievals.

~~Figure 4. Optimized total (green) and wetlands (orange) CH_4 emissions from 1993 to 2005 by assimilating NOAA/ESRL measurements for (a) global, (b) tropics (30°S–20°N), (c) northern mid-latitude (20°N–50°N) and (d) northern high-latitude (>50°N). The smooth lines indicate the 12-month average of total and wetlands CH_4 fluxes. The prior wetland CH_4 fluxes are simulated by LPJ-WSL.~~

~~Figure 5. Optimized global CH_4 emissions and emissions scale factors (posterior emissions relative to prior emissions) in the period of July 2004 to June 2005 at 4° × 5° resolution using both SCIAMACHY and NOAA/ESRL observations. a) The posterior CH_4 emissions averaged over six inversions; b) the standard deviation of the posterior CH_4 emissions over six inversions; c) the optimized scale factor averaged over six inversions.~~

Figure 46. Optimized pan-Arctic CH_4 fluxes in 2005 ~~from July 2004 to June 2005~~ at 1/2° × 2/3° resolution using both SCIAMACHY and NOAA/ESRL observations. a) BERN; b) CLM4Me; c) DLEM; d) ORCHIDEE; e) SDGVM; f) WSL.

Figure 5. Comparison of prior and posterior pan-Arctic CH_4 emissions and their uncertainties. "NOAA only" represents posterior emissions assimilating only surface measurements. "NOAA + SCIA" represents posterior emissions assimilating both surface measurements and satellite retrievals. The uncertainty of prior emissions is 100%. Scenarios are represented by their name initials: "B" for BERN, "C" for CLM4Me, "D" for DLEM, "O" for ORCHIDEE, "S" for SDGVM and "W" for WSL.

Figure 6. Distribution of the relative difference between the observed and simulated posterior SCIAMACHY column-average mixing ratios. The "DLEM + Lake" scenario includes CH_4 emissions from both wetlands and lakes and the "DLEM only" scenario only includes CH_4 emissions from wetlands. Relative difference is calculated as a percentage of absolute differences between GEOS-Chem and SCIAMACHY relative to SCIAMACHY retrievals.

~~Figure 7. Optimized CH_4 emissions from Arctic lakes from July 2004 to June 2005 at 1/2° × 2/3° resolution using both SCIAMACHY and NOAA/ESRL observations. a) BERN; b) CLM4Me; c) DLEM; d) ORCHIDEE; e) SDGVM; f) WSL.~~

~~Figure 8. Evaluation of the posterior GEOS-Chem CH_4 mole fractions from the global inversions with independent data sets. The plot shows the root mean square (rms) of differences between modeled and observed CH_4 mixing ratios. APRI indicates the average rms using different prior wetland emissions.~~

Figure 79. Evaluation of the posterior GEOS-Chem CH_4 mole fractions from the pan-Arctic nested-grid inversions with independent data sets from the NOAA flaskPAL stations, and the NOAA aircraft PFA profiles and the NIES aircraft Surgut profiles. APRI indicates the average rms using different prior wetland emissions. APOR indicates the average rms calculated from six global inversions.Black symbols indicate the rms of the forward GEOS-Chem runs and red symbols indicate the rms of the global inversions.

Table1. Summary of bias correction methods and of mean absolute satellite-model difference (ppb) for 2003-2005 before and after applying bias correction. ΔBIC is the BIC score increase of a bias correction method when referring to the latitude only method.

	Bias correction function*	Mean absolute difference	ΔBIC	R^2
No correction		9.271		
Latitude only	$p_0 + p_1\varphi + p_2\varphi^2$	6.305		0.62
Air mass factor only	$p_0 + p_1 A_F$	7.071	161	0.52
Humidity only	$p_0 + p_1 H_S$	6.786	73	0.56
Latitude + Humidity	$p_0 + p_{11}\varphi + p_{12}\varphi^2 + p_{21} H_S$	6.230	-7	0.62
Air mass factor + Humidity	$p_0 + p_{11} A_F + p_{21} H_S$	6.396	12	0.60

* p_0, p_1, p_2, p_{11}, p_{12} and p_{21} are regression parameters.

Table 2. Estimated annual CH_4 emissions (units: Tg CH_4 yr^{-1}) for TransCom 3 land regions (NAB: North American Boreal, NAT: North American Temperate, SATr: South American Tropical, SAT: South American Temperate, NAf: Northern Africa, SAf: Southern Africa, ErB: Eurasian Boreal, ErT: Eurasian Temperate, TrA: Tropical Asia, Aus: Australasia, and Eur: Europe). The priors are the range of the initial CH_4 emissions given by the six scenarios.

Region	**Priors**	**Posterior**						**Fraser et al. (2013)**	**Alexe et al. (2015)**
		Bern	**CLM4Me**	**DLEM**	**ORCHIDEE**	**SDGVM**	**WSL**		
NAB	7.9–26.0	24.3	16.2	16.8	27.4	12.0	20.7	5.1±1.1	10.3
NAT	38.5–59.2	33.2	32.8	42.8	49.2	51.2	39.7	62.5±4.4	45.6
SATr	29.6–100.0	43.0	60.8	31.4	61.0	62.3	42.1	49.6±6.4	71.8
SAT	29.1–55.8	31.2	27.1	35.2	39.1	25.6	30.5	55.8±9.5	40.2
NAf	26.8–31.2	34.0	41.3	27.9	28.0	27.7	32.0	46.9±7.3	50.6
SAf	16.0–27.0	18.4	16.2	19.0	24.2	15.6	18.7	36.6±5.8	42.0
ErB	11.5–32.7	19.2	14.3	16.5	18.7	22.2	14.9	16.5±3.8	15.4
ErT	114.9–133.5	97.0	84.9	146.1	92.7	98.3	99.8	115.9±7.3	109.6
TrA	33.1–45.8	47.3	51.4	35.8	33.1	36.4	45.1	43.5±3.2	76.8
Aus	5.8–8.3	7.3	7.7	6.6	7.9	6.3	7.3	17.6±2.7	4.3
Eur	43.6–53.5	54.9	52.2	46.4	43.5	56.5	54.1	39.6±3.7	28.9
Wetlands	121.7–278.1	166.8	164.6	130.0	203.3	161.8	160.7	192.1±16.1	169
Global	471.5–627.8	501.0	497.7	511.5	511.0	496.4	502.9	510.6±18.4	540.5

Table 3. Summary of the prior and posterior CH_4 emissions (Tg CH_4 yr^{-1}) from the Arctic from July 2004 to June 2005. The priors are the range of the initial CH_4 emissions given by the six scenarios.

	Priors	**Posterior**					
		Bern	**CLM4Me**	**DLEM**	**ORCHIDEE**	**SDGVM**	**WSL**
Alaska	2.8–3.9	3.3	2.5	2.2	2.6	1.8	2.3
Northern Canada	6.2–12.4	7.2	9.0	6.9	5.2	4.4	4.3
Northern Europe	5.6–9.7	8.5	5.8	4.8	4.6	6.7	7.5
Northern Siberia	7.0–18.0	8.2	12.7	3.8	2.0	7.2	8.8
Arctic total	25.7–39.9	27.8	30.4	18.1	14.6	20.3	20.0
Wetlands	11.4–25.6	18.7	20.4	9.2	8.8	12.5	10.9
Lakes	11.1	7.7	7.9	7.5	5.4	7.0	7.7
Other	3.2	1.4	2.1	1.4	0.3	0.9	1.4

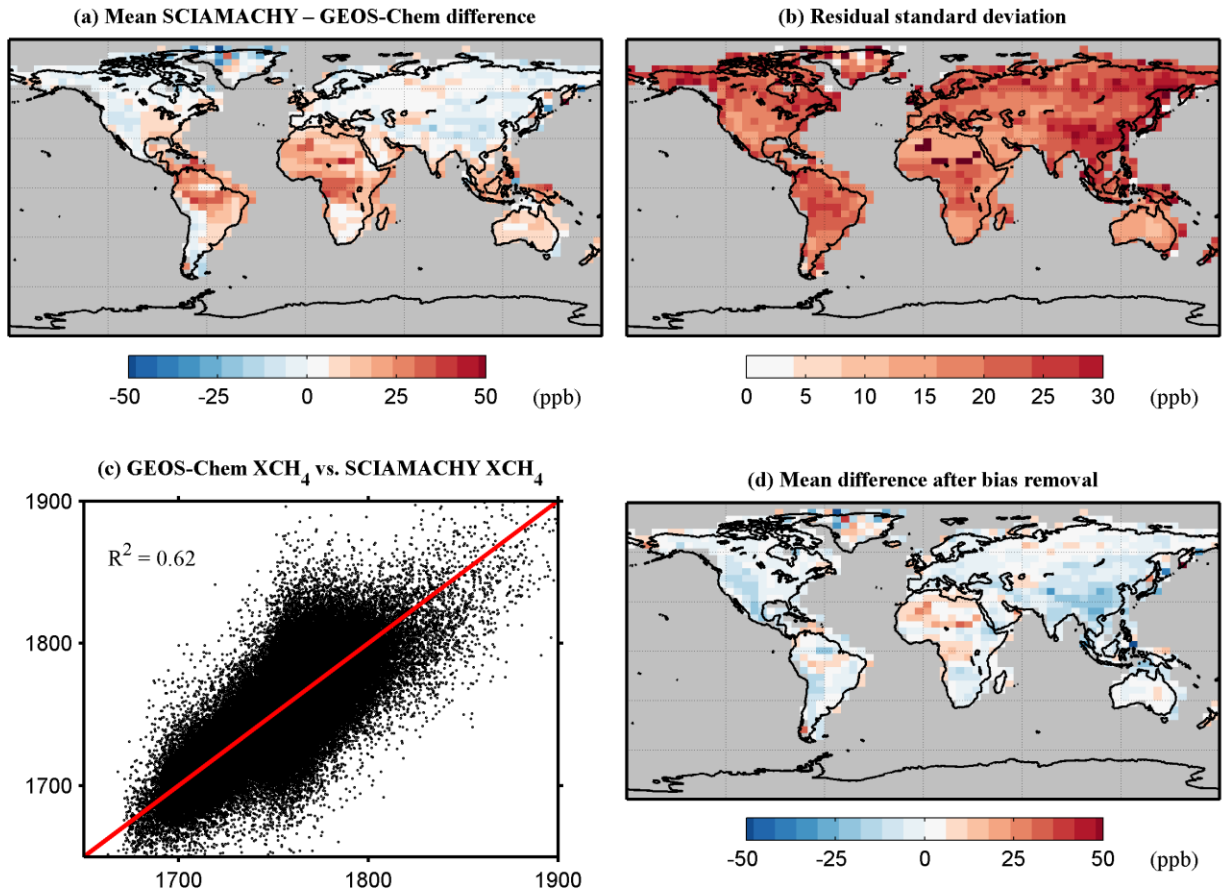
(a) Mean SCIAMACHY – GEOS-Chem difference
-50
-25
0
25
50
(ppb)
(b) Residual standard deviation
0
5
10
15
20
25
30
(ppb)
(c) GEOS-Chem XCH4 vs. SCIAMACHY XCH4
R2 = 0.62
1900
1800
1700
1700
1800
1900
(d) Mean difference after bias removal
-50
-25
0
25
50
(ppb)

~~Figure 1.~~

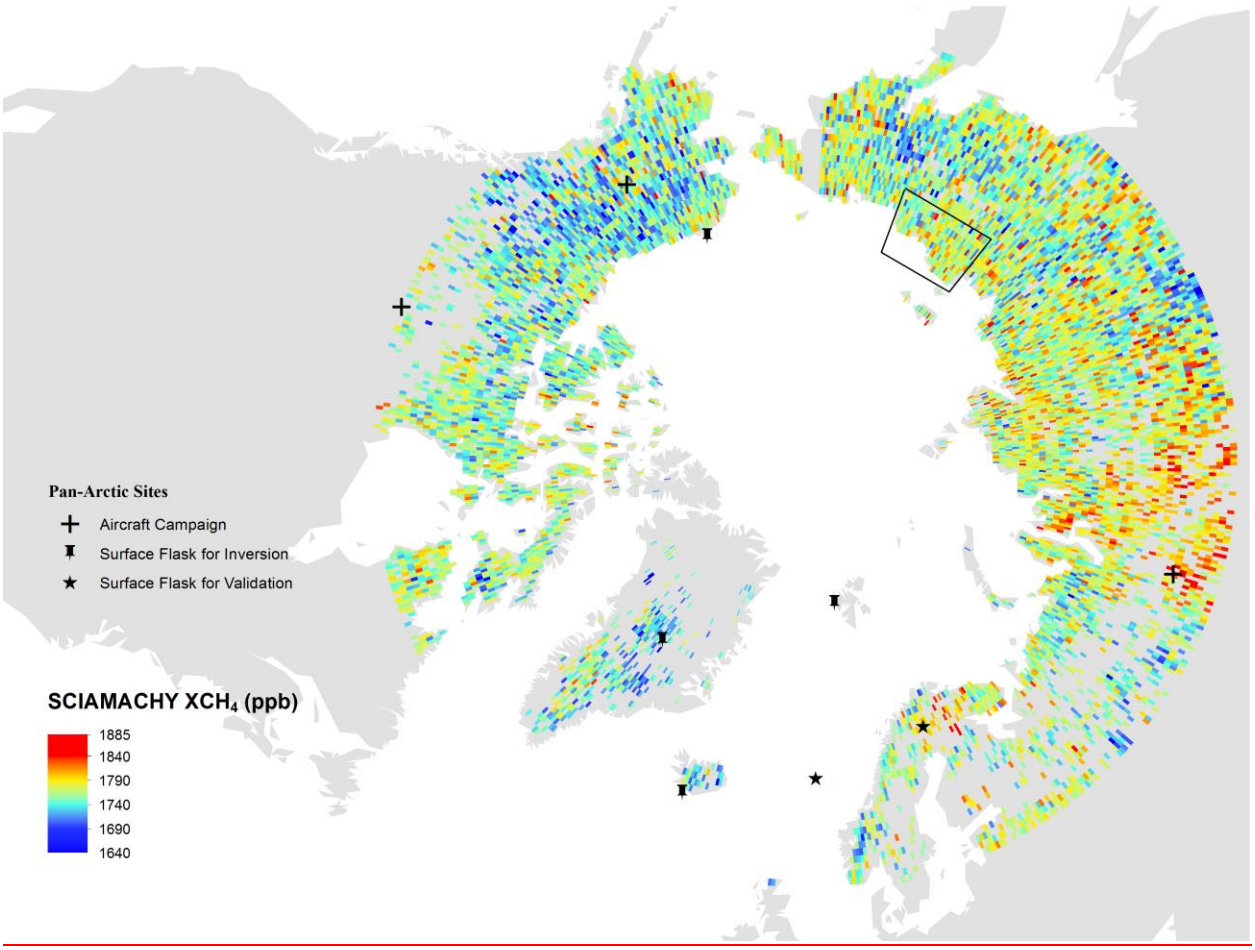
Pan-Arctic Sites
Aircraft Campaign
Surface Flask for Inversion
Surface Flask for Validation
SCIAMACHY XCH4 (ppb)
1885
1840
1790
1740
1690
1640

Figure 1.

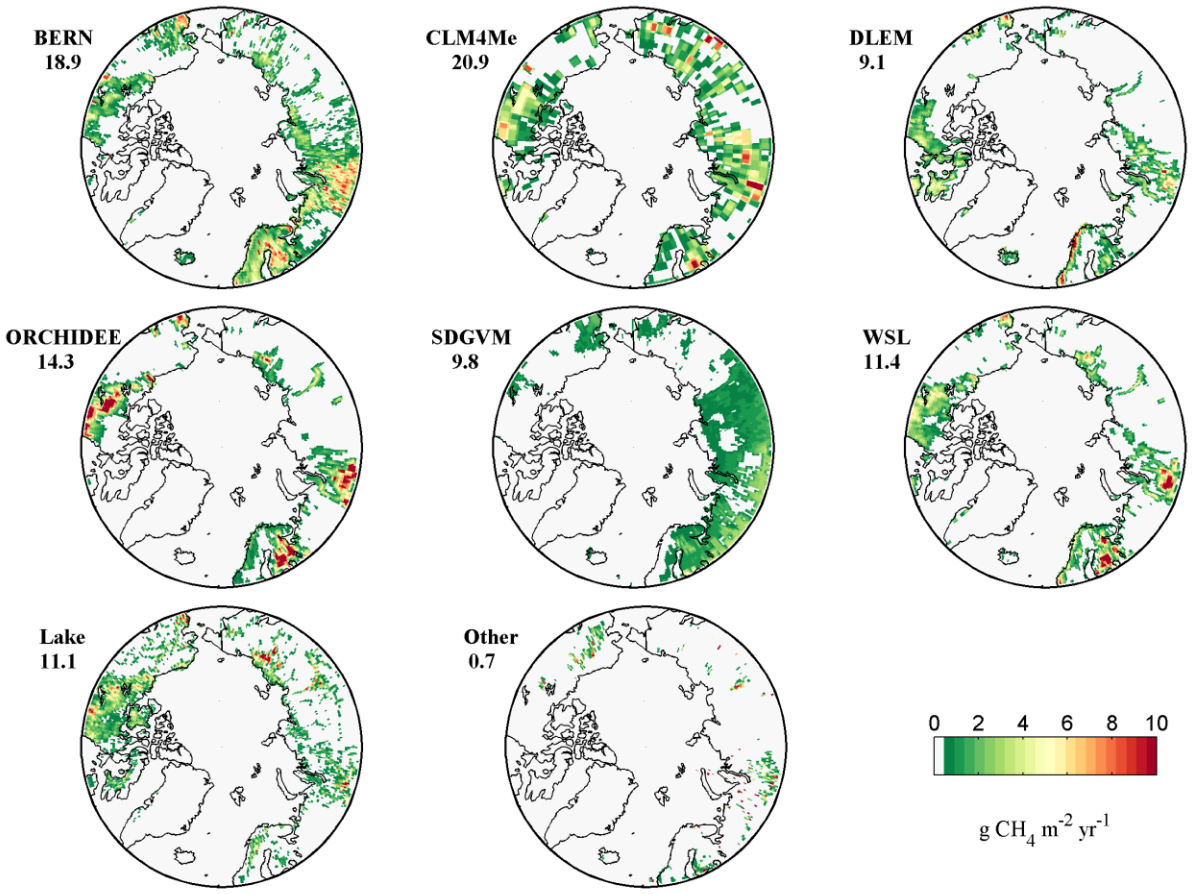
BERN
18.9
CLM4Me
20.9
DLEM
9.1
ORCHIDEE
14.3
SDGVM
9.8
WSL
11.4
Lake
11.1
Other
0.7
0 2 4 6 8 10
g CH4 m-2 yr-1

Figure 2.

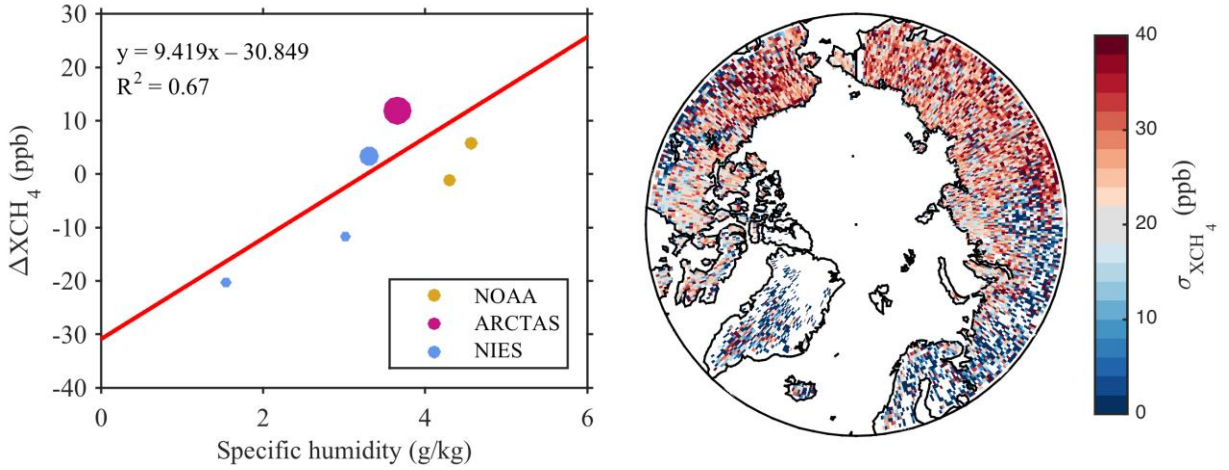
y = 9.419x – 30.849
R2 = 0.67
ΔXCH4 (ppb)
Specific humidity (g/kg)
NOAA
ARCTAS
NIES
σXCH4 (ppb)

Figure 3.

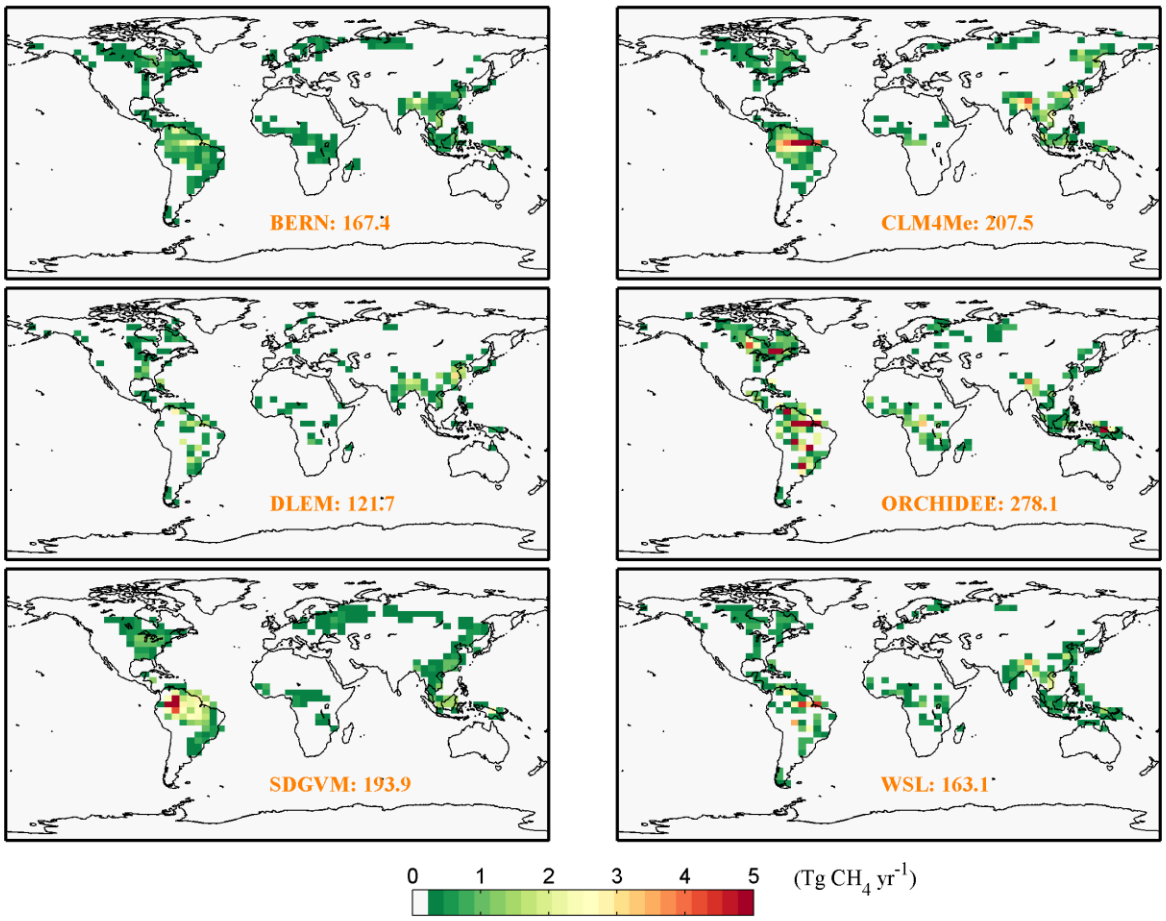
BERN: 167.4
CLM4Me: 207.5
DLEM: 121.7
ORCHIDEE: 278.1
SDGVM: 193.9
WSL: 163.1
0 1 2 3 4 5 (Tg CH4 yr-1)

~~Figure 2.~~

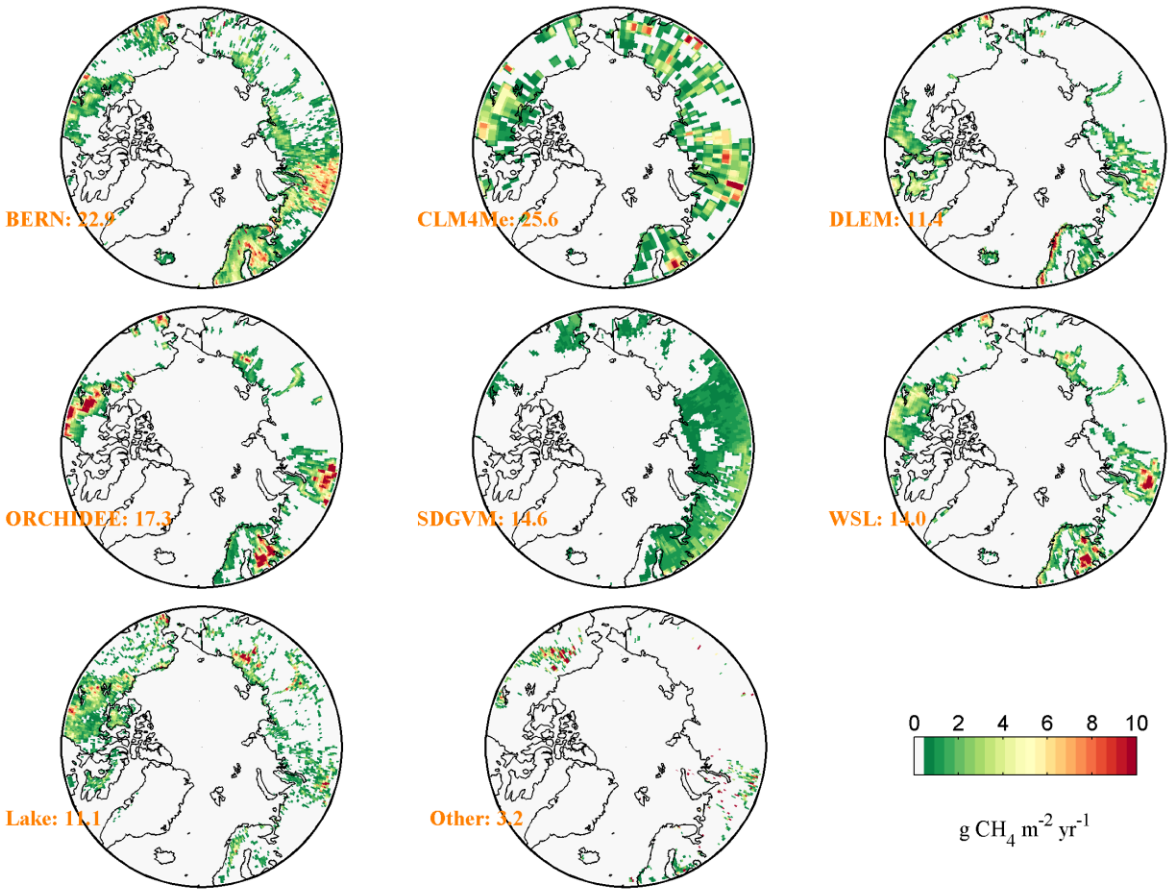
BERN: 22.0
CLM4Me: 25.6
DLEM: 11.4
ORCHIDEE: 17.3
SDGVM: 14.6
WSL: 14.0
Lake: 11.1
Other: 3.2
0 2 4 6 8 10
g CH4 m-2 yr-1

~~Figure 3.~~

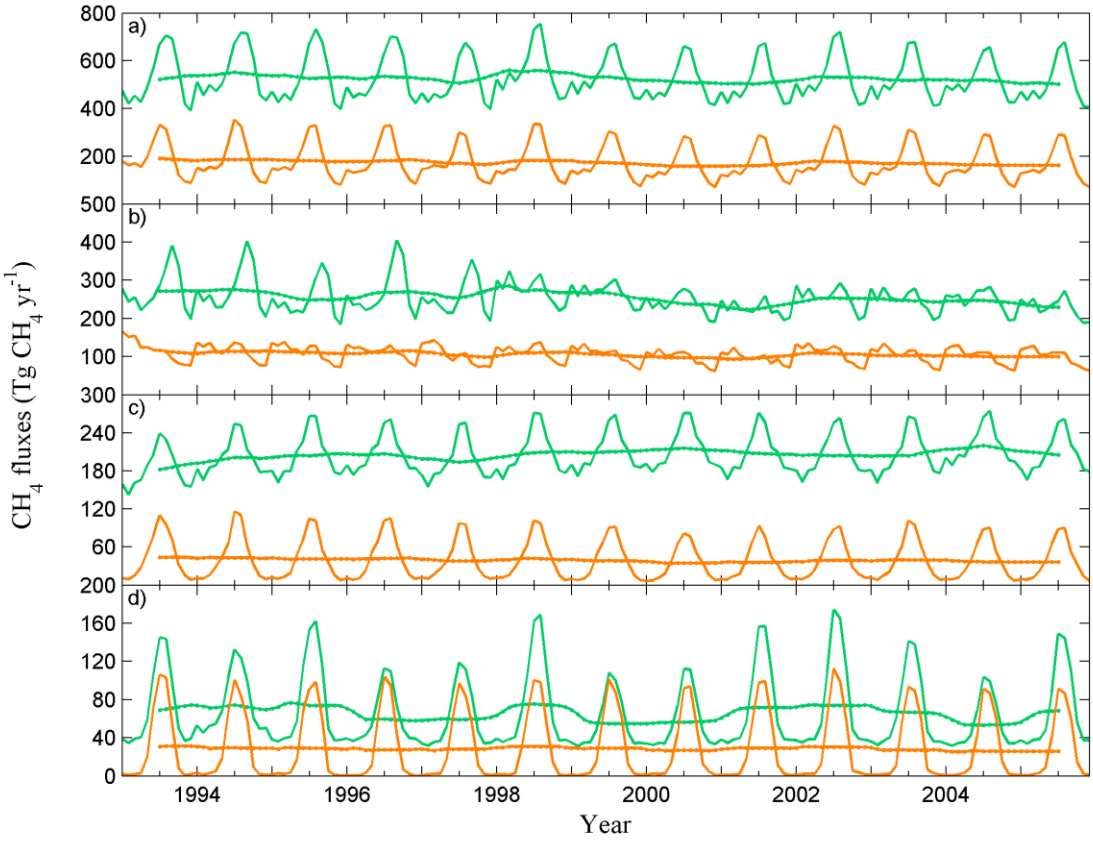
a)
b)
c)
d)
800
600
400
200
500
400
300
200
100
300
240
180
120
60
200
160
120
80
40
0
1994
1996
1998
2000
2002
2004
Year
CH4 fluxes (Tg CH4 yr-1)

~~Figure 4.~~

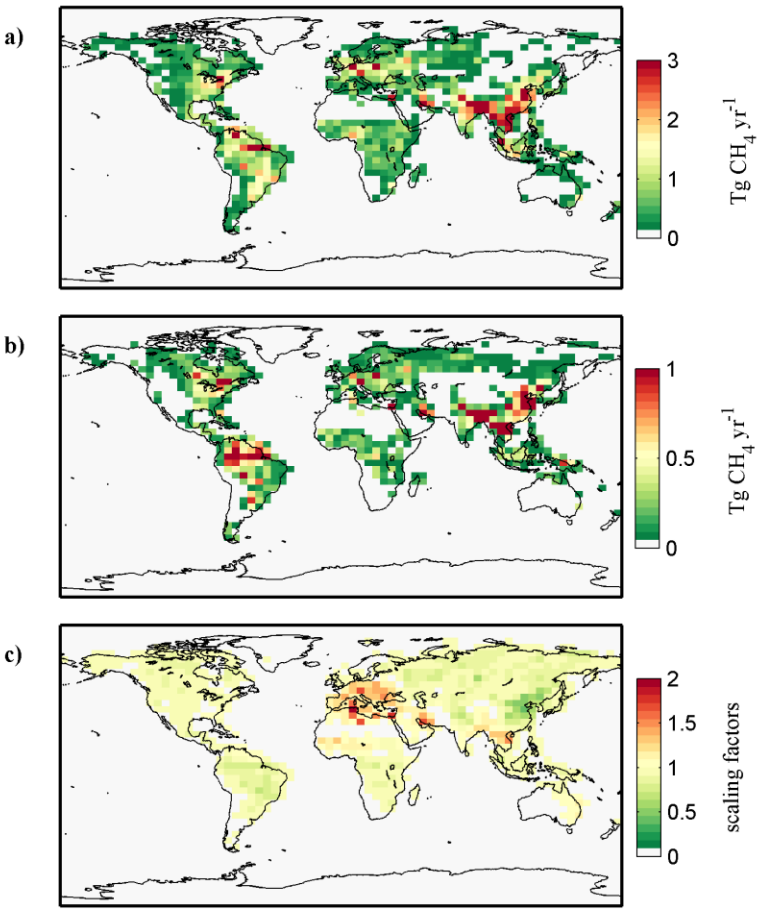

~~Figure 5.~~

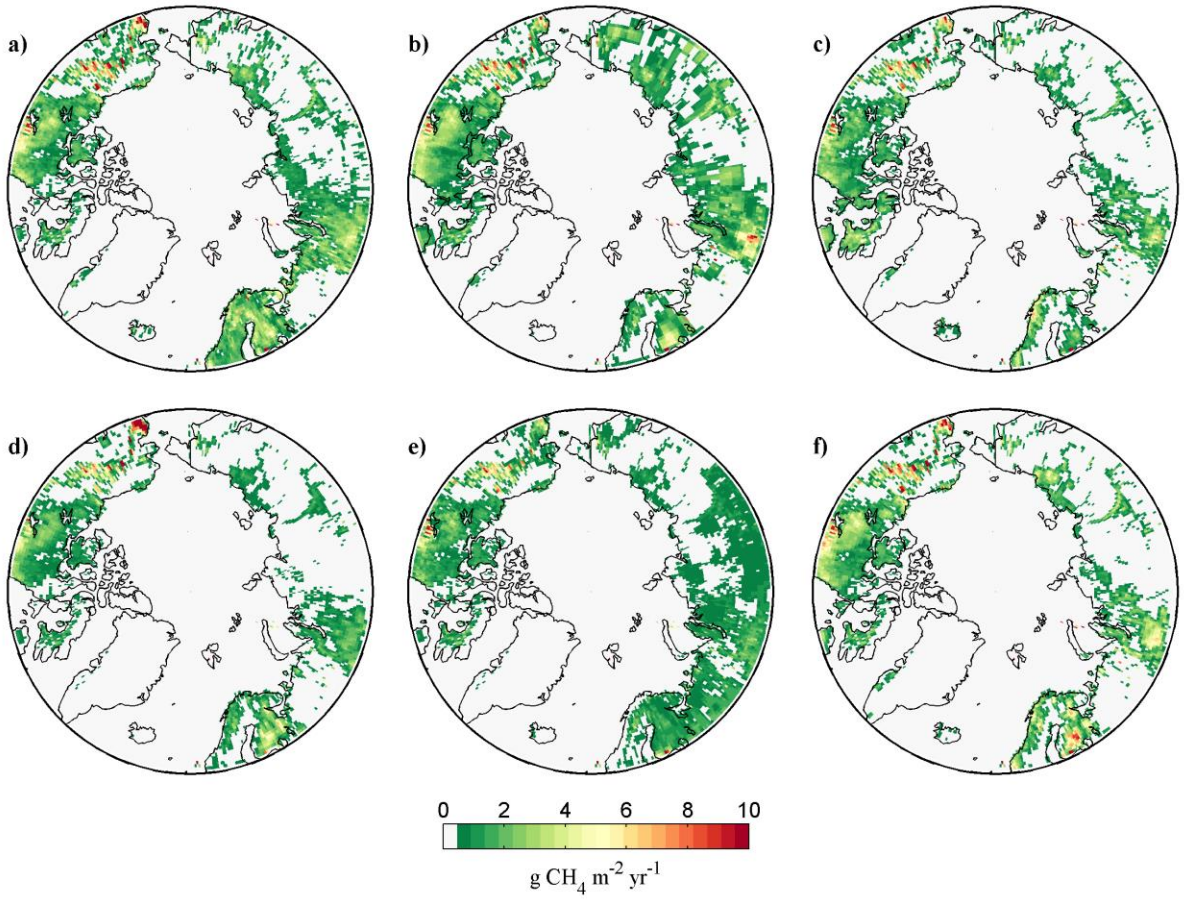

Figure 4~~6~~.

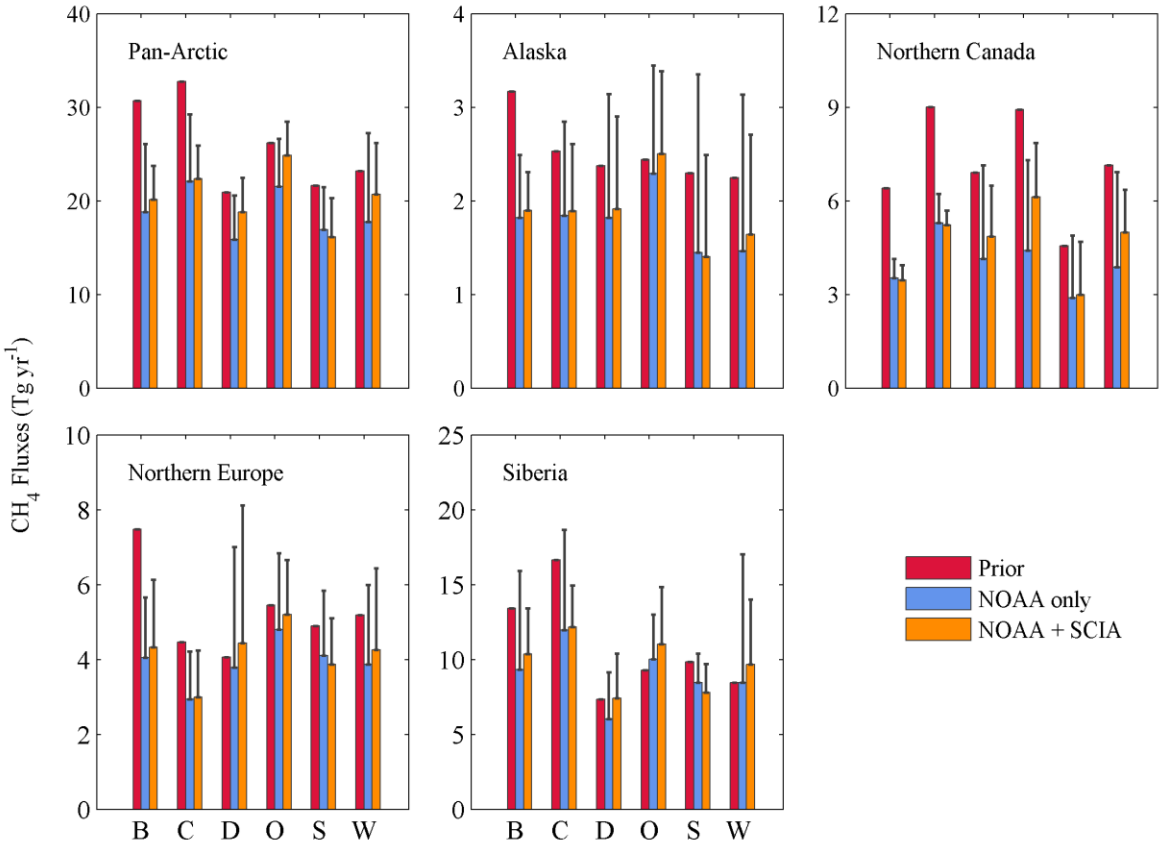
Pan-Arctic
Alaska
Northern Canada
Northern Europe
Siberia
CH4 Fluxes (Tg yr-1)
B C D O S W
Prior
NOAA only
NOAA + SCIA

Figure 5.

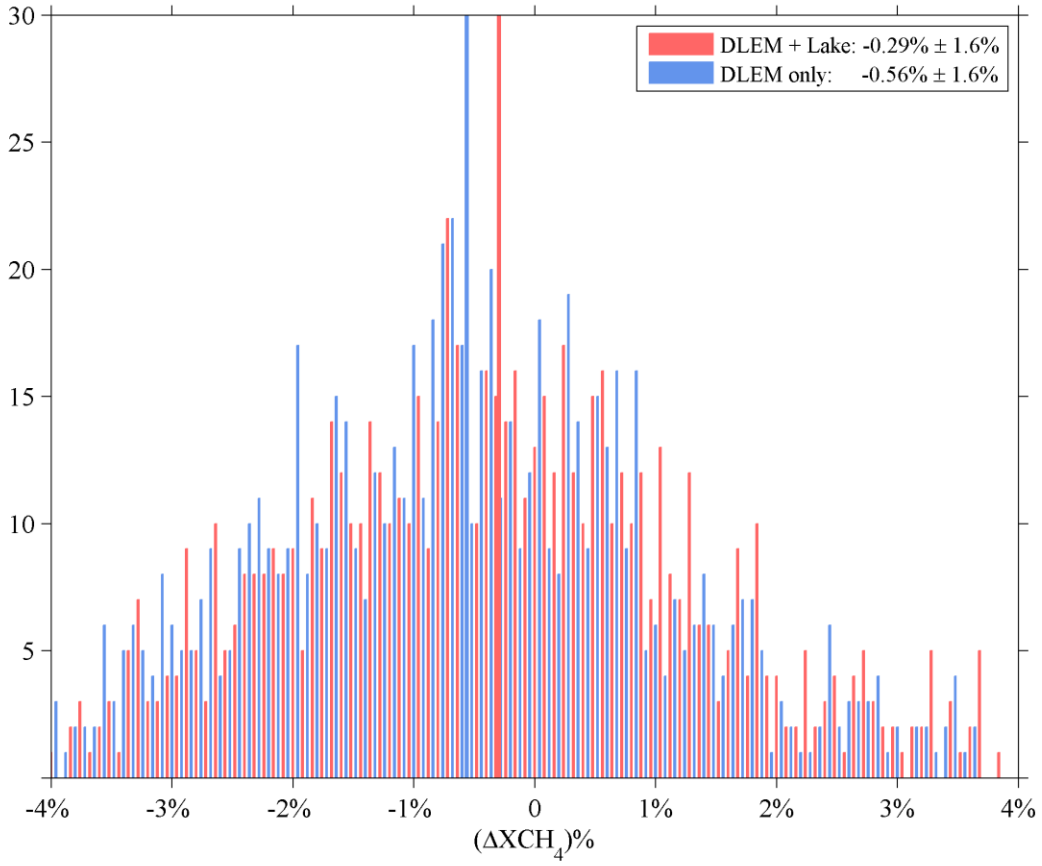
DLEM + Lake: -0.29% ± 1.6%
DLEM only: -0.56% ± 1.6%
30
25
20
15
10
5
-4%
-3%
-2%
-1%
0
1%
2%
3%
4%
(ΔXCH4)%

Figure 6.

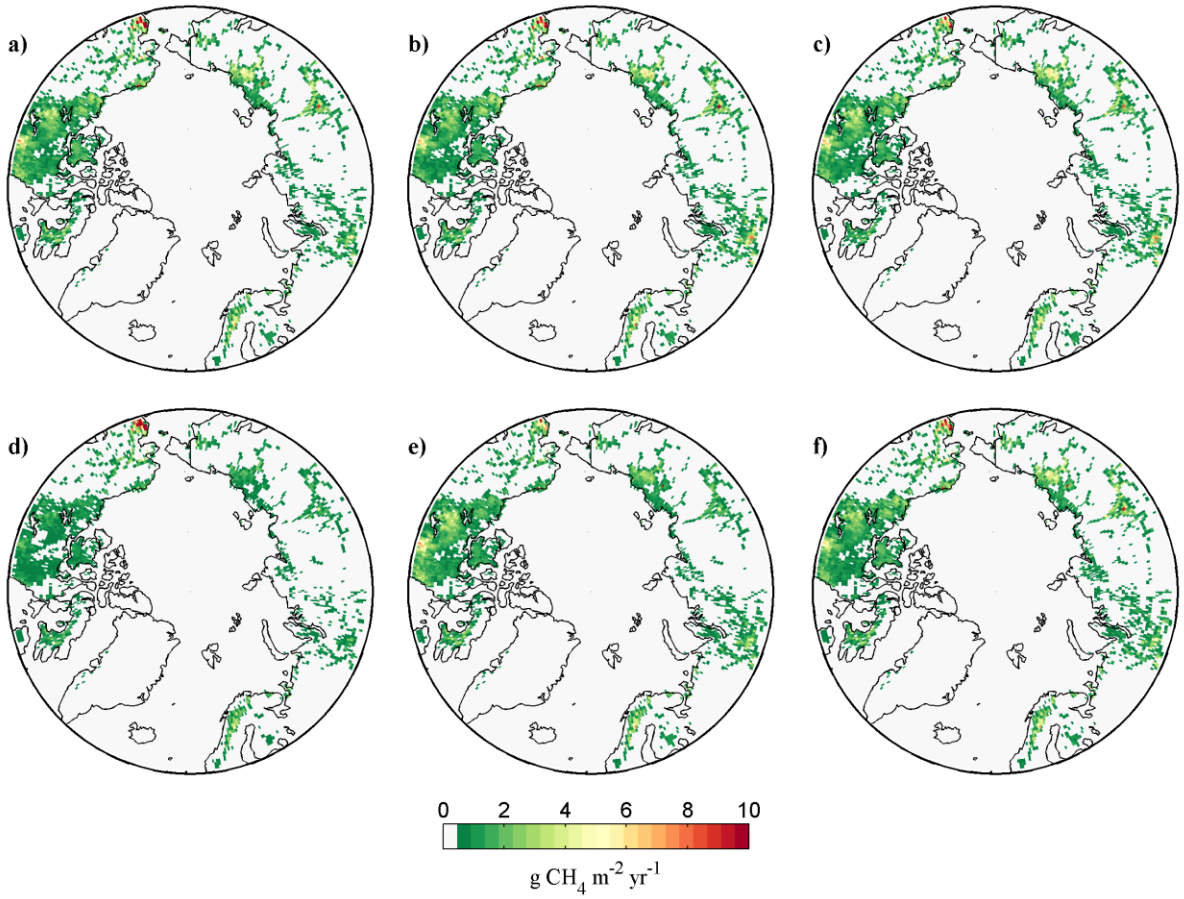

~~Figure 7.~~

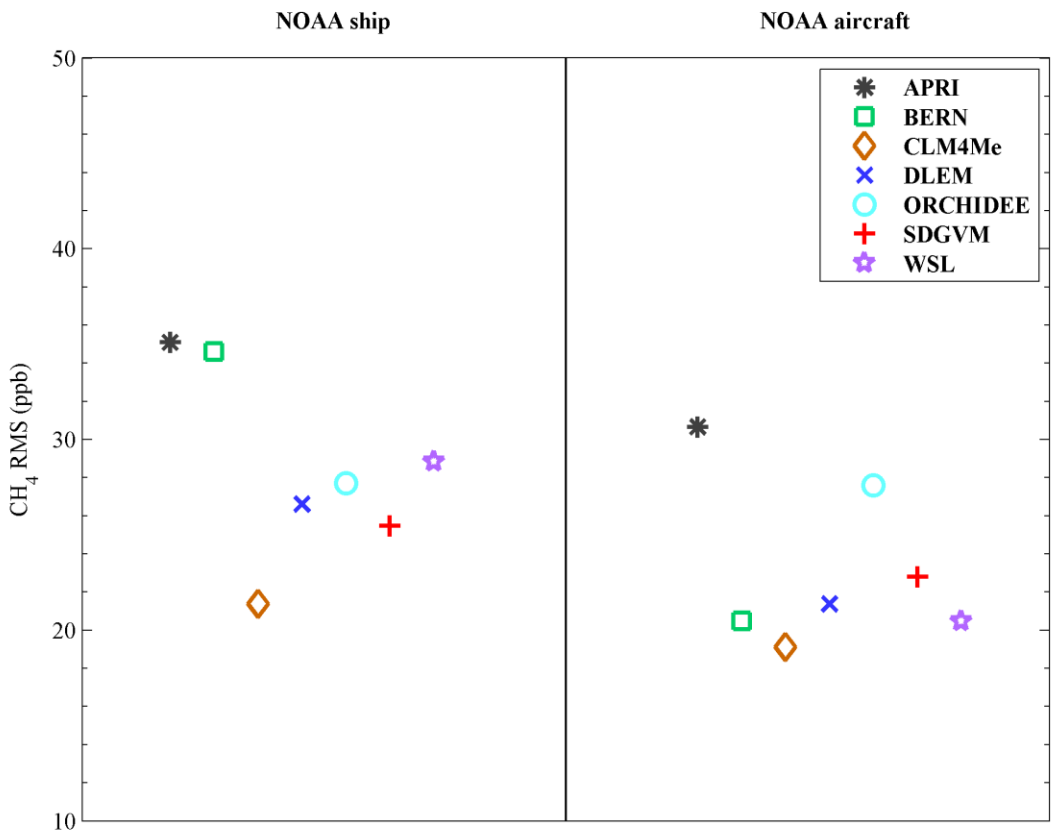
NOAA ship
NOAA aircraft
50
40
30
20
10
CH4 RMS (ppb)
APRI
BERN
CLM4Me
DLEM
ORCHIDEE
SDGVM
WSL

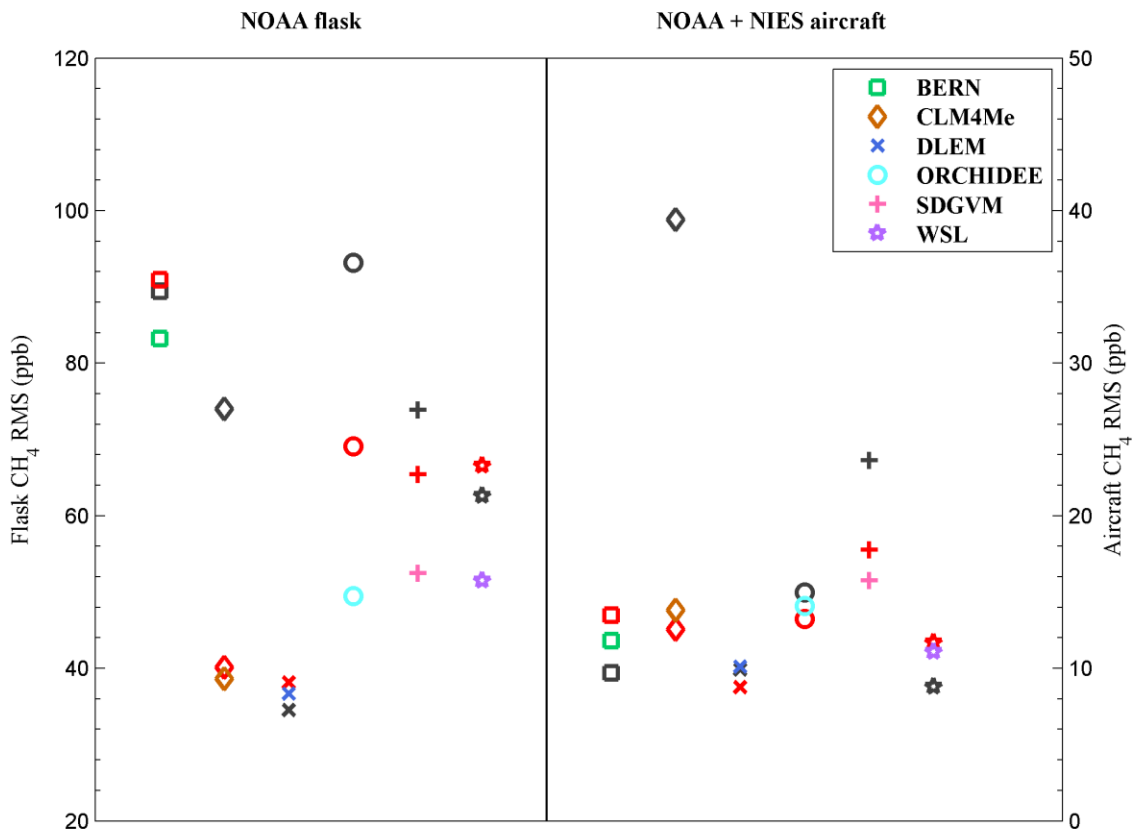
NOAA flask
NOAA + NIES aircraft
BERN
CLM4Me
DLEM
ORCHIDEE
SDGVM
WSL
Flask CH4 RMS (ppb)
Aircraft CH4 RMS (ppb)
120
100
80
60
40
20
50
40
30
20
10
0

Figure 7~~8~~.

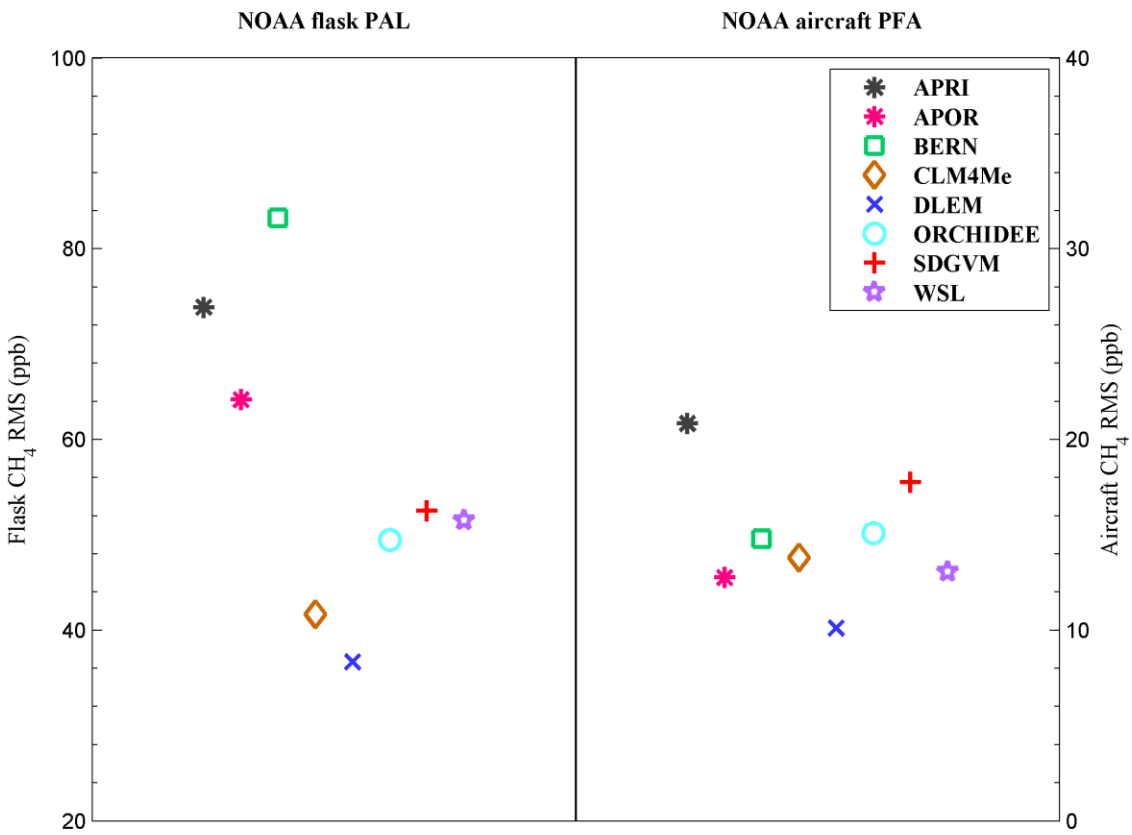
NOAA flask PAL
NOAA aircraft PFA
Flask CH4 RMS (ppb)
Aircraft CH4 RMS (ppb)
100
80
60
40
20
40
30
20
10
0
APRI
APOR
BERN
CLM4Me
DLEM
ORCHIDEE
SDGVM
WSL

~~Figure 9.~~

S1. Methods and Results

In the text S1, the steps to construct optimal initial conditions for global and nested grid inversions are described. We also describe the steps to construct an optimal GEOS-Chem CH_4 field for SCIAMACHY bias correction purpose and the comparison between our estimates and previous inversion studies in the global scale.

To start global and nested-grid inversions, the initial CH_4 field of the GEOS-Chem model needs to be optimized to minimize its error. As our focus is in the period of 2004–2005, to speed up the whole process, we only ran one inversion from 1993 to 2003 using the LPJ-WSL scenario and NOAA/ESRL measurements. The main purpose of this inversion is to construct initial CH_4 field in 2004. As presented in Fig. S2, without optimization, the LPJ-WSL scenario gives the best fit of the GEOS-Chem modeled CH_4 to the GLOBALVIEW-CH4 data (GLOBALVIEW-CH4, 2009). During the 1993–2003 inversion, GEOS-Chem was driven by GEOS-4 meteorological (met) data from NASA's Global Modeling Assimilation Office (GMAO). Relative to GEOS-5, the GEOS-4 met data has the same horizontal resolutions but less vertical hybrid sigma-pressure levels (55 vertical levels).

To construct optimal atmospheric CH_4 fields for the bias correction of SCIAMACHY retrievals at the global scale, we ran a global inversion during 2004–2005 using the LPJ-WSL wetland emission scenario and NOAA/ESRL measurements. In this inversion, the GEOS-Chem model was driven by the GEOS-5 met data. The global inversions of different scenarios that assimilated both surface measurements and satellite retrievals were then run in two sequential time windows: 2004/01–2004/12 and 2005/01–2005/12. Only the inversions in the second time window are for analysis and the first time window is designed to minimize the impacts of the

transition from GEOS-4 to GEOS-5 and from the LPJ-WSL scenario to other scenarios. In the above inversions, we included surface measurements from pan-Arctic sites but excluded satellite retrievals out of 50°S–50°N. The global inversions during 2005 also provided initial conditions and time-dependent boundary conditions for the nested grid simulations of the adjoint model. Following Turner et al. (2015), we did not optimize boundary conditions in the nested-grid inversions as did in Wecht et al. (2014). The nested grid inversions of the pan-Arctic were run at 1/2° × 2/3° resolution from July 1, 2005 to Oct 1, 2005.

Specific humidity for bias correction was retrieved from the European Centre for Medium-Range Weather Forecasts (ECMWF)'s ERA-20C reanalysis product (http://apps.ecmwf.int/datasets/data/era20c-daily), averaged by the column between the surface and 3 km altitude (Houweling et al., 2014). The air mass factor and coordinates of satellite CH_4 retrievals have been included in the SCIAMACHY IMAP v6.0. For global-scale bias correction, we first optimized the GEOS-Chem 4-D CH_4 mixing ratios using only surface measurements and then sampled the modeled XCH_4 at the coordinates and time of SCIAMACHY retrievals and with local averaging kernels applied. Following Bergamaschi et al. (2009) and Houweling et al. (2014), only satellite retrievals between 50°S and 50°N were utilized. The XCH_4 differences between SCIAMACHY and GEOS-Chem are shown in Fig. S3a. A regression relationship was then built to represent the satellite system bias by proxy factors. Turner et al. (2015) suggested that it is more likely that grid squares residual standard deviation (RSD) in excess of 20 ppb are dominated by model bias in prior emissions. Thus, we excluded such grid squares in regressions. And satellite retrievals with low precisions (the ratio of retrieval precision error to retrieval is larger than 3%) were also removed from analysis. Following Houweling et al. (2014), we did not optimize bias correction functions in the inversion cycle in the concern that this process could

cause bias correction to incorrectly account for the uncertainties caused by unaccounted model errors or even the uncertain sources and sinks. As shown in Fig. S3d, bias correction reduced model-satellite differences greatly in tropical areas of America, Africa and South Asia and also reduced the differences in Australia and some areas of the United States. And the agreement between GEOS-Chem and SCIAMACHY is also improved at the global scale (Fig. S3c). However, the model-data agreement is deteriorated in East Asia. It could be caused by the overestimate of anthropogenic CH_4 emissions from China in the EDGAR dataset (Peng et al., 2016).

The results of the global inversions are presented in Table 2 and Fig. S4. There have been many studies that assimilated surface measurements and/or satellite retrievals into a CTM inverse model to constrain global CH_4 emissions, see Kirschke et al. (2013) for review. For instance, using the same observations suite, Bergamaschi et al. (2009) estimated that in 2004, CH_4 emissions in global, tropical (30°S–30°N), northern extratropical (30°N–90°N) and southern extratropical (90°S–30°S) zonal areas were 506.7 Tg CH_4 yr^{-1}, 323.5 Tg CH_4 yr^{-1}, 172.8 Tg CH_4 yr^{-1} and 10.4 Tg CH_4 yr^{-1}, respectively. These large-scale estimates are consistent with our calculations: 284.5–319.6 Tg CH_4 yr^{-1} (tropical), 165.3–206.6 Tg CH_4 yr^{-1} (northern extratropical) and 10.0–13.9 Tg CH_4 yr^{-1} (southern extratropical). This agreement could imply that the GEOS-Chem adjoint and TM5-4DVAR are consistent in the atmospheric transport, chemistry and inverse modeling methods. In contrast to Bergamaschi et al. (2009), our inversions allocate more emissions to extratropical regions. As a result, the tropical total (SATr + NAF + SAF + TrA) of the six inversions is in the range of 114.1–169.7 Tg CH_4 yr^{-1}, which is much lower than their estimate of 203.2 Tg CH_4 yr^{-1}. The likely reason for this discrepancy is that we did not optimize bias correction functions in the inversion cycle. Our posterior wetland CH_4 emissions estimated

in the Bern, CLM4Me, SDGVM and WSL scenarios are close to the estimate of 161 Tg CH_4 yr^{-1} for 2003–2007 in Bloom et al. (2010). The latter was based on CH_4 and gravity spaceborne data to constrain large-scale methanogenesis. Our estimates are also close to the inferred wetland CH_4 emissions (175±33 Tg CH_4 yr^{-1}) by Kirschke et al. (2013). By using artificial neural networks, Zhu et al. (2013) estimated that from 1990 to 2009, annual wetland CH_4 emissions from northern high latitudes (> 45°N) were in the range of 44.0–53.7 Tg CH_4 yr^{-1}, agreeing with the estimates of the Bern, CLM4Me and SDGVM scenarios.

Fig. S4a shows that CH_4 fluxes are the highest in the Amazon, China, Southeast Asia, North America and Europe where there are either a large area of wetlands and rice paddies or advanced coal and oil industries or both. Our results indicate that the Eurasian temperate zone, including China, North America and Europe, emitted much more CH_4 than any other geographic zones (Table 2), implying the dominance of anthropogenic sources in the global CH_4 inventory. As presented in Fig. S4c, our inverse modeling reduced the CH_4 emissions from China, the Amazon basin and the Eurasian boreal region (scale factor < 1) but increased the emissions in Europe and Southeast Asia (scale factor > 1) relative to the prior.

Fig. S6 shows the difference between the modeled and observed CH_4 mixing ratios at NOAA ship board sampling stations and aircraft vertical profile sites under different wetland scenarios before and after the global scale inversions. For most scenarios, inversion improves the representation of CH_4 mixing ratios in GEOS-Chem at both marine and inland boundary layers and free troposphere. For example, the BERN scenario inversion reduced the bias by about 18 ppb for ship stations and about 6 ppb for aircraft sites. Also the DLEM scenario inversion reduced the bias by about 20 ppb for ship stations and about 19 ppb for aircraft sites. For the

CLM4Me and SDGVM scenarios with low prior biases, the inversions did not improve the performance. This could be caused by the errors introduced by the inversion process itself. For example, as the optimization is designed to address total emissions, the representation of diurnal variability in GEOS-Chem could be made worse during inversion.

Table S1. NOAA/ESRL stations used in the inversion.

Station ID	Latitude	Longitude	Altitude [m]	Station Name
ALT	82.45	-62.52	210.0	Alert, Nunavut, Canada
ZEP	78.90	11.88	475.0	Ny-Alesund, Svalbard (Spitsbergen), Norway and Sweden
SUM	72.58	-38.48	3238.0	Summit, Greenland
BRW	71.32	-156.60	11.0	Barrow, Alaska, USA
ICE	63.34	-20.29	127.0	Heimay, Vestmannaeyjar, Iceland
CBA	55.20	-162.72	25.0	Cold Bay, Alaska, USA
SHM	52.72	174.10	40.0	Shemya Island, Alaska, USA
UUM	44.45	111.10	914.0	Ulaan Uul, Mongolia
NWR	40.05	-105.58	3526.0	Niwot Ridge, Colorado, USA
AZR	38.77	-27.38	40.0	Terceira Island, Azores, Portugal
WLG	36.29	100.90	3810.0	Mt. Waliguan, People’s Republic of China
BMW	32.27	-64.88	30.0	Tudor Hill, Bermuda, UK
IZO	28.30	-16.48	2360.0	Tenerife, Canary Islands, Spain
MID	28.21	-177.38	7.7	Sand Island, Midway, USA
ASK	23.18	5.42	2728.0	Assekrem, Algeria
MLO	19.53	-155.58	3397.0	Mauna Loa, Hawai, USA
KUM	19.52	-154.82	3.0	Cape Kumukahi, Hawaii, USA
GMI	13.43	144.78	6.0	Mariana Islands, Guam

RPB	13.17	-59.43	45.0	Ragged Point, Barbados
CHR	1.70	-157.17	3.0	Christmas Island, Republic of Kiribati
SEY	-4.67	55.17	7.0	Mahe Island, Seychelles
ASC	-7.92	-14.42	54.0	Ascension Island, UK
SMO	-14.24	-170.57	42.0	Tutuila, American Samoa, USA
CGO	-40.68	144.68	94.0	Cape Grim, Tasmania, Australia
CRZ	-46.45	51.85	120.0	Crozet Island, France
TDF	-54.87	-68.48	20.0	Tierra Del Fuego, La Redonda Isla, Argentinia
PSA	-64.92	-64.00	10.0	Palmer Station, Antarctica, USA
SYO	-69.00	39.58	14.0	Syowa Station, Antarctica, Japan
HBA	-75.58	-26.50	33.0	Halley Station, Antarctica, UK
SPO	-89.98	-24.80	2810.0	South Pole, Antarctica, USA

Table S2. NOAA aircraft profiles used for validation.

CODE	Location	Latitude (deg)	Longitude (deg)	Start Date	End Date
PFA	Poker Flat, Alaska, United States	65.07	-147.29	06/27/1999	06/05/2015
ESP	Estevan Point, British Columbia, Canada	49.6	-126.4	11/22/2002	06/09/2015
DND	Dahlen, North Dakota, USA	48.1	-98.0	09/21/2004	05/31/2015
LEF	Park Falls, Wisconsin, USA	45.9	-90.3	04/10/1998	05/28/2015
FWI	Fairchild, Wisconsin, USA	44.7	-91.0	09/20/2004	11/18/2005
NHA	Worcester, Massachusetts, USA	43.0	-70.6	09/21/2003	06/10/2015
BGI	Bradgate, Iowa, USA	42.8	-94.4	09/13/2004	11/18/2005
HFM	Harvard Forest, Massachusetts, USA	42.5	-72.2	11/11/1999	11/18/2007
WBI	West Branch, Iowa, USA	42.4	-91.8	09/14/2004	05/28/2015
OIL	Oglesby, Illinois, USA	41.3	-88.9	09/16/2004	11/19/2005
THD	Trinidad Head, California, USA	41.0	-124.2	09/02/2003	05/16/2015
BNE	Beaver Crossing, Nebraska, USA	40.8	-97.2	09/15/2004	05/11/2011
CAR	Briggsdale, Colorado, USA	40.6	-104.6	11/09/1992	04/21/2015
HIL	Homer, Illinois, USA	40.1	-87.9	09/16/2004	05/21/2015
TGC	Sinton, Texas, USA	27.7	-96.9	09/09/2003	06/05/2015
HAA	Molokai Island, Hawaii, USA	21.2	-158.9	05/31/1999	04/22/2008
RTA	Rarotonga, Cook Islands	-21.3	-159.8	04/16/2000	05/29/2015

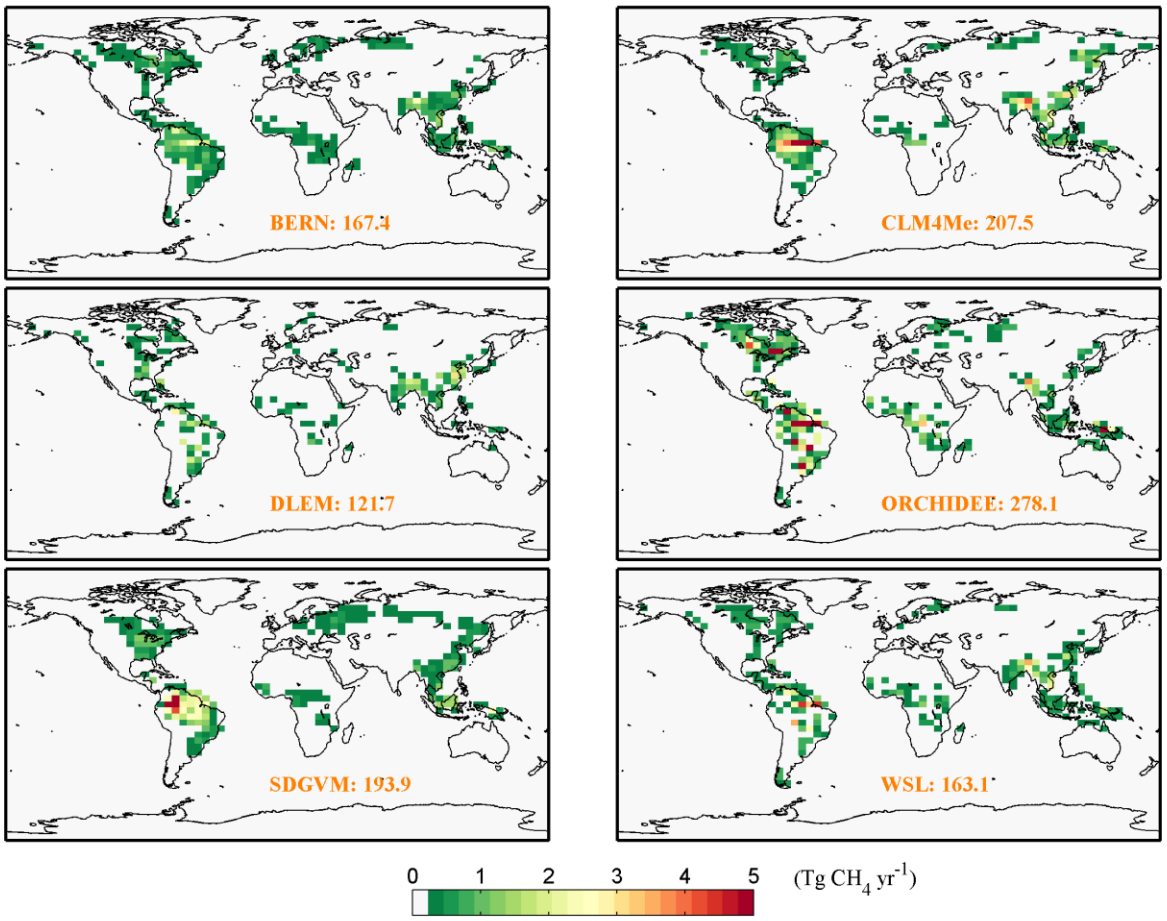

Figure S1. Average of prior wetland CH_4 annual emissions during 2004–2005 from six different wetland biogeochemical models used for the GEOS-Chem global inversion at 4° × 5° resolution. Annual total emission (orange) is presented in units of Tg CH_4 yr^{-1}.

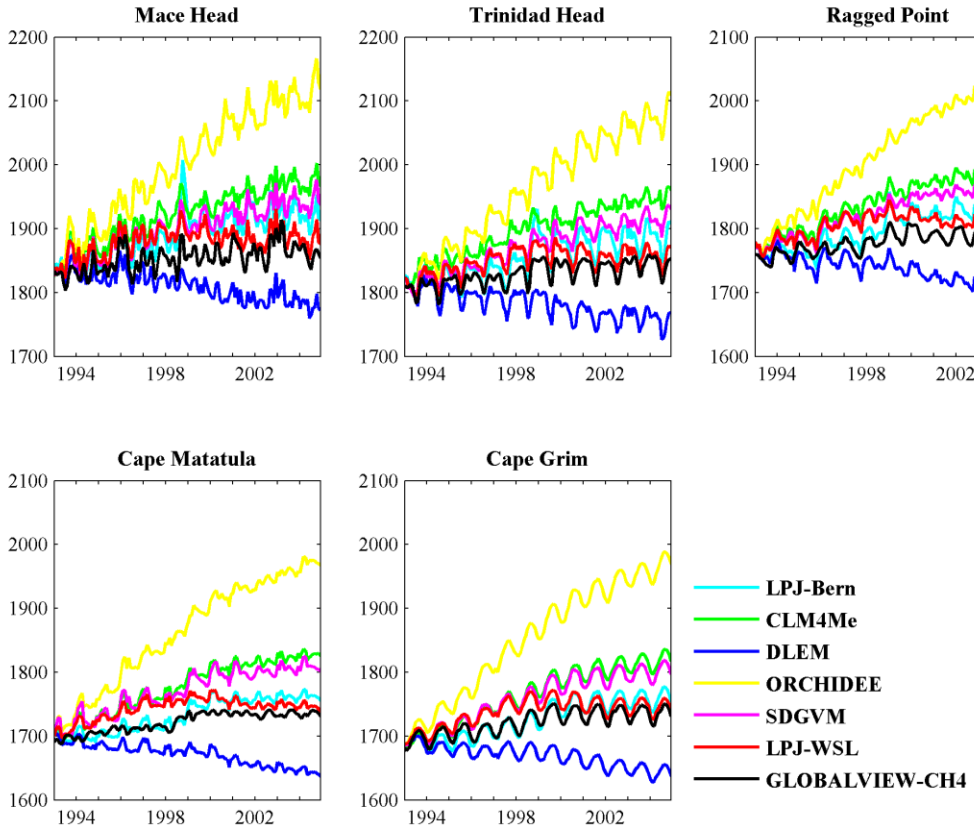

Figure S2. The comparison between the GEOS-Chem simulated and GLOBALVIEW-CH4 atmospheric CH_4 (units: ppbv) at five stations (Mace Head, Ireland; Trinidad, California; Ragged Point, Barbados; Cape Matatula, Samoa; Cape Grim, Tasmania). The wetland CH_4 emissions used are pre-optimized model simulations provided by the WETCHIMP project.

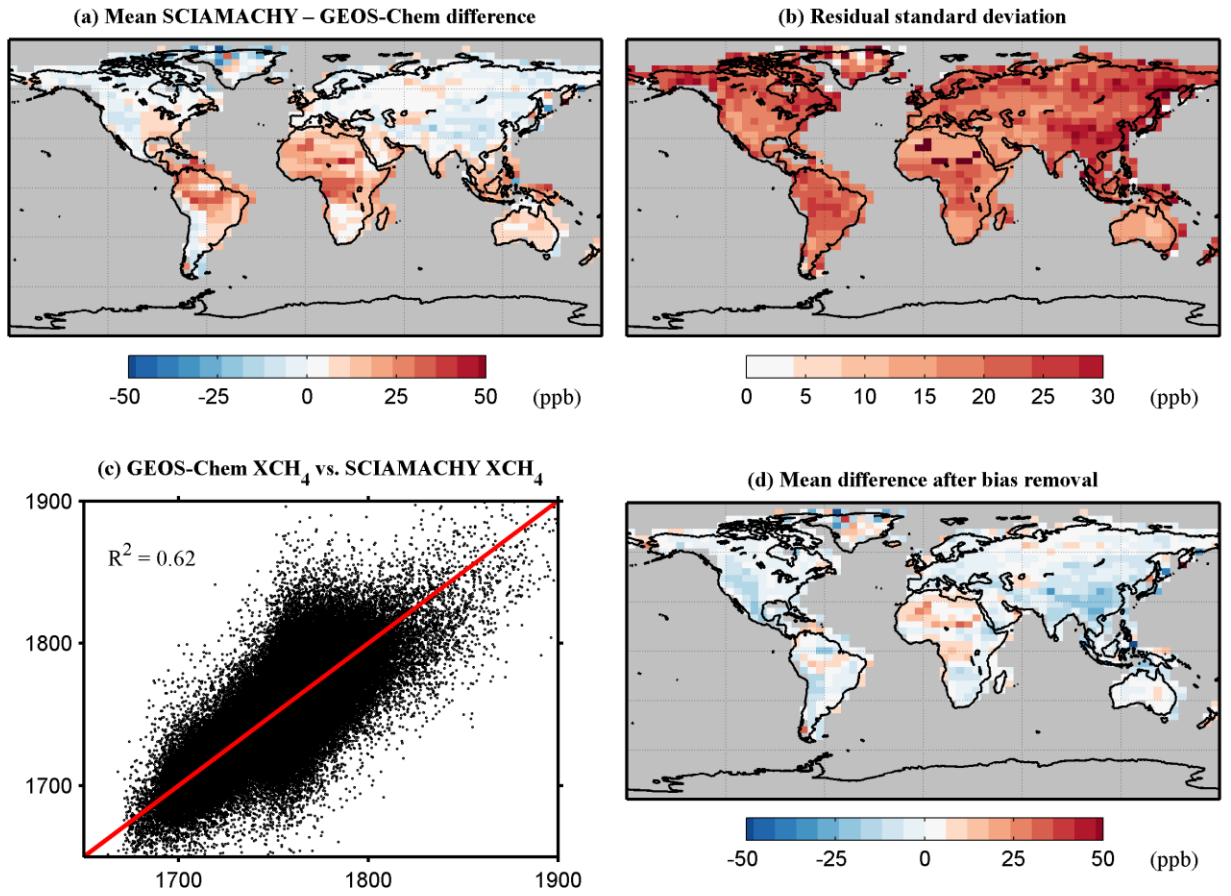

Figure S3. Comparison of column averaged CH_4 mole fractions from SCIAMACHY with those from GEOS-Chem model calculated with prior emissions. (a and b) show the mean bias and residual standard deviation of the satellite-model difference, (c) shows the comparison of the model (x axis) and satellite (y axis) XCH_4 after applying the "latitude + humidity" correction from the linear regression (weighted R^2 is shown inset and the red 1:1 line is also shown), and (d) shows the satellite-model difference after bias removal.

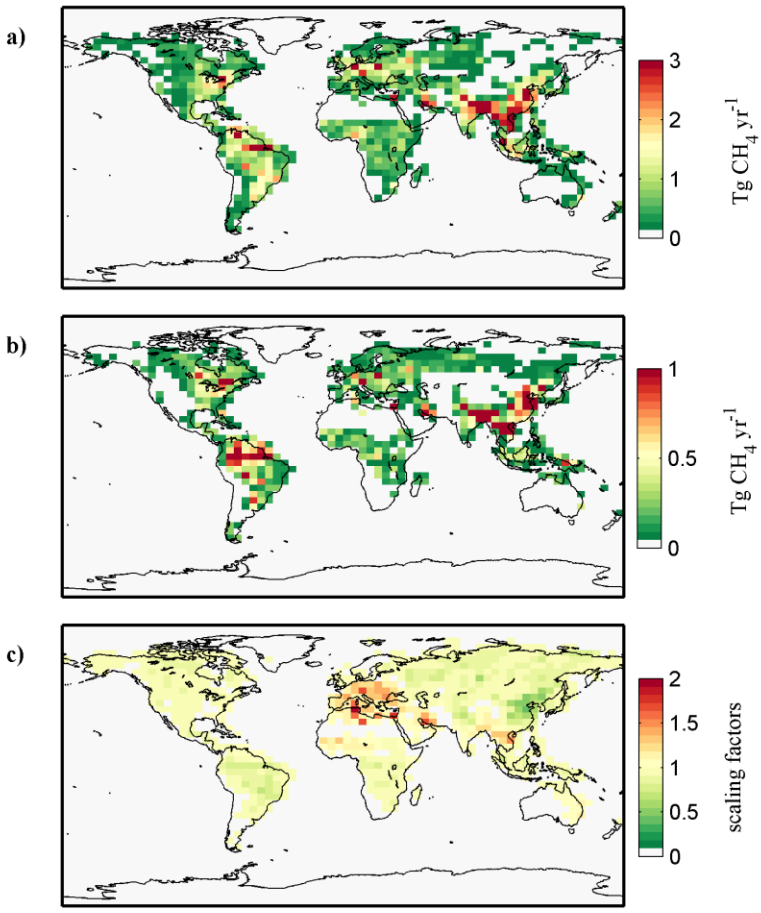

Figure S4. Optimized global CH_4 emissions and emission scale factors in 2005 at 4° × 5° resolution. Emission scale factor is defined as posterior emissions relative to prior emissions. a) Posterior CH_4 emissions averaged over inversions of six scenarios; b) standard deviation of posterior CH_4 emissions over inversions of six scenarios; c) optimized emission scale factors averaged over inversions of six scenarios.

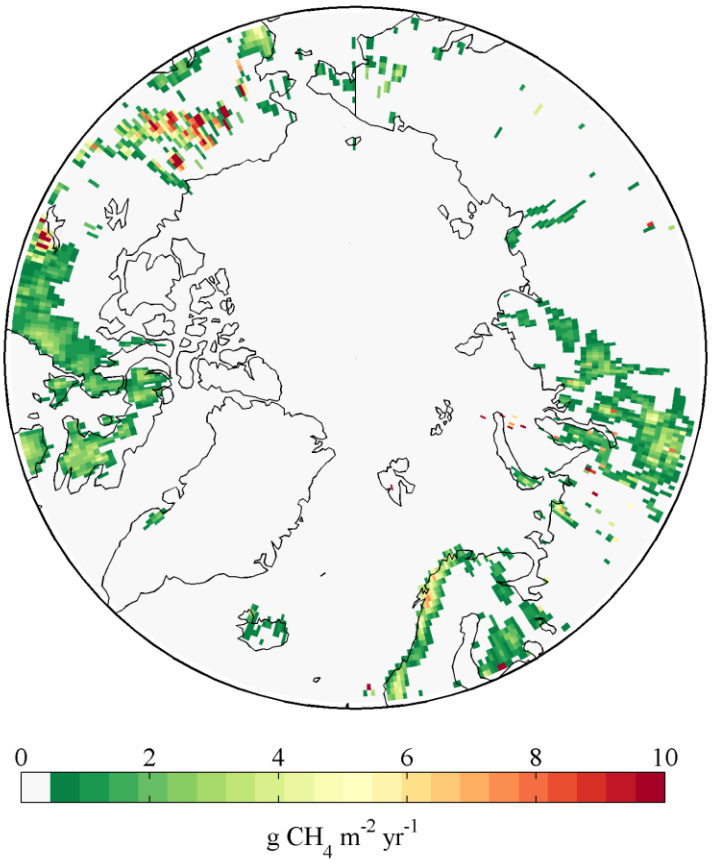

Figure S5. Posterior CH_4 emissions from the pan-Arctic in 2005 estimated by the inversion of the "DLEM wetland only" scenario. The "DLEM wetland only" scenario uses the simulated wetland CH_4 emissions from the DLEM model and does not incorporate CH_4 emissions from pan-Arctic lakes.

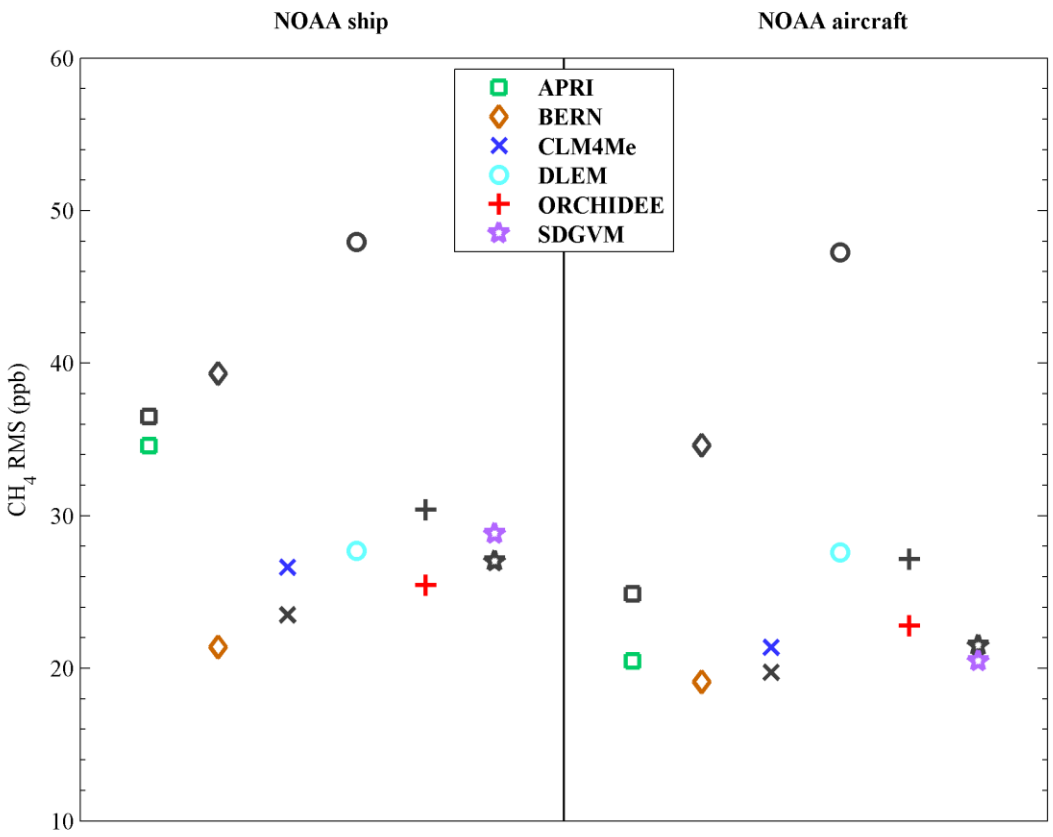

Figure S6. Evaluation of posterior GEOS-Chem CH_4 mole fractions from the global inversions with independent data sets. The plot shows the root mean square (rms) of differences between the modeled and the observed CH_4 mixing ratios. Black symbols indicate the rms of the forward GEOS-Chem runs.